Title
Cortical mechanisms underlying verbal working memory

Author
Fegen, David

Publication Date
2012

Peer reviewed|Thesis/dissertation

Cortical mechanisms underlying verbal working memory

David Andrew Fegen

A dissertation submitted in partial satisfaction of the

requirements for the degree of

Doctor of Philosophy

in

Neuroscience

in the

Graduate Division

Of the

University of California, Berkeley

Committee:

Professor Mark D'Esposito, Chair
Professor Robert Knight
Professor Jonathan Wallis
Professor David Brillinger

Fall 2012

Cortical mechanisms underlying verbal working memory

by David Andrew Fegen

Abstract

Cortical mechanisms underlying verbal working memory

by

David Andrew Fegen

Doctor of Philosophy in Neuroscience

University of California, Berkeley

Professor Mark D'Esposito, Chair

Verbal working memory refers to the limited-capacity store responsible for maintaining and manipulating task-relevant information in a verbal form over short time-periods. The cortical regions that underlie this type of memory can be dissociated into control and storage regions. Control processes may involve operations such as the identification and selection of relevant information and the assembly and initial execution of articulatory rehearsal programs. In contrast, storage regions are where the actual task-relevant information is rehearsed. Presumably, control and storage regions transfer information among each other within a functionally connected network.

To study the cortical network formed during the delay period of a verbal working memory task, the first study was specifically designed to investigate functional connectivity. This involved several innovations to standard verbal working memory paradigms including visual pacing cues to ensure subvocal rehearsal over long delay periods and imaging only the left hemisphere to achieve a high temporal resolution. While the functional connectivity results counterintuitively led to a null result, it was demonstrated that middle frontal gyrus (MFG) and superior parietal lobule (SPL) were active during encoding and the start of the delay period, as well as at the end of the delay period, suggesting they were involved in control processes. In contrast, it was demonstrated that inferior frontal gyrus (IFG), premotor (PM) and Sylvian-parietal-temporal junction (area Spt) were active throughout encoding and the entire delay period, suggesting they were involved in storage/rehearsal processes.

In a second follow-up study, the presentation rate of the visual pacing cues was altered to control subvocal rehearsal rate. Therefore, along with memory load, rehearsal rate was manipulated over long delay periods in a verbal working memory task. Results demonstrated that control regions MFG and SPL were not sensitive to manipulations in rehearsal rate, but exhibited non-linear memory load

effects. Conversely, storage/rehearsal regions IFG, PM and area Spt demonstrated approximately linear rehearsal rate and memory load effects. Additionally, memory load effects were found to diminish through time in all areas, while rehearsal rate effects persisted through the entire delay period in storage/rehearsal areas. It was also revealed that rehearsal rate and memory load were confounded behaviorally as subjects strategically increased their rehearsal rate to manage an increased memory load, until the load became so great that their rehearsal rate began to decrease. It was also discovered that high capacity individuals have less activity in MFG, IFG and SPL, but more activity in PM. Analyzing this same dataset with a functional connectivity analysis also led to a counterintuitive connectivity result: as task-demands increased, functional connectivity decreased. When fully investigated it was determined that increased task demands led to decreased standard deviation of the fMRI BOLD signal, which in turn led to decreased functional connectivity. These results help clarify the counterintuitive functional connectivity results of the first study.

The relationship between signal variability and functional connectivity was utilized in a third study which also used visual pacing circles and long blocks of activity, but this time in combination with jittered time intervals between rehearsals to maximize signal variability. Substitute tasks were made for the encoding period (listen word) and delay period (subvocal rehearsal) of standard verbal working memory tasks and the timing and network properties of the active cortical regions were investigated. Results demonstrated that during the listen word condition activity in primary auditory cortex preceded area Spt, and that primary auditory cortex and area Spt formed a functional network. In contrast, during the subvocal rehearsal condition activity occurred first in PM, then in area Spt, followed by IFG. These three regions also formed a functional network in the subvocal rehearsal condition. Together these experiments provide novel insights into the cortical mechanisms underlying verbal working memory.

TABLE OF CONTENTS

List of Figures and Tables

Abbreviations

ANTS:	Advanced Normalization Tools
BA:	Brodmann area
BOLD:	blood oxygen level dependent
CSPLIN:	cubic spline function
DTI:	diffusion tensor imaging
ECoG:	electrocorticography
EEG:	electroencephalography
EPI:	echo-planar imaging
FDR:	False Discovery Rate
FIR:	finite impulse response
fMRI:	functional magnetic resonance imaging
HRF:	hemodynamic response function
MEG:	magnetoencephalography
MNI:	Montreal Neurological Institute
PLS:	partial least squares
ROI:	region of interest
SynN:	symmetric normalization
TR:	repetition time
WM:	working memory

cortical regions:

FFA:	fusiform face area
HG:	Heschl's gyrus (BA 41)
IFG:	inferior frontal gyrus (BA 44/45)
IFGpo:	inferior frontal gyrus pars operculum (BA 44)
IFGpt:	inferior frontal gyrus pars triangularis (BA 45)
MFG:	middle frontal gyrus (BA 9/46)
PFC:	prefrontal cortex
PM:	premotor (BA 6)
SPL:	superior parietal lobule (BA 7)
Spt:	Sylvian-parietal-temporal junction
STG:	superior temporal gyrus
STS:	superior temporal sulcus

Acknowledgments

First and foremost, I must thank Mark for providing his encouragement, support and resources. Without him, none of this would be possible. Also for setting an example of unwavering and determined pursuit of scientific discovery.

I must also thank Brad for his willingness to share his time, ideas and technical knowledge. These projects would be entirely different without his input.

And thanks to all the other current and former lab members who have helped along the way.

Thank you.

Dedication

To Jenn, with hidden strength and radiant beauty.
To Liam or Keira, whichever may be.
To my parents, for always being there.
To Devon, for her energy and enthusiasm.
To Chowder and Mila, for making every bit of life humorous.

This is for you.

1

INTRODUCTION

1.1 Background

The motivation of this work was to explore the cortical networks that subserve working memory, and more specifically, verbal working memory. From my first exposure to the field of cognitive neuroscience until the present day, I have found the topic of networks highly fascinating.

I begin in Chapter 1 by examining what is known about working memory from a theoretical viewpoint followed by what is known individually about the cortical regions that subserve working memory. Next I explore what is known about neural communication, cortical networks, and specifically cortical networks underlying working memory. I then turn to the design of a novel verbal working memory paradigm specifically designed to study cortical networks with connectivity analyses. Finally, in Chapters 2-6 I explore these concepts within the context of my own work.

1.2 Theoretical Background

Task-relevant information is temporarily kept in an active state through active maintenance processes, collectively referred to as working memory (WM). Since the time of Baddeley's influential WM model (Baddeley 1986), cortical and subcortical regions have been thought to be involved in both control (i.e. Baddeley's central executive) and storage operations (i.e. Baddeley's two storage subsystems). However, recent work suggests there is no neural evidence for such dedicated storage buffers as Baddeley's model proposes (Postle 2006; D'Esposito 2007). Rather than considering "storage" as a passive receptacle capable of holding information, recent WM models propose that information is maintained or "stored" by the repeated reactivation of the cortical regions involved in the initial perception of the task-relevant information, the so-called emergent-property view (Postle 2006). The emergent-property view is similar to models that propose that WM is not a separate system but the subset of long-term memory representations that are currently in the focus of attention (Anderson 1983; Cowan 1995; Oberauer 2002; Ruchkin et al. 2003). One major criticism of these activated long-term memory models is that they do not easily account for how the ordinal position of items is flexibly remembered in WM, as WM allows for the temporary retention of

information in any configuration. The emergent-property view improves on long-term activated models by postulating that information is encoded in multiple ways such that when a memory is retrieved from long-term memory multiple representations of the memory are reactivated (visual, auditory, etc.). Because a verbal memory code is known to be an efficient way of remembering serial order (O'Connor & Hermelin 1972, 1973; Glenberg & Fernandez 1988), the emergent-property view asserts that WM is achieved by first activating long-term representations and then repeatedly cycling through the verbally coded representation of these items via speech production systems (Page & Norris 1998). In other words, the emergent-property view asserts that task-relevant representations are "stored" through the action of covert articulatory rehearsal. Rehearsal is one mechanism by which transient representations can be reactivated and is defined as the repeated selection of, or the repeated attention to, relevant representations (Curtis & D'Esposito 2003).

1.3 Individual Cortical Areas Supporting Verbal Task-Relevant Information

Therefore, the process of maintaining verbal task-relevant information can be thought to involve two types of regions: regions involved in control operations versus regions involved in storage operations. Control operations may involve processes such as the identification and selection of relevant information and the assembly and initial execution of an articulatory rehearsal program (in situations with verbal information). As explained in detail above, storage operations are now thought to be where the actual task-relevant information is rehearsed.

As mentioned, rehearsal is proposed to be initiated by control processes. While many verbal WM studies implicate the inferior frontal gyrus (IFG; Brodmann areas (BA) 44/45 or "Broca's area") in a rehearsal circuit (Paulesu et al. 1993; Awh et al. 1996), it is unclear if the region is contributing to storage of the information in some way (i.e. storing motor plans), or is only needed for control processes in order to initiate the rehearsal process in other regions. Similarly, many studies implicate the middle frontal gyrus (MFG, BA 9/46) in the maintenance of task-relevant information (Fuster & Alexander 1971; Kubota & Niki 1971), however, the exact role of the region in maintenance has been heavily debated. While some models of MFG function emphasize a storage role (Funahashi et al 1993; D'Esposito et al. 2000; Constantinidis et al. 2001), other models emphasize its role in exerting top-down control over the posterior cortical regions that store the task-relevant information (D'Esposito et al. 2000; Miller & Cohen 2001; Sakai et al. 2002). Superior parietal lobule (SPL, BA 7) has been implicated as being the phonological store (Smith et al. 1995; Smith et al. 1996; Awh et al. 1996), while others have instead argued for a more top-down role (e.g. directing attention) in verbal WM tasks (Becker et al. 1999). Recent evidence suggests that Sylvian-parietal-temporal junction (area Spt) is critical for verbal WM serving as an auditory-motor interface, associating verbal information with the motor codes to produce them (Buchsbaum et al. 2005; Buchsbaum & D'Esposito 2008). While somewhat less debated, it is

thought that superior temporal sulcus/gyrus (STG/STS) contains the perceptual (echoic) memory stores of the rehearsed verbal items (Buchsbaum et al. 2005), the cerebellum compares the output of subvocal articulation with the contents of the phonological store (Desmond et al. 1997; Chen & Desmond 2005), and premotor (PM, BA 6) areas are thought to actually generate the motor plans and codes.

1.4 Mechanisms of Neural Communication

Anatomically, excitatory neurons have long-range projections, while inhibitory neurons have short-range projections. Ascending or feed-forward cortico-cortical projections are generally thought to originate in superficial layers of cortex (layer 2/3) and terminate in superficial and deep layers of cortex (layers 2/3 & 4), while descending or feed-backward cortico-cortical projections are generally thought to originate in deeper layers of cortex (layers 5 & 6) and project to superficial layers of cortex (layer 2/3) (Douglas & Martin 2004).

However, much less is known about the mechanism of communication between cortical areas. The traditional model of long range cortico-cortical communication states that neurons send messages down their axons while receiving groups of neurons integrate this information and modulate their firing based on its contents. Recently, a new theory known as "communication-through-coherence" has gained popularity. Specifically, the theory states that only coherently oscillating neuronal groups can communicate (Fries 2005). Recent experimental evidence has been found which not only supports this hypothesis (Fries 2005; Varela et al. 2001), but also suggests at least two consistent findings. One consistent finding is that disparate regions seem to have synchronous oscillations in the beta frequency range (Brovelli et al. 2004; Lachaux et al. 2005; Tallon-Baudry et al. 2001; Tallon-Baudry et al. 2004). The second standard finding is that the temporal windows of synchronous activity between regions generally lasts 50-300ms (Varela et al. 2001). However, it should be noted that neither has been consistently and reliably shown in a higher-level cognitive task, such as in a working memory paradigm.

1.5 Cortical Networks and Working Memory

It is becoming clear that distributed cortical networks are required for complex cognition, however, the available methods to study these networks in behaving animals and humans are technically difficult and are therefore rarely utilized. Despite this, there is some strong evidence to suggest that the prefrontal cortex (PFC) exerts top-down control over posterior sensory regions that maintain task-relevant information. Specifically, by transiently lesioning the PFC through cooling in monkeys, it was revealed that neural spiking was attenuated in the inferotemporal cortex during a delayed-match-to-sample task (Fuster et al. 1985). A second study that separated bottom-up sensory signals from top-down signals utilizing a posterior split-brain procedure in monkeys, found that PFC neurons were

able to reactivate object-selective representations in inferotemporal cortex (Tomita et al. 1999). In humans, it was found that when patients with PFC lesions were completing delayed-match-to-sample tasks that distractors during the delay period led to larger event-related potentials in posterior cortex, relative to control subjects (Chao & Knight 1998). These results all support a role of the PFC in suppressing behaviorally irrelevant representations.

A simpler way (although still technically challenging) to study cortical networks than cooling or lesion studies are connectivity analyses in fMRI. Generally these analyses are divided into two types, functional and effective connectivity. Functional connectivity is defined as the "temporal correlations between remote neurophysiological events", while effective connectivity is defined as "the influence one neural system exerts over another" (Friston 1994). However, these methods have proven particularly challenging to apply to working memory tasks due to the low-pass filtering properties of the functional magnetic resonance imaging (fMRI) blood oxygen level dependent (BOLD) signal which leads to peak activity 4-6 seconds after the onset of neural activity. Specifically, while the goal of most WM studies is to investigate cortical activity during the delay period (when the task-relevant information is being maintained and manipulated), the delay period is always preceded by an encoding period. Therefore, activity during the encoding period can interfere with the activity of the delay period, which in general only last 10-15 seconds in duration. To overcome this difficulty, a special functional connectivity technique was developed specifically to measure the individual cognitive components of WM tasks: beta-series correlation (Rissman et al. 2004). Essentially each period of a WM task (encoding, delay, retrieval) is modeled with the traditional general linear model and the resulting parameter estimates (beta values) within each period are correlated across trials. While this technique has led to some extremely important insights concerning connectivity in WM, there still are some questions and concerns about the technique. For example, it is not clear how computing correlations on beta values that summarize many seconds of activity relate to correlations directly on fMRI BOLD time courses.

Due to some of these reasons, only a few studies have provided direct evidence that the commonly described distributed cortical regions found during the maintenance of task-relevant information are actually communicating with each other with functional connectivity analyses (Buchsbaum et al. 2005; Narayanan et al. 2005; Fiebach et al. 2006; Gruber et al. 2007; Woodward et al. 2006). Interestingly, two verbal WM studies have revealed evidence for separate ventral and dorsal processing streams in the auditory association cortex (Buchsbaum et al. 2005; Narayanan et al. 2005). Specifically, IFG was more correlated with STG/STS ("ventral stream"), while MFG was more correlated with area Spt, PM, and motor regions ("dorsal stream"). Strikingly, this mirrors neuroanatomical studies in monkeys that revealed neurons in the anterior portion of STG projecting to IFG and neurons in posterior STG projecting to MFG (Romanski et al. 1999; Romanski 2004; Scott & Johnsrude 2003). Relative to functional connectivity analyses, there are even fewer studies implementing effective connectivity analyses and none that

specifically investigate WM. However, there have been some studies investigating the PFC in cortical networks that may relate to WM. Specifically, in a visuomotor mapping task, Granger causality revealed a top-down influence from the PFC to parietal cortex (Roebroeck et al. 2005) and in a visual attention task the analysis demonstrated a top-down influence of the frontal eye fields and intraparietal sulcus on visual occipital cortex. Additionally, in a speeded-processing task Granger causality revealed that the PFC exerted more directed influences over other cortical areas in slower than faster individuals (Rypma et al. 2006). In summary, there is little evidence of cortical networks subserving human cognitive behavior and even less known about cortical networks specifically subserving WM, primarily due to the technical challenges of the available methods and analyses.

1.6 Verbal Working Memory Task Optimized for Connectivity

While most fMRI studies are designed to optimally investigate univariate activity, very few fMRI studies are specifically designed for connectivity analyses. To do so required several innovations to typical fMRI WM tasks. As necessitated by the sluggish BOLD signal that is measured with fMRI (Henson 2006), we developed a WM paradigm with extremely long delay periods (45 seconds) to ensure that activity during the delay period was not contaminated with activity from the encoding period. To keep subjects behaviorally engaged over these long delay periods we used repeating visual pacing cues to prompt subjects when to subvocally rehearse, resulting in long blocks of highly consistent maintenance rehearsal activity. Furthermore, we used a high-temporal resolution fMRI protocol to increase the number of data-points that can be used in connectivity analyses. Since language is often lateralized to the left hemisphere (approximately 95% of the time in right handed people; Knecht et al. 2000), we only collected fMRI data from the left hemisphere. This allowed us to achieve a repetition time (TR) of 800ms, much faster than the average TR of 2 seconds employed in most fMRI studies. These long blocks of pure maintenance rehearsal activity together with the high temporal resolution fMRI protocol should provide more than enough data-points to ensure adequate statistical power for various connectivity techniques.

1.7 Experimental Overview

The first study (Chapter 2) was therefore specifically designed to study connectivity during the delay period of a verbal WM task. While this study ultimately gave us counterintuitive functional connectivity results, we realized that by using visual pacing cues to prompt rehearsal, we could manipulate subvocal rehearsal rate. Therefore, in the second study we used the same basic design (with long 45 second delay periods) except that we manipulated both memory load and rehearsal rate and quantified the effects of the two factors in individual cortical areas (Chapter 3). Subsequently, the same dataset was then analyzed with a functional connectivity analysis, which produced a counterintuitive result that was then examined in

complete detail (Chapter 4) and helps explain the previous counterintuitive functional connectivity result (from Chapter 2). The results of the second study directly led to a third study, which involved finding substitute conditions for the encoding and delay periods of verbal WM tasks where signal variability could be maximized so that connectivity could be investigated (Chapter 5).

2

TEMPORAL DISSOCIATION OF CONTROL AND STORAGE/REHEARSAL REGIONS

2.1 Introduction

Behavioral studies of verbal WM have provided evidence that there are two stages involved in WM tasks: an effortful first stage followed by an automatized second stage (Naveh-Benjamin & Jonides 1984; Aldridge et al. 1987; Greene 1987; Phaf & Wolters 1993). The first stage is thought to engage control processes such as the identification and selection of the relevant information, followed by the assembly and initial execution of an articulatory rehearsal program (in situations with verbal information). By contrast, the second stage requires less attention as the rehearsal becomes automatized and the motor programs are repeatedly executed. If these two behavioral stages are also dissociable and distinct at the neural level, this model predicts some cortical areas will be active at the start of rehearsal and then decline with time, while other cortical areas will remain constantly active throughout the duration of rehearsal.

While a few fMRI studies have found some evidence supporting this model (Chein & Fiez 2001; Buchsbaum et al. 2005), they did not precisely control the subject's behavior making it difficult to interpret their findings. For example, it is not known if a region showing decreasing activity over the delay period is because subjects have encoded the items in the first few seconds and have stopped rehearsing, or because the region is truly not needed as rehearsal continues (i.e. only part of stage one). Moreover, since it takes 12-16 seconds for fMRI BOLD activity to return to baseline (Henson 2006), many studies have utilized delay periods that are too short to discern if activity in a region has returned to baseline.

We propose that cortical areas involved in maintaining task-relevant verbal information can be broadly dissociated via time into cortical regions involved in

control processes from those involved in storage/rehearsal. To test this hypothesis, a WM task that allows precise control over subvocal rehearsal rates, combined with very long delay periods and a scanning acquisition with high temporal resolution, will be utilized. This experimental paradigm will be explored with fMRI experiments in young, healthy participants. We predict that in order to actively maintain task-relevant verbal information MFG and SPL will be involved in processes that will be required at times when high control is needed (at the start of the delay period and near retrieval), while IFG, PM and area Spt will be involved in storage/rehearsal processes that will persist from the encoding period all the way through the delay period.

2.2 Methods

2.2.1 Subjects

Twenty-seven subjects gave informed written consent according to procedures approved by the University of California and participated in the study. All were right-handed, native English speakers, had normal or corrected-to-normal vision and normal hearing. All subjects were healthy with no neurological or psychiatric disease. One subject was eliminated due to excessive head movement (>3mm in any single run) and one subject was eliminated for poor behavior performance (below chance accuracy for order probe). This left a total of twenty-five subjects (14 females; age: 18-31, mean: 22.2).

2.2.2 Experimental Stimuli

Letters were pseudorandomly chosen from a pool of 19 letters (b,c,d,f,g,h,j,k,l,m,n,p,q,r,s,t,v,x,z) with the only constraint being that a letter could not be repeated within the same trial. Vowels (a,e,i,o,u) and the letter "y" were removed so subjects could not chunk letter sequences into words. The letter "w" was removed because it has two syllables. Letters were converted into a female voice for auditory presentation with text-to-speech software (Nuance Speechify, Burlington, MA).

2.2.3 fMRI Task

Memory load (3,5-letters) was manipulated over long 45 second delay periods (Figure 2.1). Specifically, during encoding subjects were simultaneously visually and auditorily presented with either 3 (sub-span) or 5 (above-span) letters at a rate of one letter/per second. During a 45 second delay period, subjects were required to subvocally rehearse one letter, in the original order, with each visual pacing cue (flashing gray circle). Each pacing cue was visually presented for 400msec and the interval between pacing circles was 300msec, resulting in a rehearsal rate of 1.4Hz (1 rehearsal every 400+300=700msec). This rate was chosen based on free overt rehearsal pilot data. Critically, to ensure subjects were subvocally rehearsing one

letter with each visual pacing cue through the entire delay period, at the end of each trial subjects were prompted with an order probe (red circle) to verbally report which letter they were on. Because the correct answer depended on the number of rehearsals over a fixed time period (delay period), the correct answer was randomly varied by slightly altering the number of rehearsals over the delay period (either 59, 60, or 61 rehearsals). Therefore, subjects could not use a simple rule to answer the order probe correctly (e.g. always the second letter). After the order probe subjects were prompted with a recall probe (green triangle) to verbally report the original list of letters in order. Verbal answers for the order and recall probes were digitally recorded and manually scored after the experiment.

In a control task, instead of letters subjects heard noise (same letters used in real trials except played backwards) followed by a 45 second period where they were instructed to observe the flashing gray circles without subvocally rehearsing. At the end of the trial subjects were instructed to say "square" as soon as they saw the blue square probe appear. To ensure subjects remained attentive during these long periods, catch trials were included where the blue square appeared before the full 45 seconds so that subjects never knew when they would have to answer. In order to optimize signal-to-noise, catch trials were grouped in order to keep non-task periods the same duration as task trials. Therefore, two catch trials with 17 second delay periods were presented sequentially or catch trials with a 10 second and 24 second delay periods were presented sequentially. One group of catch trials was pseudorandomly chosen for each run with the only constraint being that there were an equal number of catch trials across all 10 runs.

Each fMRI session contained ten runs that lasted approximately nine minutes each. Each run contained two 5-lettter task trials, two 3-letter task trials, two control trials, and two catch trials. Task and control/catch trials were presented in a pseudorandom order with the constraint that the condition types alternate. In total, each fMRI session contained 40 task trials, 20 control trials, and 20 catch trials.

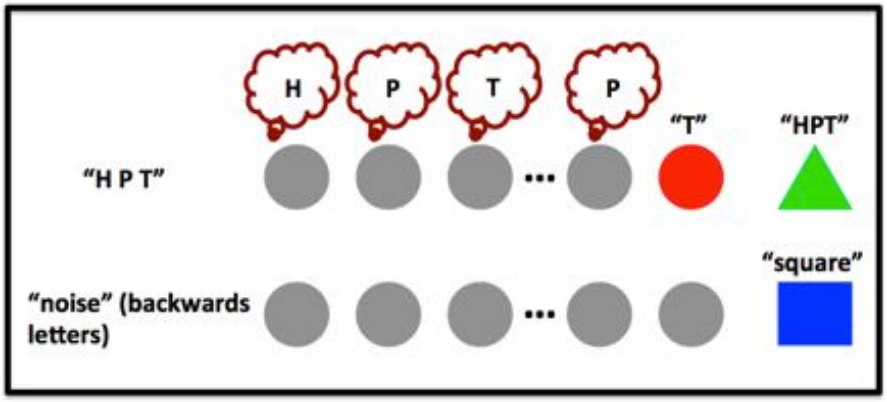

Figure 2.1: fMRI task design. Subjects (n=25) were visually and auditorily presented with either three (below span) or five (above span) letters that they were instructed to maintain over a 45 second delay period. During the delay period a repeating visual pacing cue prompted subjects to subvocally rehearse one letter, in the original order. To ensure subjects were subvocally rehearsing one letter with each pacing circle, an order probe (red circle) prompted subjects to verbally report which letter they were on. Immediately after, a recall probe (green triangle) appeared which prompted subjects to verbally report the original list of letters, in order, to ensure they remembered the original information they were supposed to. For control trials, subjects were instructed to listen to the noise during encoding before attending to the visual pacing cues without subvocally rehearsing, and verbally saying "square" as soon as they saw a blue square. To ensure subjects paid attention during control trials, catch trials were included that were identical to control trials except with shortened delay periods so that subjects never knew when control trials would end.

2.2.4 Functional Magnetic Resonance Imaging

2.2.4.1 Acquisition

fMRI data will be collected on a Siemens whole-body 3.0 Tesla magnet (Berlin/Munich, Germany) at the UC Berkeley Brain Imaging Center. Functional volumes will be acquired with an echo-planar imaging (EPI) pulse sequence (TR=801ms; TE= 20ms; FA=20°; FOV=183mm; matrix: 76 x 76; in-plane resolution: 2.4mm x 2.4mm). Each functional volume consists of 17 contiguous left hemisphere 3mm thick sagittal slices separated by a 0.5mm interslice gap set to cover lateral temporal cortex and extending as far medially as possible using AutoAlign Head (Siemens™). Using a 3D Flash sequence and an automatic segmentation algorithm, AutoAlign performs slice positioning in an automatic and reproducible way on each individual participant once a user has manually positioned the desired slices on an atlas brain. Additionally, high-resolution structural MP Flash T1 weighted images were acquired for precise anatomical localization.

Presentation software (Neurobehavioral Systems, Albany, CA) was used for auditory and visual stimulus delivery. Auditory stimuli were delivered via MR-Confon headphones. Visual stimuli were presented via a liquid crystal display projector

(Avotec, FL) which displayed images on a screen located in the center of the scanner bore. Subjects viewed the screen by looking at a mirror mounted on the radiofrequency coil. Overt responses in the fMRI scanner were recorded with a dual-channel, noise cancelling fiber optical microphone system and noise reduction software (Optoacoustics Ltd., Or-Yehuda, Israel).

2.2.4.2 Pre-Processing

MRI data were converted to NifTI format. Functional data were realigned to the first acquired volume using the AFNI (Cox 1996) program 3dVolreg and spatially smoothed with a 5-mm full-width at half-maximum Gaussian kernel. One subject was removed for excessive head motion (>3mm within a single run). All subsequent statistical analyses were performed on these realigned and smoothed images.

In order to view the functional results on the group anatomy of the same subjects who generated them, a study specific group template was created with the program Advanced Normalization Tools (ANTS: http://www.picsl.upenn.edu/ANTS/). In an iterative fashion, each subject's high-resolution anatomical scan was nonlinearly warped (symmetric normalization algorithm, SyN) into registration with one another, and a group mean image was generated. The study specific group template was then normalized to Montreal Neurological Institute (MNI) space with a 12-parameter affine transformation. Each subject's high-resolution anatomical scan was nonlinearly normalized to this study specific group template in MNI space utilizing the SyN algorithm (ANTS). These warping parameters were then applied to the native space EPI data/statistical maps as needed to transform them into normalized template space. The study specific group template and group functional data were converted to surface maps for visualization purposes (SUMA: http://afni.nimh.nih.gov/afni/suma).

2.2.4.3 Statistical Analyses

Regression modeling within each subject was performed with the AFNI program 3dDeconvolve. Block regressors were generated by convolving a boxcar function with an incomplete gamma function. For all trials, encoding periods were modeled as blocks with durations matching stimulus presentation lengths (three second block for 3-letter trials, five second block for 5-letter trials). The delay period of every task, control, and catch trial were modeled as blocks. To reduce collinearity between encoding and delay period regressors, a two second gap was introduced between regressors. For analyses involving different phases of the delay period, the delay period was divided into three separate 14 second segments. Therefore early delay was modeled as a block 2-16s into the delay period, mid delay as a block 16-30s into the delay period, and late delay as a block 30-44s into the delay period. Order probe and recall probe periods were separately modeled as gamma functions. For each scanning run a set of nuisance regressors (constant term plus linear, quadratic, and polynomial terms) were included to remove low frequency noise. Head movement was also regressed out of the time series data. Statistical contrasts

at the single-subject level were carried out in native space and were computed as weighted sums of the estimated beta coefficients divided by an estimate of the standard error, resulting in a *t*-statistic. Each subject's *t*-statistic map was normalized to group template space. Random effects group analyses were computed on *t*-values instead of beta coefficients because *t*-values are more normally distributed at the group level (Thirion et al. 2007). Left-hemisphere group results were corrected for multiple comparisons by thresholding to $q<0.05$ using the False Discovery Rate (FDR) method.

2.2.4.3 fMRI BOLD Correlation Analysis

To analyze the delay period, 68 second blocks including encoding, delay and retrieval periods were extracted from the longer runs of data. Area Spt regions of interest (ROI) were used to extract time series from each extracted block. Critically, area Spt ROIs were derived from the encoding period (from the contrast [$TASK_{ALL}$ - CONTROL]) and therefore were not biased in any way toward activity during the delay period. At the single-subject level, multiple linear regression (3dDeconvolve) was carried with covariates for the seed ROI (area Spt) time series, head movement, and baseline detrending for each extracted block (constant plus linear term) all included in the regression model. r^2 values were converted to correlation coefficient r values before being transformed into a more normal distribution with Fisher's Z transform. Data was normalized to group template space and random effects group analyses were performed.

2.2.4.4 Beta-series Correlation Analysis

To specifically investigate connectivity during the different cognitive stages of a WM task, a beta-series correlation analysis was performed (Rissman et al. 2004). The same general linear model as described above was modified to compute a parameter estimate (beta value) for every trial. Beta values were then sorted according to the stage they belonged to (encoding, delay, retrieval) and then concatenated together along the time dimension, forming a time series. Area Spt ROIs were then used to extract a beta-series time series from this data and entered as a covariate into a regression model (3dDeconvolve). r^2 values were converted to correlation coefficient r values before being transformed into a more normal distribution with Fisher's Z transform. Data was normalized to group template space and random effects group analyses were performed.

2.2.4.5 Analysis of Behavioral Data

fMRI behavioral data was scored for the order probe (red circle) and recall probe (green triangle). Order probe was classified correct if the single correct letter was reported. If the letter identity was incorrect but the letter order was correct in the recall portion, trial was scored as correct (but incorrect in recall scoring). Recall data was scored on a letter-by-letter basis requiring both letter identity and letter

position to be correct to be classified as correct. The mean value of each condition was computed for each subject and then used to compute the group mean.

2.3 Results

2.3.1 fMRI Behavioral Data

Analysis of order probe (red circle) behavioral data revealed that the decrease in accuracy for 3-letter when compared to 5-letter was not significant (p=0.12,df=24, permutation paired t-test) (Figure 2.2). However, there was a significant load effect evident between 3 and 5-letters with the recall probe (green triangle) behavioral data (p<0.0001,df=24, permutation paired t-test).

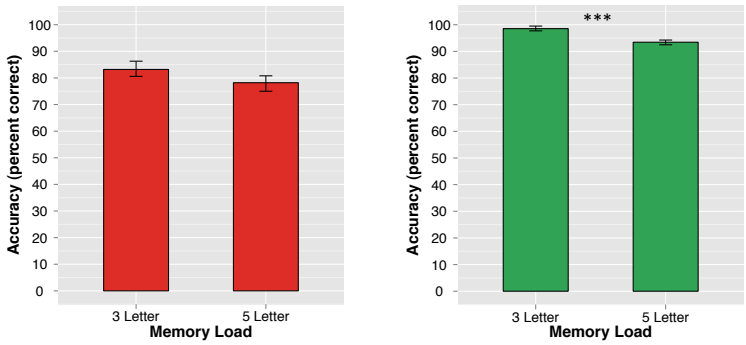

Figure 2.2: fMRI behavioral results. Order probe (red circle) accuracy on left, recall probe (green triangle) accuracy on right. Results show that as memory load increased, accuracy decreased for both the order probe and the recall probe, however, the decrease in order probe accuracy was not statistically significant while the decrease in recall probe accuracy was significant. Data plotted are group means. Error bars represent bootstrapped within-subject 95% confidence intervals. ***p<0.0001.

2.3.2 Functional Magnetic Resonance Imaging Results

To investigate how the activity profiles of different cortical regions varied through time, trials were divided into encoding, delay (early: 2-16 seconds, mid: 16-30 seconds, late: 30-44 seconds) and retrieval (recall probe). Results revealed that during the encoding period MFG (and inferior frontal sulcus), IFG, PM, area Spt and SPL were active (Figure 2.3). However, in early delay mainly IFG, PM and area Spt were active, with only a small area of SPL remaining active. By mid delay these same regions with more surrounding areas of cortex remained active. By the end of the delay period, MFG, frontal polar and SPL were active while IFG, PM and area Spt continued to be active. During retrieval mainly STG/STS was active.

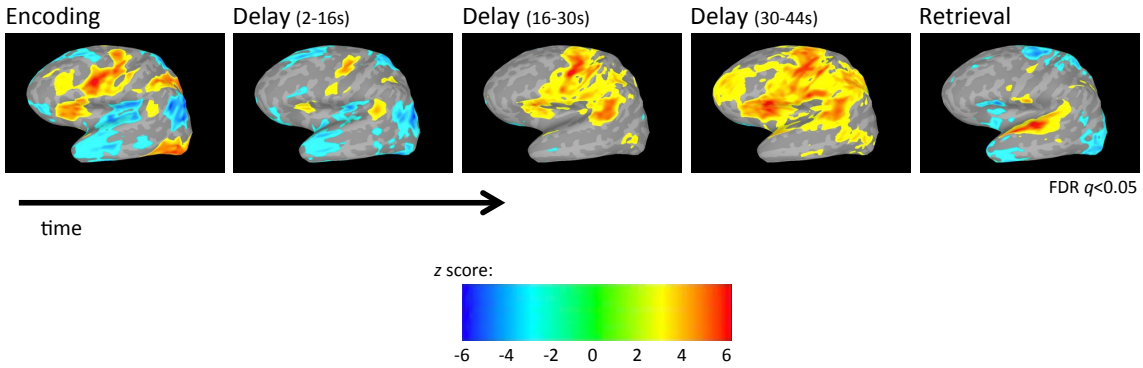

Figure 2.3: fMRI results through time. Activity estimates (*t*-values) for encoding, delay (early, mid, and late) and retrieval time periods (recall probe) were entered into a paired *t*-test for task (3 and 5-letter) versus control. Results show that during the encoding period MFG, IFG, PM, area Spt and SPL were active. However, by early delay (2-16 seconds) only IFG, PM and area Spt (and a small region of SPL) remained active. By mid delay (16-30 seconds) these same regions with more surrounding cortex remained active. By the end of the delay period (30-44 seconds), MFG, frontal polar and SPL were active while IFG, PM and area Spt continued to be active. During retrieval mainly STG/STS was active. Data from left hemisphere; data shown are *z*-scores thresholded at FDR $q<0.05$ for the five time periods in order to compare changes across time.

2.3.3 Connectivity Results

To determine if the active regions (or any other regions) from the univariate analysis formed a network, we performed a correlation analysis on the fMRI BOLD time series as well as a functional connectivity analysis specifically designed for WM studies, beta-series correlation (Rissman et al. 2004). For each subject, an area Spt ROI time series was used as the "seed" time series and correlated with a time series from every voxel in the brain. Area Spt was used as the seed region because of its central importance in verbal working memory (Hickok et al. 2003; Buchsbaum et al. 2005; Hickok et al. 2009) and for comparison to previous verbal working memory functional connectivity studies that also used area Spt as a seed region (Buchsbaum et al. 2005). Results revealed that at a conventional voxelwise statistical threshold (FDR $q<0.05$) neither analysis demonstrated any regions significantly correlated with area Spt. At a low threshold ($p<0.05$) some regions showed significant connectivity, but only in the beta-series correlation analysis, including IFG, PM and SPL. None of the task-active regions were significant in the fMRI BOLD correlation analysis. However, due to the issue of multiple comparisons in fMRI (thousands of voxels) a threshold this low is not statistically valid. For the fMRI BOLD correlation analysis 68 second task blocks were used that included encoding, delay and retrieval periods to include as many time-points in the analysis as possible. The same analysis performed on 45 second task blocks only including the delay period gave similar results.

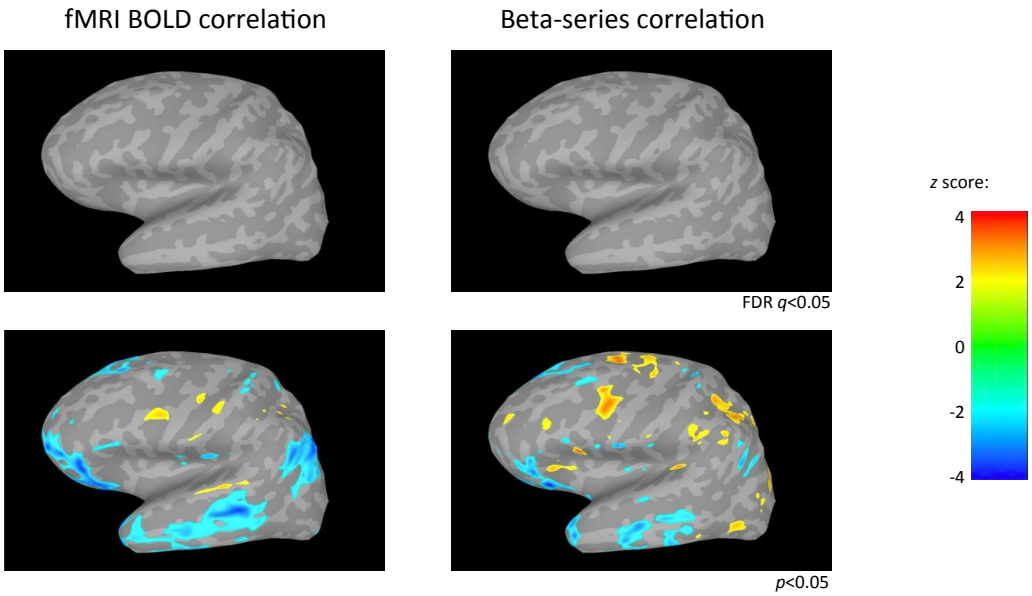

Figure 2.4: Functional connectivity results. An area Spt seed was used in an fMRI BOLD correlation analysis (left) and a beta-series correlation analysis (right). Correlation values were Fisher z transformed and submitted to a paired *t*-test to determine connectivity differences between task (3 and 5-letter) and control. At a typical conventional voxelwise statistical threshold (FDR $q<0.05$) no regions demonstrated significant connectivity with area Spt. At a lower threshold ($p<0.05$) there seems to be a few task active regions (IFG, PM, SPL) that demonstrated connectivity with area Spt, but only in the beta-series correlation analysis. fMRI BOLD correlation analysis included 68 second task blocks that included encoding, delay and retrieval periods. Beta-series correlation analysis included only the delay period. Data from left hemisphere; data shown are *z*-scores thresholded at FDR $q<0.05$ and uncorrected $p<0.05$.

2.4 Discussion

In this fMRI study we attempted to dissociate control and storage/rehearsal regions by enforcing subvocal rehearsal over long delay periods. We demonstrated behaviorally that subjects were successfully rehearsing throughout the long delay periods and that MFG and SPL areas were only active during encoding and near the end of the delay period, while IFG, PM and area Spt showed sustained activation throughout encoding and the entire delay period. Functional connectivity analyses did not produce any statistically valid results.

2.4.1 Control Regions

Our results demonstrate that MFG and SPL areas are control regions since they were only active during encoding and during the end of the delay period, times when high control is required. High control is likely required during encoding as the task-relevant information is being identified and selected, before articulatory plans are

repeatedly executed. The end of the delay period may also be a period of high control as subjects have been rehearsing the information for a long time and require extra attention to stay on task. Additionally, subjects may be anticipating the difficult retrieval tasks (order and recall probes) at the end of trials and may be increasing the amount of attention they devote to the task.

While many studies have implicated the MFG in the maintenance of task-relevant information (Fuster & Alexander 1971; Kubota & Niki 1971), the region's exact role in maintenance has been debated. While early models emphasized MFG's role in the storage of task-relevant information (Funahashi et al. 1993; D'Esposito et al. 2000; Constantinidis et al. 2001), the MFG is now thought to be involved in exerting top-down control over the posterior cortical regions that store task-relevant information (D'Esposito et al. 2000; Miller & Cohen 2001; Sakai et al. 2002). Our results are in agreement with these later theories and findings and point to the MFG being involved in top-down control. Similarly, early on SPL was implicated as being the phonological store in the maintenance of task-relevant information (Smith et al. 1995; Smith et al. 1996; Awh et al. 1996), but recently others have instead argued for a more top-down control role (e.g. directing attention) during verbal WM tasks (Becker et al. 1999). Our results agree with these later findings and suggest that SPL is not likely involved in storage as it is not consistently active throughout the delay period.

2.4.2 Storage/Rehearsal Regions

In contrast, our results demonstrate that IFG, PM and area Spt are storage/rehearsal regions that are active throughout encoding and the long delay periods. This seems to implicate these areas in the "storage" or rehearsal of task-relevant information in verbal working memory.

While many verbal WM studies implicate the IFG in a rehearsal circuit (Paulesu et al. 1993; Awh et al. 1996), the temporal pattern of activity of the region is not typically reported. Thus, it is unclear if during the repeated rehearsals that occur during the maintenance of task-relevant information the IFG is involved in each instance of a rehearsal, implying it is contributing to storage of the information in some way (i.e. storing motor plans), or it is only needed for control processes in order to initiate the rehearsal process in other regions. A recent study involving the execution of overlearned action plans did not find sustained activity in IFG, instead only finding activity in the region at the start and end of the functional segments of the hierarchical action plans (Koechlin & Jubault 2006). This evidence seems to implicate IFG in more of a control role. Our results seem to be at odds with this last study, instead implicating IFG in more of a storage/rehearsal region that is required during each rehearsal of information. However, the way in which we discouraged chunking of our stimuli, as well as forced the rehearsal of each item separately at a set rate, might prevent subjects from creating hierarchical action plans leading to the contrasting results.

While it was first believed that the phonological store was thought to be SPL, recent evidence suggests that area Spt is the phonological store, as this area is thought to serve as an auditory-motor interface, associating verbal information with the motor codes to produce them (Buchsbaum et al. 2005; Buchsbaum & D'Esposito 2008). Our results agree with this as area Spt was active throughout the long delay periods. PM areas are also thought to be involved in storage/rehearsal as these areas are thought to actually generate the motor codes. Our results agree with these findings.

2.4.3 Connectivity

Considering this task was specifically designed to investigate connectivity during the delay period (long delay periods with constant behavior, high temporal resolution by imaging only the left hemisphere) and given the robust univariate activity results, it was surprising that both connectivity analyses gave null results. This issue was examined in detail with a very similar design paradigm in Chapter 4.

3

THE EFFECT OF MEMORY LOAD AND REHEARSAL RATE ON VERBAL WORKING MEMORY CIRCUITRY

3.1 Introduction

Over the years, neuroimaging studies have used memory load manipulations to investigate various processes within WM. Increasing the memory load is believed to increase the amount of task-relevant information that must be transiently remembered and is thought to increase general cognitive demands. These manipulations seem to activate numerous cortical regions, including those thought to be involved in storage/rehearsal such as the IFG, PM and area Spt (i.e. the "phonological loop"), as well as control regions such as MFG and SPL (Rypma et al. 1999; Zarahn et al. 2005). Therefore, memory load manipulations seem to engage many different cognitive processes and cortical areas, and the contribution of each region to verbal WM is unclear.

While many studies have manipulated memory load, neuroimaging studies have only indirectly manipulated rehearsal (through articulatory suppression, etc.) and no study has explicitly manipulated subvocal rehearsal rate in the context of a

memory load. Increasing rehearsal rate may increase demands on motor planning, selection of motor plans, initial execution of motor programs, and the repeated selection or attention to task-relevant representations. Therefore, it is unknown if control areas thought to be involved in verbal WM, such as MFG and SPL, will be sensitive to manipulations in rehearsal rate. It is also unknown if the various cortical areas involved in verbal WM can be dissociated based on orthogonal manipulations of memory load and subvocal rehearsal rate. Dissociating cortical areas on these parameters may lead to insights about the processes being performed in the various regions implicated in verbal WM.

Furthermore, the two task manipulations may be related behaviorally. Specifically, manipulations in memory load may be behaviorally confounded with rehearsal rate. While this issue has never been directly studied, a few behavioral studies revealed that recall increases linearly with rehearsal rate (Hulme et al. 1984; Cowan et al. 1998; Dasi et al. 2008), suggesting that with a higher memory load subjects may strategically employ a faster rehearsal rate to maintain more task-relevant information. It is currently unclear how this potential confound may impact neuroimaging studies, but it may help explain why memory load effects in cortical areas are so variable and inconsistent (Postle et al. 1999; Rypma et al. 1999a,b; Rypma et al. 2002; Buchsbaum et al. 2005; Narayanan et al. 2005; Zarahn et al. 2005).

Therefore, in order to 1) investigate if MFG and SPL areas that show memory load effects also show rehearsal rate effects, 2) dissociate some of the component processes of verbal WM, and 3) investigate the confound of rehearsal rate and memory load, we orthogonally manipulated rehearsal rate and memory load over long delay periods in a maintenance rehearsal verbal working memory task.

In general, we predict that manipulations in rehearsal rate will primarily affect regions thought to be involved in storage/rehearsal such as IFG, PM and area Spt. We predict that memory load manipulations at all loads will affect these regions since more attention per item will be required as the memory load increases. In contrast, we predict that only once a certain memory load threshold is exceeded will control regions be recruited, such as MFG and SPL. Finally, since we believe that rehearsal rate and memory load will dissociate processes within verbal WM, we do not expect any regions to exhibit a rehearsal rate by memory load interaction.

3.2 Methods

3.2.1 Subjects

Twenty-eight subjects gave informed written consent according to procedures approved by the University of California and participated in the study. All were right-handed, native English speakers, had normal or corrected-to-normal vision and normal hearing. All subjects were healthy with no neurological or psychiatric

disease. One subject was eliminated due to falling asleep in the scanner and three subjects were eliminated for failing to follow instructions (subvocally rehearsing when instructed not to). This left a total of twenty-four subjects (13 females; age: 18-32, mean: 21.3).

3.2.2 Experimental Stimuli

Letters were pseudorandomly chosen from a pool of 19 letters (b,c,d,f,g,h,j,k,l,m,n,p,q,r,s,t,v,x,z) with the only constraint being that a letter could not be repeated within the same trial. Vowels (a,e,i,o,u) and the letter "y" were removed so subjects could not chunk letter sequences into words. The letter "w" was removed because it has two syllables. Letters were converted into a female voice for auditory presentation with text-to-speech software (Nuance Speechify, Burlington, MA).

3.2.3 Behavioral Task (performed prior to fMRI scanning)

In order to determine the effect of memory load on rehearsal rate, prior to being informed about any details of the fMRI experiment, subjects performed a verbal working memory task. Subjects were instructed: "The goal is to remember the letters in order and say them out loud at the green triangle [recall probe]. To remember the letters, please rehearse the letters out loud starting at the beep." Subjects were instructed to overtly rehearse in a normal speaking voice. During the encoding period, Subjects were simultaneously visually and auditorily presented with either 2, 4, 6, or 8-letters at a rate of one letter/per second. Following the last letter there was a 1 second pause before a 500ms beep sounded which informed subjects to start overtly rehearsing the letters presented to them during encoding. During the 15 second delay period, subjects were instructed to fixate on a white cross-hair displayed on a black background. After the delay period subjects were prompted with a recall probe (green triangle that appeared on the screen) and given four seconds to overtly recall in order as many of the original letters as possible. Overt rehearsal and recall responses were recorded by a digital recorder and subsequently manually transcribed and scored.

Each subject was given a total of five blocks of trials with two minute breaks between blocks. The first block was a practice block that was not scored and the remaining four blocks were test blocks. The first trial of each block was not scored as a matter of practice due to restart confounds. Each block contained eight scored trials, two of each memory load, which were randomly ordered for each subject. Therefore, each subject had a total of eight trials of each memory load.

3.2.4 fMRI Behavioral Task

Memory load (2, 4, 6-letters) and rehearsal rate (0.8, 1.1, 1.4, 1.7, 2.0, 2.3, 2.6Hz) were independently manipulated resulting in a fully crossed 3x7 factorial design (Figure 3.1). Specifically, during encoding subjects were simultaneously visually and

auditorily presented with either 2, 4, or 6-letters at a rate of one letter/per second. During a 45 second delay period, subjects were required to subvocally rehearse the sequence one letter at a time, in the original order, with each visual pacing cue (flashing gray circle). Each pacing cue was visually presented for 300msec while the interval between pacing cues was altered in order to control rehearsal rate. Specifically, subjects were paced to rehearse at 0.8Hz (1 rehearsal/1250msec=0.8Hz), 1.1Hz, 1.4Hz, 1.7Hz, 2.0Hz, 2.3Hz, and 2.6Hz (1 rehearsal/385msec=2.6Hz), rates chosen based on free overt rehearsal pilot data. Critically, to ensure subjects were subvocally rehearsing one letter with each visual pacing cue through the entire delay period, at the end of each trial subjects were prompted with an order probe (red circle) and given two seconds to verbally report the last letter they had subvocally rehearsed. Because the correct answer depended on the number of rehearsals over a fixed time interval, the correct answer varied trial-by-trial both as a function of how many letters subjects were supposed to rehearse as well as the pacing rate, so subjects could not use a simple rule to answer the order probe correctly (e.g. always the second letter). Because the memory load and rehearsal rate were independently and randomly chosen for every trial, the correct answer also randomly varied among all possible letter positions. After the order probe subjects were prompted with a recall probe (green triangle) and given four seconds to verbally report the original list of letters in order. Verbal answers for the order and recall probes were digitally recorded and manually scored after the experiment.

In a control task, instead of letters subjects heard noise (same letters used in real trials except played backwards) that lasted the same duration as letters in real trials followed by a 45 second period where they were instructed to observe the flashing gray circles without subvocally rehearsing. All seven rehearsal rates were presented to each subject. At the end of the trial subjects were given fours seconds to say "square" as soon as they saw the blue square probe appear. To ensure subjects remained attentive during these long periods, catch trials were included where the blue square appeared before the full 45 seconds so that subjects were never aware as to when the trial would end. Delay periods in catch trials were pseudorandomly chosen from a set distribution spanning from 25%-75% of the normal 45 second delay periods (11,13,15,17,18,20,22,23,25,27,29,30,32,34 seconds), with the constraint that once a duration was used it could not be repeated. Control and catch trials were randomly intermixed.

Each fMRI session contained ten runs that lasted approximately eight minutes each. Each run contained an average of four task trials, one control trial, and one catch trial presented in a randomized order. For all trial types, memory load and rehearsal rate were independently and pseudorandomly chosen with the constraint that all conditions had to occur before a condition could be repeated. In total, each fMRI session contained 42 task trials, 14 control trials, and 14 catch trials. Memory load and rehearsal rate were fully crossed in the task condition (3x7=21), resulting in two trials per condition. Due to limited time load and rate were not fully crossed in

control trials, however, over the 14 control trials each rehearsal rate was presented twice.

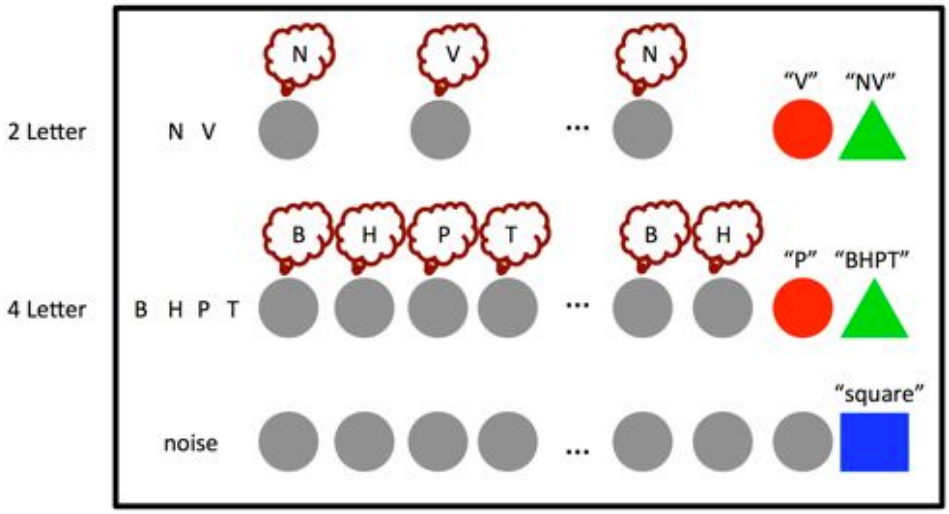

Figure 3.1: fMRI task design. Subjects (n=24) were visually and auditorily presented with either 2, 4, or 6-letters that they were instructed to maintain over a 45 second delay period. During the delay period a repeating visual pacing cue prompted subjects to subvocally rehearse one letter, in the original order. The rehearsal rate at which subjects were paced was varied across seven rates: 0.8, 1.1, 1.4, 1.7, 2.0, 2.3, and 2.6Hz. Therefore, memory load and rehearsal rate were independently varied resulting in a fully crossed 3x7 factorial design. To ensure subjects were subvocally rehearsing one letter with each pacing circle, an order probe (red circle) prompted subjects to verbally report which letter they were on. Immediately after, a recall probe (green triangle) appeared which prompted subjects to verbally report the original list of letters, in order, to ensure they remembered the original information they were supposed to. For control trials, subjects were instructed to listen to the noise during encoding before attending to the visual pacing cues without subvocally rehearsing, and verbally saying "square" as soon as they saw the blue square. To ensure subjects paid attention during control trials, catch trials were included that were identical to control trials except with pseudorandomly shortened delay periods from 11-34 seconds, so that subjects never knew when control trials would end.

3.2.5 Functional Magnetic Resonance Imaging

3.2.5.1 Acquisition

MR data were acquired with a Siemens TIM/Trio 3 Tesla scanner (Berlin/Munich, Germany). Functional data were obtained using a 32-channel radiofrequency head coil and a 2-shot T_2^*-weighted EPI sequence sensitive to BOLD contrast (TR = 2000msec, TE = 25msec, 224mm field of view with a 72x72 matrix size, in-plane resolution 3.1mm x 3.1mm). Each functional volume contained 34 contiguous

3.3mm-thick axial slices separated by a 0.5mm interslice gap acquired in an interleaved fashion. High-resolution whole-brain MP Flash T_1-weighted scans were acquired for anatomical localization.

Presentation software (Neurobehavioral Systems, Albany, CA) was used for auditory and visual stimulus delivery. Auditory stimuli were delivered via MRI-compatible form-fitting foam insert earphones (Sensimetrics, MA). Visual stimuli were presented via a liquid crystal display projector (Avotec, FL), which displayed images on a screen located in the center of the scanner bore. Subjects viewed the screen by looking at a mirror mounted on the radiofrequency coil. Overt responses in the fMRI scanner were recorded with a dual-channel, noise cancelling fiber optical microphone system and noise reduction software (Optoacoustics Ltd., Or-Yehuda, Israel).

3.2.5.2 Pre-Processing

MRI data were converted to NifTI format. Functional data were slice-time corrected, realigned to the first acquired volume using the AFNI (Cox 1996) program 3dVolreg and spatially smoothed with a 5-mm full-width at half-maximum Gaussian kernel. No runs were removed for excessive head motion (>3mm within a single run). All subsequent statistical analyses were performed on these realigned and smoothed images.

In order to view the functional results on the group anatomy of the same subjects who generated them, a study specific group template was created with the program ANTS. In an iterative fashion, each subject's high-resolution anatomical scan was nonlinearly warped (SyN algorithm) into registration with one another, and a group mean image was generated. The study specific group template was then normalized to MNI space with a 12-parameter affine transformation. Each subject's high-resolution anatomical scan was nonlinearly normalized to this study specific group template in MNI space utilizing the SyN algorithm (ANTS). These warping parameters were then applied to the native space EPI data/statistical maps as needed to transform them into normalized template space. The study specific group template and group functional data were converted to surface maps for visualization purposes (SUMA).

3.2.5.3 Statistical Analyses

Regression modeling within each subject was performed with the AFNI program 3dDeconvolve. Block regressors were generated by convolving a boxcar function with an incomplete gamma function. For all trials, encoding periods were modeled as blocks with durations matching stimulus presentation lengths (two second block for 2-letter trial, four second block for 4-letter trial, six second block for 6-letter trial). The delay period of every task, control, and catch trial were also modeled as blocks. Each delay period condition was modeled with a separate regressor ($LOAD_{[2L,4L,6L]}$ x $RATE_{[0.8,1.1,1.4,1.7,2.0,2.3,2.6\ Hz]}$). To reduce collinearity between encoding

and delay period regressors, a two second gap was introduced between the two regressors. Therefore, for analyses involving the entire delay period, a 43-second block regressor was placed beginning two seconds into the delay period. For analyses involving different phases of the delay period, the delay period was divided into three separate 14 second segments. Therefore, the early delay period was modeled as a block 2-16 seconds into the delay period, the middle of the delay period as a block 16-30 seconds into the delay period, and the end of the delay period as a block 30-44 seconds into the delay period. Order probe and recall probe periods were separately modeled as gamma functions. For each scanning run a set of nuisance regressors (constant term plus linear, quadratic, and polynomial terms) were included to remove low frequency noise. Head movement was also regressed out of the time series data. Statistical contrasts at the single-subject level were carried out in native space and were computed as weighted sums of the estimated beta coefficients divided by an estimate of the standard error, resulting in a *t*-statistic. Therefore, for linear trend analyses beta coefficients were used in linear trend contrasts for LOAD (-1,0,+1) and RATE (-1,-0.667,-0.333,0,+0.333,+0.667,+1) at the single-subject level and resulting *t*-statistics were used in further analyses. Each subject's *t*-statistic map was normalized to group template space. Random effects group analyses were computed on *t*-values instead of beta coefficients because *t*-values are more normally distributed at the group level (Thirion et al. 2007). Left-hemisphere group results were corrected for multiple comparisons by thresholding to $q<0.05$ using the FDR method.

3.2.5.4 Region of Interest Definition

To further investigate the effects of memory load and rehearsal rate in cortical areas commonly implicated in verbal working memory, ROI analyses were performed. ROIs for MFG, SPL, IFG, PM, and area Spt were created. IFG was subdivided into anterior (IFG pars operculum: IFGpo, BA 44) and posterior portions (IFG pars triangularis: IFGpt, BA 45) because of evidence that the two subdivisions have both functional (Wagner et al. 2001; Badre & Wagner 2007) and anatomical connectivity (Frey et al. 2008) differences. In general, cortical ROIs were first anatomically constrained and then searched within for the most active voxels in native space on a subject-by-subject basis. In the end, each subject had a native-space top-10 voxel region defined for every area of interest.

In general, anatomical regions were derived from the Harvard-Oxford Cortical and Subcortical Structural Atlas (included in FSL: http://www.fmrib.ox.ac.uk/). Regions were taken in normalized space at 100% thresholded probability and non-linearly reverse normalized for each subject using the SyN algorithm (ANTS). Functional activity was assessed with statistical contrasts computed on the single-subject level for each voxel as a *t*-statistic for the contrast [$TASK_{ALL}$ > $CONTROL_{ALL}$] over 43 seconds of the delay period (not including the first two seconds). Therefore, these ROIs were not biased to a particular time phase of the delay period (since the whole delay period was used) or biased to a particular task condition (since all task

conditions were included). For group analyses, single subject *t*-statistic maps were spatially normalized and then tested against zero with a one-sample *t*-test.

Specifically, the exact way in which each ROI was created slightly differed based upon the functional and anatomic details of each region. IFGpo and SPL regions for each subject were first defined anatomically (Harvard-Oxford atlas) and then searched within for the voxel with the highest *t*-value. Once the highest *t*-value was located, the nine contiguous highest *t*-value voxels were found, giving a top-10 voxel ROI for each subject.

Because this procedure led to anatomically heterogeneous subject-to-subject ROIs for IFGpt, MFG and PM regions, a different procedure was used. For example, generally subjects had activation in inferior PM (near the temporal lobe) as well as in mid PM (near the intersection with the inferior frontal sulcus). Therefore, when the top voxels were searched in the large purely anatomical PM masks, some subject's top-10 voxel ROIs were created in inferior PM while other subjects had their PM ROI in mid-PM. In order to make these ROIs more anatomically homogenous, the top *t*-value voxel within each anatomical region (Harvard-Oxford atlas) at the group level was located. A 10mm sphere was placed around this top-voxel and the sphere was re-intersected back with the original atlas mask. The group mask for each ROI was non-linearly reverse normalized for each subject and the top-10 highest *t*-value contiguous voxels were found for each ROI in each subject in native space, as described above.

Because area Spt is functionally (as opposed to anatomically) defined, at the group level the voxel with the highest *t*-value located near the Sylvian fissure at the parietal-temporal boundary was located (so no Harvard-Oxford atlas mask was used). A 10mm sphere was placed around this top-voxel and this group mask was non-linearly reverse normalized into native space for each subject. Within each subject's sphere the top-10 highest *t*-value contiguous voxels were located, giving a top-10 voxel Spt ROI for each subject. Subsequently, each subject's Spt ROI was manually assessed. In four subjects the Spt ROIs were incorrectly located within SPL. In these four subjects the top voxel was manually located that was clearly in the planum temporale and still within each subject's sphere search space, and this top voxel was used to create top-10 voxel ROIs.

3.2.5.5 Analysis of Behavioral Data

Behavioral data collected prior to fMRI scanning was scored for rehearsal rate over the delay as well as recall of letters at the end of the delay period. One subject was eliminated due to whispering rehearsals that could not be scored (subject was not removed from fMRI analyses). Trials in which subjects used elaborative rehearsal (e.g. if the letters were "sdnz" and the subject began rehearsing, "San Diego, New Zealand") were eliminated for failing to follow instructions (instructed only to rehearse the given letters). Overt rehearsals were manually recorded by counting the number of letters spoken over the full delay period (15 seconds) as well as over

the first half (7.5 seconds) and the second half (7.5 seconds). Recall data was scored two different ways. In order to determine the effect of rehearsal rate on accuracy, trials were classified as "all correct" (all letters in trial correct and in correct position) or as "error" (any letter in trial incorrect or in incorrect position). This was used to classify the rehearsal rate data in Figure 3.2. However, for the individual-differences analyses a more sensitive measure of recall was utilized by scoring each letter in each trial individually. So a 6-letter trial had a possible minimal score of 0/6 or a possible maximum score of 6/6 correct. Both the letter identity and letter position had to be correct in order for a letter to be classified as correct. This data was used in the correlations in Figure 3.10. For both rate and recall, the mean value of each condition was computed for each subject and then used to compute the group mean.

Behavioral data collected during fMRI scanning was scored for the order probe (red circle) and recall probe (green triangle). Order probe was classified correct if the single correct letter was reported. If the letter identity was incorrect but the letter order was correct in the recall portion, trial was scored as correct (but incorrect in recall scoring). Recall data was scored on a letter-by-letter basis requiring both letter identity and letter position to be correct to be classified as correct (same as second recall scoring method above). The mean value of each condition was computed for each subject and then used to compute the group mean. When noted, permutation ANOVA and permutation linear contrast tests were performed with the R package lmPerm (http://cran.r-project.org/web/packages/lmPerm/index.html), while two-sample permutation tests were performed with the R package DAAG (http://cran.r-project.org/web/packages/DAAG/index.html).

3.3 Results

3.3.1 Behavioral Data (prior to fMRI scanning)

To determine if memory load and rehearsal rate were confounded behaviorally, subjects performed an overt free rehearsal working memory task. To first determine if there was an effect of load on recall, each trial was categorized as either all correct (all letters in trial correct/correct position) or error (any letter wrong in a trial/incorrect position) to generate an accuracy score for each subject. A permutation repeated-measures ANOVA was performed on the recall data with LOAD modeled as a within-subject factor and SUBJECT modeled as a random effect. The main effect of LOAD was significant (p<0.0001, df=3,66). Post-hoc permutation linear contrast tests revealed a significant linear decreasing trend for LOAD (linear coefficient=-0.62, p<0.0001, df=66), confirming that recall decreased with increasing memory load.

To investigate the effect of load on rehearsal rate, a permutation repeated-measures ANOVA was performed on the free rehearsal rate data with LOAD modeled as a within-subject factor and SUBJECT modeled as a random effect (Figure 3.2A). The

main effect of LOAD was significant (p<0.0001, df=3,66). Post-hoc paired two-sample permutation tests revealed that rehearsal rate significantly increased with memory load until the 8-letter condition, at which point rehearsal rate significantly decreased: 2-letter versus 4-letter (p<0.0001, df=22), 4-letter versus 6-letter (p<0.01, df=22), and 6-letter versus 8-letter (p<0.001, df=22). In other words, subjects displayed a U-shaped curve with increases in rehearsal rate across increases in low memory loads, but with decreases in rehearsal rate across increases in high memory loads. When trials were divided into all correct versus error, there were significant differences between 6-letter (unpaired two-sample permutation test: p<0.01) and 8-letter (unpaired two-sample permutation test: p<0.001) trials. Specifically, subjects rehearsed faster in all correct trials and slower in error trials in both 6 and 8-letter trials.

To determine if rehearsal rate changed during the delay period, the overt rehearsal rate in the first half of delay period (first 7.5 seconds) and the last half of delay period (last 7.5 seconds) were analyzed separately. A 2-way permutation repeated-measure ANOVA was performed with LOAD and TIME modeled as within-subject factors and SUBJECT modeled as a random effect (Figure 3.2B). There was a significant LOADxTIME interaction (p<0.001, df=3,66). Post-hoc paired two-sample permutation tests across TIME phases were preformed. Significant differences between the first and last time phases of the delay period were found for 2-letter (p<0.05, df=22) and 8-letter (p<0.05, df=22), while a marginally significant difference was found for 4-letter (p=0.06, df=22). No significant difference was found for 6-letter (p=0.11, df=22). Dividing each trial into all correct or error (as above) revealed that the pattern of effects did not change. Specifically, in 2-letter and 4-letter subjects rehearsed faster in the first half of the delay period relative to the second half, while in 8-letter subjects rehearsed slower in the first half but faster in the second half. In the 6-letter condition, the rehearsal rate for all correct trials was approximately the same for the first and second half of the delay period, but during trials with errors, rehearsal was slower in the first half and faster in the second half. During all correct trials, the 4-letter condition was significant (paired two-sample permutation test: p<0.05, df=22) while during error trials, the 6-letter (paired two-sample permutation test: p=0.065, df=20) and 8-letter conditions (paired two-sample permutation test: p=0.098, df=22) there was a trend towards significance.

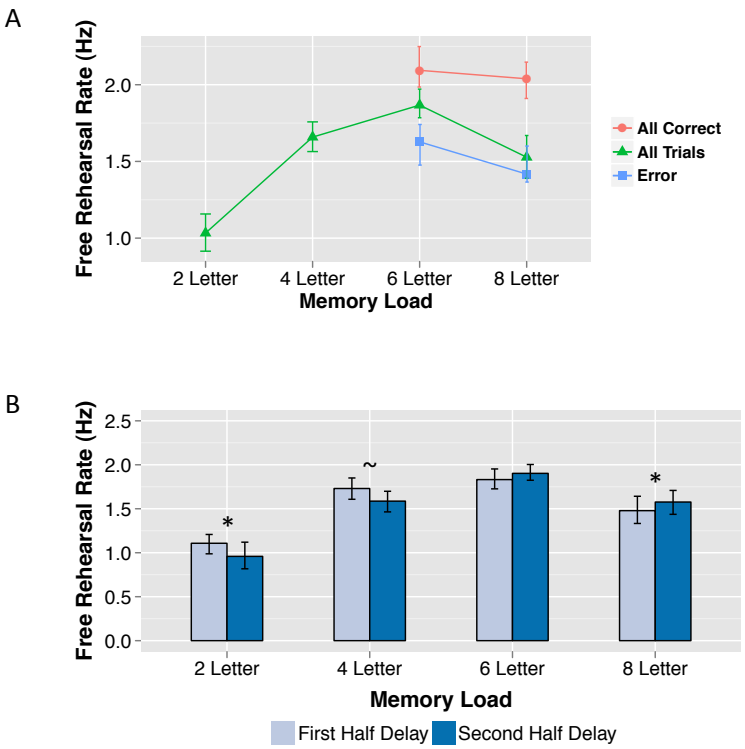

Figure 3.2: Overt free rehearsal behavioral data. Prior to the fMRI experiment, subjects overtly rehearsed either two, four, six, or 8-letters over a fifteen second delay period in a working memory task. ***A,*** For each memory load, mean rehearsal rate (number of letters/second) is plotted. In general, as the memory load increased subjects rehearsed at a faster rate until the memory load exceeded a certain threshold at which point subjects' rehearsal rate decreased. Trials were divided into either all correct (all letters correct/correct position) or error (any letter incorrect/wrong position). Trials classified as all correct had a faster rehearsal rate than trials classified as error. ***B,*** Rehearsal rate in the first half of the delay period (first 7.5 seconds) versus the second half of the delay period (last 7.5 seconds) for each memory load condition. In general, subjects rehearsed faster in the first half of the delay period for two and 4-letter conditions, but faster in the second half of the delay period for 6 and 8-letter conditions. Data plotted are group means. Error bars represent bootstrapped within-subject 95% confidence intervals. *p<0.05, ~p<0.10.

3.3.2 fMRI Behavioral Data

A permutation 2-way repeated-measures ANOVA was performed on the order probe data with LOAD and RATE modeled as within-subject factors and SUBJECT modeled as a random effect (Figure 3.3). The main effect of LOAD was significant (p<0.0001, df=2,46), the main effect of RATE was significant (p<0.0001, df=6,138), while the interaction of LOADxRATE was not significant (p=0.24, df=12,276). Post-hoc permutation tests revealed a significant decreasing linear trend for LOAD (linear coefficient=-10.31, p<0.0001, df=46) and RATE (linear coefficient=-42.259, p<0.0001, df=138) on order probe accuracy.

A permutation 2-way repeated-measures ANOVA was performed on the recall probe data with LOAD and RATE modeled as within-subject factors and SUBJECT modeled as a random effect (Figure 3.3). The main effect of LOAD was significant (p<0.0001, df=2,46) while the main effect of RATE (p=0.77, df=6,138) and the interaction of LOADxRATE (p=0.85, df=12,276) were not significant. Post-hoc permutation tests revealed a significant decreasing linear trend for LOAD (linear coefficient=-8.49, p<0.0001, df=46) on recall probe accuracy, but not for RATE (linear coefficient=-0.12, p=1.0, df=138).

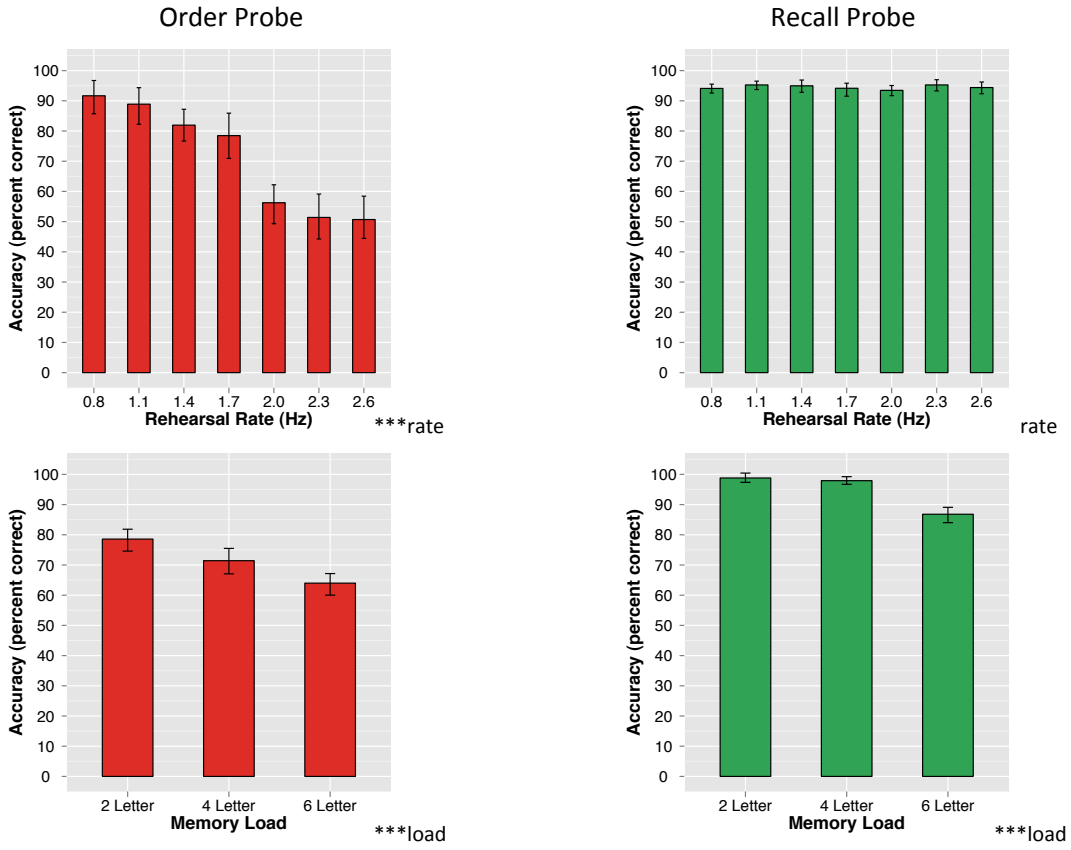

Figure 3.3: fMRI behavioral results. Order probe (red circle) accuracy on left, recall probe (green triangle) accuracy on right. Effect of rate on top, effect of memory load on bottom. Data from order probe and recall probe were separately entered into a permutation 2-way repeated measures ANOVA (LOAD, RATE); statistics show the main effect of each factor and are displayed in the lower right corner of each plot. Results show that as the rehearsal rate increased it became more difficult to correctly answer the order probe, with a large decrease in accuracy between 1.7 and 2.0 Hz (top-left). Conversely, rehearsal rate did not affect the recall probe (top-right). However, both probes showed a memory load effect as accuracy decreased from two, to four, to 6-letters. There was no LOADxRATE interaction for either probe. Data plotted are group means. Error bars represent bootstrapped within-subject 95% confidence intervals. ***p<0.0001.

3.3.3 Functional Magnetic Resonance Imaging Results

To identify cortical regions sensitive to memory load and, separately, regions sensitive to rehearsal rate, a 43-second delay period activity estimate (*t*-value) for each of the 21 conditions ($LOAD_3$ x $RATE_7$) for every subject was entered into a 2-way repeated-measures ANOVA with LOAD and RATE modeled as within-subject factors and SUBJECT modeled as a random effect (Figure 3.4). Resulting non-directional F values were assigned direction based on linear trend analyses. Results demonstrated a positive main effect of LOAD in many areas commonly implicated in verbal working memory including MFG, IFG, PM, area Spt and SPL. Additionally, superior frontal gyrus, inferior parietal lobule, and anterior temporal lobe areas demonstrated load effects. A main effect of RATE was found in IFG, PM, area Spt, and occipital lobe. No cortical areas revealed a significant LOADxRATE interaction.

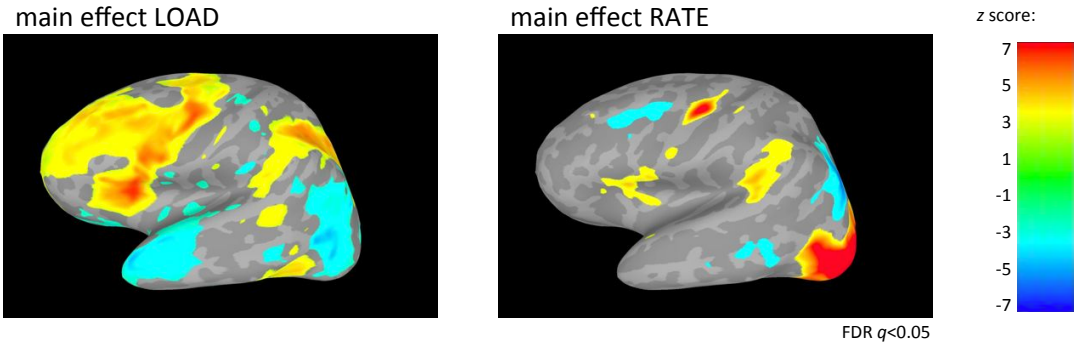

Figure 3.4: fMRI ANOVA results. Activity estimates (*t*-values) for each condition for 43 seconds of the delay period were entered into a 2-way repeated measures ANOVA (LOAD, RATE). Resulting non-directional *F* values were converted to *z*-scores and assigned direction based on linear trend (LOAD, RATE) analysis. A positive main effect of memory LOAD can be visualized across many regions implicated in verbal working memory including MFG, IFG, PM, area Spt and SPL. In contrast, a positive main effect of rehearsal RATE is mainly restricted to IFG, PM, area Spt and occipital lobe regions. Analysis of control trials (visual pacing cues in the absence of subvocal rehearsal) revealed only occipital lobe activation (data not shown). No region demonstrated a LOADxRATE interaction. Data from left hemisphere; data shown are *z*-scores thresholded at FDR $q<0.05$.

As demonstrated in Figure 3.4, the occipital lobe demonstrated a main effect of RATE presumably due to the changing frequency of visual pacing cues with changing rehearsal rate. To ensure that IFG, PM and area Spt were not also simply responding to visual sensory input, a repeated measures ANOVA with RATE modeled as a within-subject factor and SUBJECT modeled as a random effect was performed on the control conditions which included all seven rehearsal rates without the requirement to subvocally rehearse. Occipital lobe was the only region

that demonstrated a main effect of RATE confirming that IFG, PM and area Spt were not activated simply by the visual pacing cues (results not shown).

To investigate how these effects changed through the delay period, activity estimates (*t*-values) for the early delay (2-16 seconds), mid delay (16-30 seconds), and late delay period (30-44 seconds) for each condition were generated. The estimates from each phase were entered into separate 2-way repeated measures ANOVAs with LOAD and RATE modeled as within-subject factors and SUBJECT modeled as a random effect (Figure 3.5). The main effect of LOAD during the early delay period revealed a similar pattern of activation as the main effect of LOAD when averaged across the entire delay period. However, the main effect of LOAD diminished through the delay period and by the late delay period only IFG and PM exhibited LOAD effects. Conversely, areas that exhibited a main effect of RATE during the early delay period did not exhibit decreasing activity in the later delay periods. There were no cortical regions that exhibited a significant LOADxRATE interaction in any phase of the delay period.

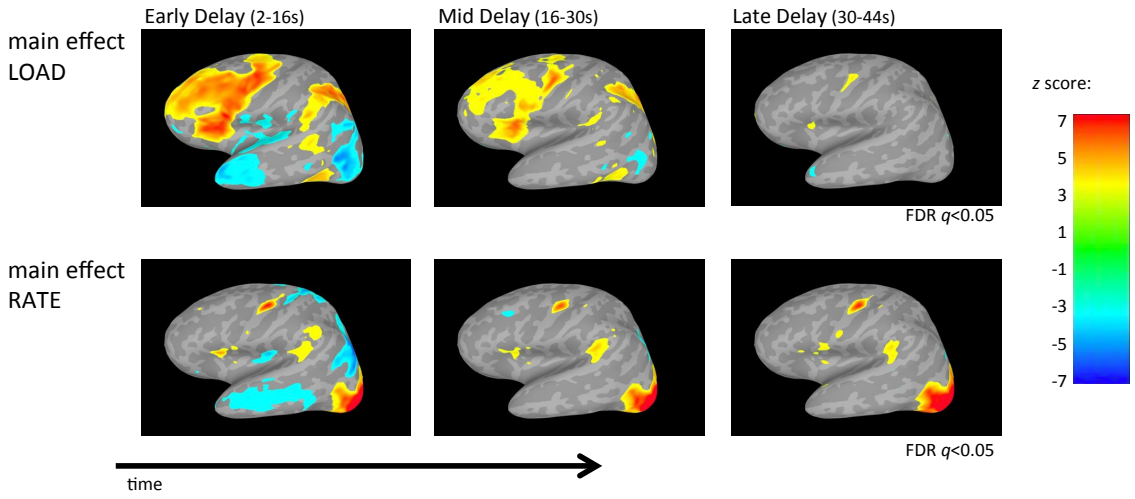

Figure 3.5: fMRI ANOVA results across time. Activity estimates (*t*-values) for each condition for the early, mid, and late delay period time phases were separately entered into a 2-way repeated measures ANOVA (LOAD, RATE). Resulting non-directional *F* values were converted to *z*-scores and assigned direction based on linear trend (LOAD, RATE) analysis. Results show that the main effect of memory LOAD decreased through time. By late delay, only IFG and PM exhibited load effects. In contrast, the main effect of RATE was primarily restricted to IFG, PM and area Spt (and occipital lobe) and were constant through the delay period without decreasing. No region demonstrated a LOADxRATE interaction during any part of the delay period. Data from left hemisphere; data shown are *z*-scores thresholded at FDR $q<0.05$ for the three time periods in LOAD and RATE separately in order to compare changes across time.

To determine which regions were sensitive to both memory load and rehearsal rate, as well as those sensitive to load but not rate, a conjunction analysis was carried out. Linear trend analyses for LOAD and RATE were independently thresholded at the group level and two separate conjunction analyses were performed. One analysis for voxels showing both a significant linear trend in load and rate, [$LOAD_{(FDR\ q<0.05)}$] ∩ [$RATE_{(FDR\ q<0.05)}$], and a second analysis for voxels showing a significant linear trend in load but not rate, [$LOAD_{(FDR\ q<0.05)}$] ∩ [$RATE_{(p>0.95)}$] (Figure 3.6). Results demonstrate that IFG, PM and area Spt were sensitive to both LOAD and RATE, while primarily MFG and SPL were sensitive to LOAD but not RATE.

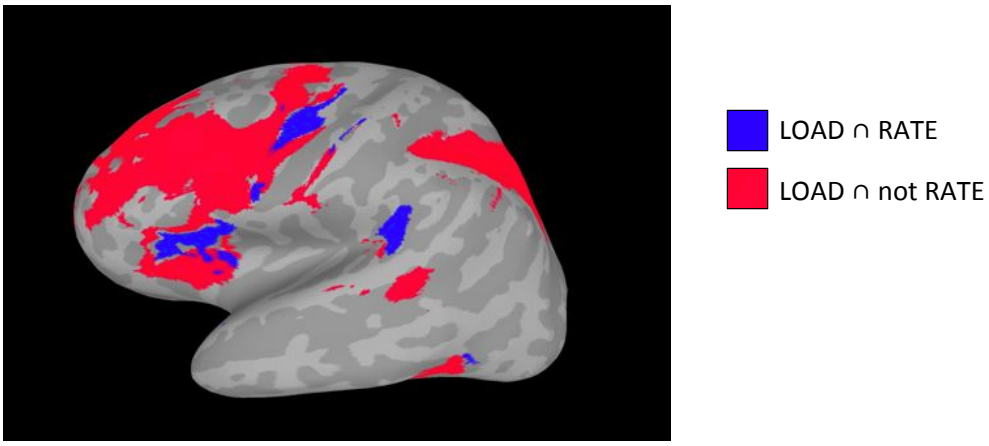

Figure 3.6: Conjunction analysis. Linear trend analysis for LOAD and RATE were independently thresholded at the group level and two separate conjunction analyses were performed: [$LOAD_{(FDR\ q<0.05)}$] ∩ [$RATE_{(FDR\ q<0.05)}$], and [$LOAD_{(FDR\ q<0.05)}$] ∩ [$RATE_{(p>0.95)}$]. Separate conjunction maps (blue, red) were then combined into one figure for visualization (as shown above). Results show that IFG, PM and area Spt were sensitive to LOAD and RATE, while primarily MFG and SPL areas were responsive to LOAD but not RATE. Data from left hemisphere.

3.3.4 Region of Interest Results

To determine the pattern of memory load and rehearsal rate effects in cortical regions commonly recruited during verbal working, an ROI analysis was performed. For each ROI, a 2-way repeated-measures ANOVA was carried out on the ROI extracted *t*-values with LOAD and RATE modeled as within-subject factors and SUBJECT modeled as a random effect (Figure 3.7). Two patterns of results emerged. MFG and SPL revealed a main effect of LOAD with no main effect of RATE, while IFGpt, IFGpo, PM and area Spt revealed a main effect of both LOAD and RATE. Furthermore, MFG and SPL exhibited a non-linear pattern of activity for memory LOAD (activity levels the same in 2 and 4-letter conditions before a significant increase in the 6-letter condition), while PM and area Spt exhibited a more linear

pattern of activity across LOAD (approximately constant increase in activity from 2 to 4 to 6-letter conditions). Additionally, the RATE effects in PM and area Spt appear approximately linear. No region revealed a LOADxRATE interaction. For full statistical results see Table 3.1.

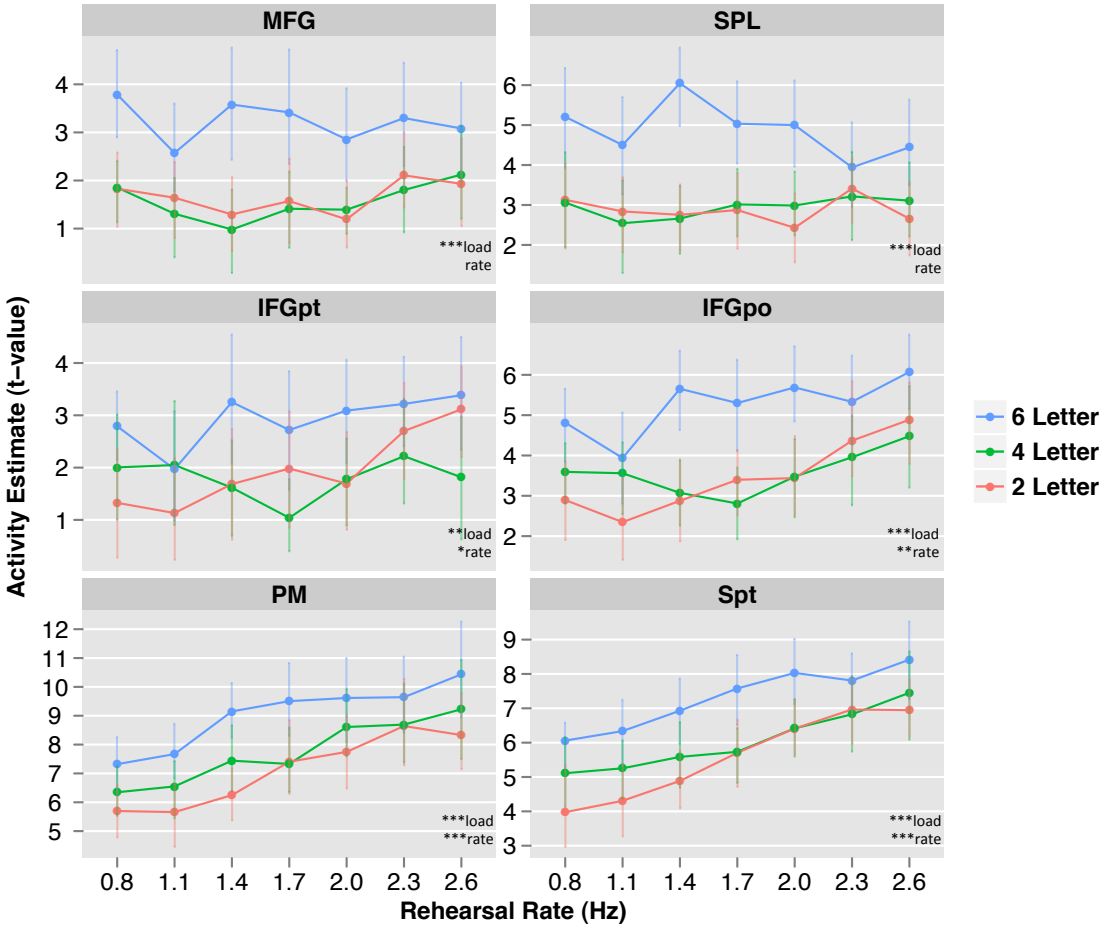

Figure 3.7: ROI analysis of key verbal working memory regions. Activity estimates (*t*-values) are plotted for 43 seconds of the delay period for each rehearsal rate (x-axis) and memory load (different colors). Data for each ROI was separately entered into a 2-way repeated measures ANOVA (LOAD, RATE); statistics show the main effect of each factor and are displayed in the lower right corner of each plot. Results show that MFG and SPL are sensitive to only memory load but not rehearsal rate, and that memory load effects appear non-linear. In contrast, IFGpt, IFGpo, PM and area Spt are all sensitive to load and rate. Furthermore, especially within PM and area Spt, the effects of load and rate appear to be approximately linear. There was no significant LOADxRATE interaction in any ROI. Data plotted are group means. Error bars represent bootstrapped within-subject 95% confidence intervals. ***p<0.0001, **p<0.001, *p<0.05.

Table 3.1: ANOVA results for each region of interest.

	MFG	SPL	IFGpt	IFGpo	PM	Spt
LOAD(df=2,46)	F=17.01	F=13.68	F=9.285	F=23.97	F=22.65	F=28.39
	p<0.0001	p<0.0001	p<0.001	p<0.0001	p<0.0001	p<0.0001
RATE(df=6,138)	F=1.56	F=0.716	F=2.487	F=4.696	F=13.57	F=12.93
	p=0.16	p=0.637	p<0.05	p<0.001	p<0.0001	p<0.0001
LOADxRATE (df=12,276)	F=0.786	F=1.568	F=1.341	F=1.438	F=0.884	F=0.796
	p=0.665	p=0.1	p=0.195	p=0.148	p=0.564	p=0.654

To investigate how these effects changed through the delay, the delay period was divided into early (2-16 seconds), mid (16-30 seconds), and late (30-44 seconds) phases and the ROI analysis was repeated. For each ROI, a 3-way repeated-measures ANOVA was performed on the ROI extracted fMRI *t*-values with LOAD, RATE, and PHASE modeled as within-subject factors and SUBJECT modeled as a random effect (Figure 3.8). All ROIs showed a PHASExLOAD interaction (all ROIs: $p<0.001$), while no ROI showed a PHASExRATE interaction (all ROIs: $p>0.10$). Subsequently, to investigate the PHASExLOAD interaction, the activity estimates (*t*-values) were collapsed over RATE and ROI. As illustrated in Figure 3.9, the PHASExLOAD interaction appears to be the result of activity during the 2 and 4-letter conditions increasing over the delay period and eventually reaching the level of the 6-letter condition, which remained constant through the delay period.

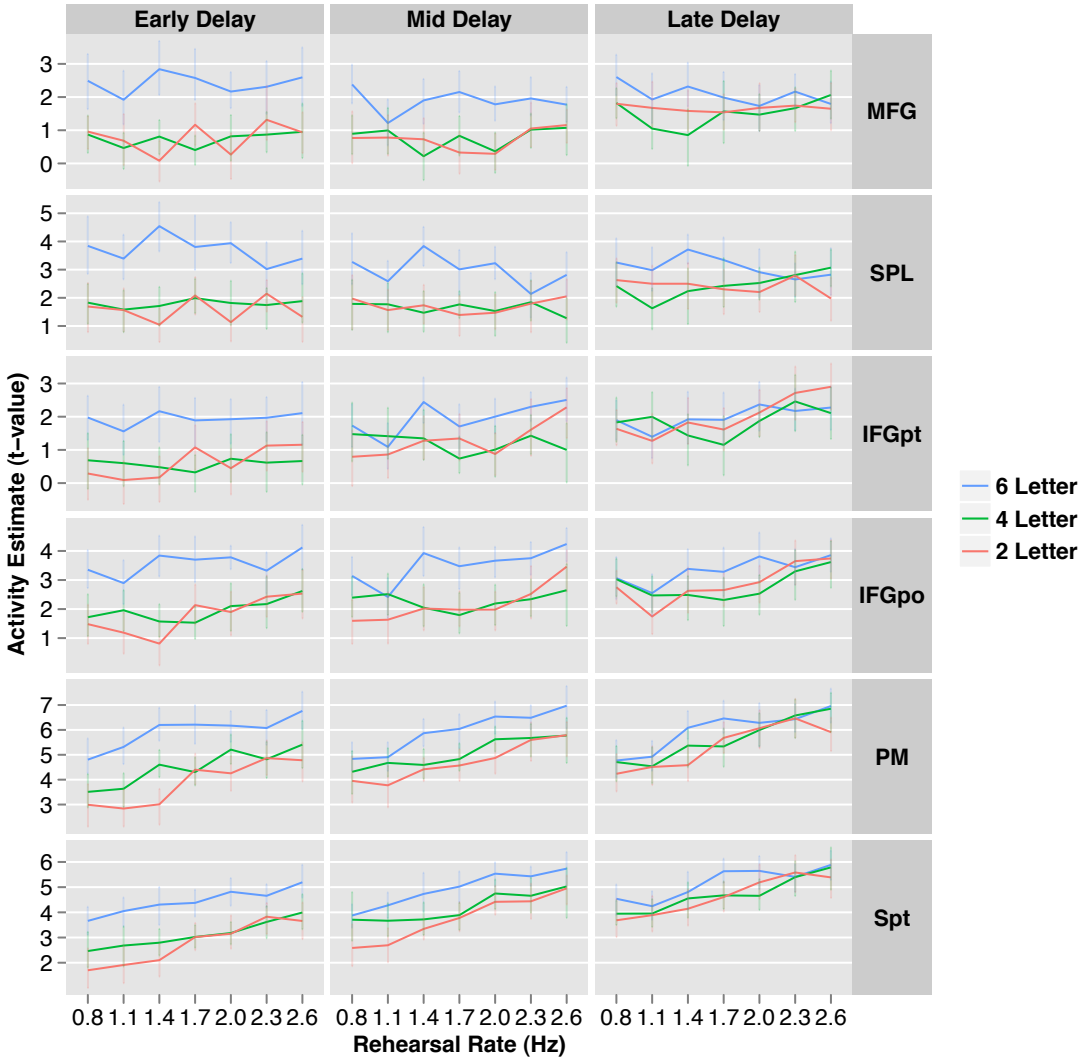

Figure 3.8: ROI analysis of key verbal working memory regions through time. Activity estimates (*t*-values) plotted for the early (2-16 seconds), mid (16-30 seconds), and late (30-44 seconds) delay period time phases (columns) for each rehearsal rate (x-axis) and memory load (different colors). Data for each ROI was separately entered into a 3-way repeated measures ANOVA (PHASE, LOAD, RATE). Results demonstrate a reduction in load effects through time as all regions revealed a PHASExLOAD interaction ($p<0.001$). Conversely, rehearsal rates remained constant through time as no region demonstrated a PHASExRATE interaction ($p>0.10$). There was no LOADxRATE interaction. Data plotted are group means. Error bars represent bootstrapped within-subject 95% confidence intervals.

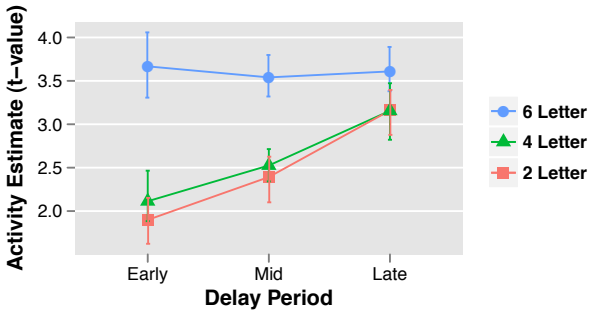

Figure 3.9: Mean activity across all ROIs through time. Activity estimates (*t*-values) from Figure 3.8 were averaged over rehearsal rate and ROI to investigate the PHASExLOAD interaction. Figure shows mean activity estimates across memory loads through early (2-16 seconds), mid (16-30 seconds), and late (30-44 seconds) delay period time phases. Results reveal the dissipating load effects were due to activity in the 6-letter condition remaining constant through the delay period while activity in the 2 and 4-letter conditions increased through time. Data plotted are group means. Error bars represent bootstrapped within-subject 95% confidence intervals.

3.3.5 Individual Differences

To examine individual differences in verbal working memory, each subject's behavioral data performed prior to fMRI scanning was correlated with their fMRI BOLD data. Specifically, the 8-letter recall letter data and 8-letter overt free rehearsal rate data were each separately correlated (Spearman rank correlation) with the *t*-value for the linear trend in memory load and rehearsal rate, both computed over the entire delay. The 8-letter condition was chosen since it was the most difficult and therefore most likely to capture individual differences. Results demonstrated that for fMRI BOLD memory load values, MFG, SPL and IFGpo were significantly negatively correlated (Table 3.2, Figure 3.10A). Thus, subjects that had higher recall accuracy (or faster free rehearsal rates) had smaller fMRI BOLD memory load effects. For fMRI BOLD rehearsal rate values, only PM was significantly positively correlated with 8-letter recall accuracy (Table 3.2, Figure 3.10B). Thus, subjects that had higher recall accuracy (or faster free rehearsal rates) had larger fMRI BOLD rate effects.

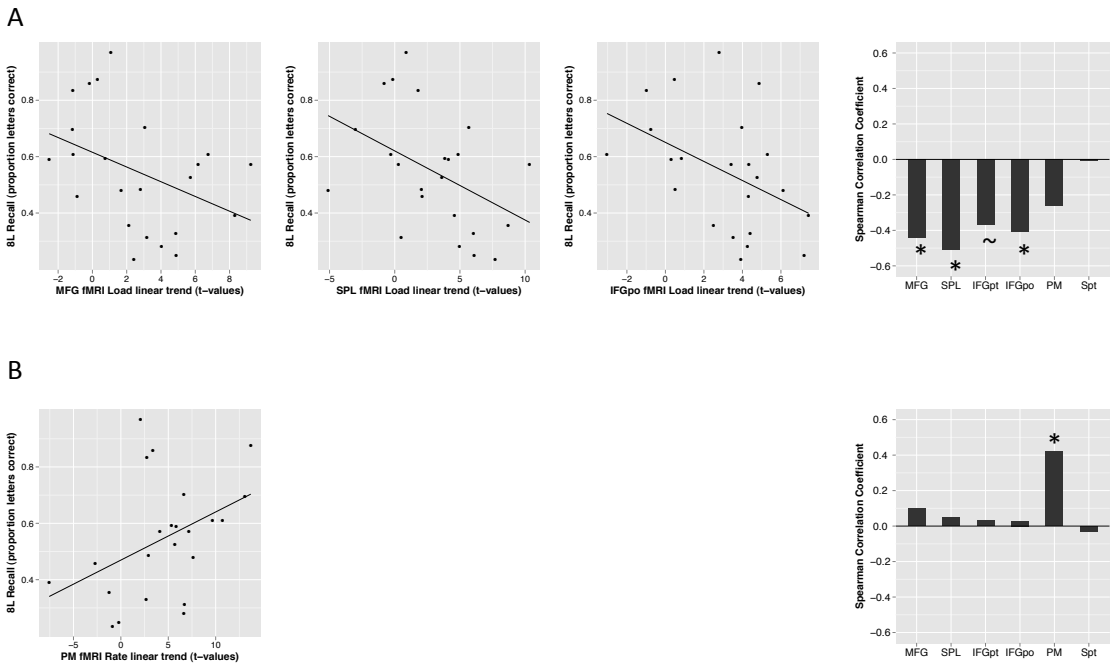

Figure 3.10: Brain-behavior correlations. For each subject, activity estimates (beta values) were used in separate linear trend contrasts for memory load and rehearsal rate. Resulting linear trend *t*-values for each subject were correlated with 8-letter recall accuracy collected prior to the fMRI scan. ***A,*** fMRI BOLD linear trend in memory load correlated with 8-letter recall accuracy. Scatterplots shown for MFG, SPL and IFGpo. Bar graph shows group Spearman correlation coefficient values across ROIs (top right). Results demonstrate a negative correlation in MFG, SPL and IFGpo, such that subjects with higher recall accuracy had smaller fMRI BOLD load effects. ***B,*** fMRI BOLD linear trend in rate correlated with 8-letter recall accuracy. Scatterplot shown for PM (bottom left). Bar graph shows group Spearman correlation coefficient values across ROIs (bottom right). Results demonstrate a positive correlation in PM such that subjects with higher recall accuracy had larger fMRI BOLD rate effects. Note that recall accuracy was correlated with free overt rehearsal rate, yet only recall accuracy is presented in figure (see Results for details). Line on scatterplots represents linear regression line. *p<0.05, ~p<0.10.

Table 3.2: Brain-behavior correlation results for each region of interest.

fMRI Load, linear trend:

		MFG	SPL	IFGpt	IFGpo	PM	Spt
8L Recall	Spearman's rho	-0.44	-0.51	-0.37	-0.41	-0.26	-0.006
	p-value	0.034	0.014	0.080	0.049	0.23	0.98
8L Rate	Spearman's rho	-0.54	-0.50	-0.38	-0.34	-0.27	0.076
	p-value	0.0084	0.017	0.074	0.12	0.21	0.73

fMRI Rate, linear trend:

		MFG	SPL	IFGpt	IFGpo	PM	Spt
8L Recall	Spearman's rho	0.10	0.050	0.033	0.029	0.42	-0.031
	p-value	0.64	0.82	0.88	0.90	0.046	0.89
8L Rate	Spearman's rho	0.084	0.11	-0.055	-0.020	0.34	0.062
	p-value	0.70	0.61	0.80	0.93	0.11	0.77

3.4 Discussion

In this fMRI study we investigated the effects of rehearsal rate and memory load in the context of verbal working memory by orthogonally varying the two factors. We demonstrated that MFG and SPL regions were not sensitive to rehearsal rate, but exhibited non-linear load effects that dissipated through the delay period. In contrast, IFG, PM and area Spt demonstrated approximately linear increases in activity with both increasing rehearsal rate and memory load, with the effects of rehearsal rate persisting through the long delay periods. Additionally, we demonstrated that memory load effects in all regions of interest dissipate through time (not just MFG and SPL), that memory load and rehearsal rate are confounded behaviorally and that individual differences in verbal span may be partially explained through high capacity individuals having less activity in MFG, SPL, and IFG, but more activity in PM.

3.4.1 Control Regions

Control processes are thought to involve organizational operations such as the allocation of attention, selection of relevant information, and the assembly and initiation of motor programs. Two supposed control regions, MFG and SPL, have

been shown to be sensitive to memory load manipulations (Rypma et al. 1999; Zarahn et al. 2005) however, it is not clear exactly why. This study demonstrates that the same MFG and SPL regions that exhibit memory load effects do not show rehearsal rate effects. Therefore, this seems to suggest that MFG and SPL regions are not involved in certain rehearsal maintenance control operations in verbal WM that can be expected to increase with increasing rehearsal demands, such as motor planning, selection of motor plans, initial execution of motor programs, and the repeated selection or attention to task-relevant representations. While these results may seem at odds with the literature that demonstrates increased MFG activity when a single, just-visualized stimulus is "refreshed" (Raye et al. 2002; Johnson et al. 2005), new work suggests that refreshing and articulatory rehearsal are two independent mechanisms of maintenance (Camos et al. 2009).

However, while our results demonstrate MFG and SPL areas are not sensitive to rehearsal rate, they are sensitive to memory load. Specifically, activity levels at 2 and 4-letter were approximately equal, before greatly increasing at 6-letter, thus demonstrating a non-linear load effect. Non-linear load effects (or "threshold" load effects) have been shown previously in these regions (Cohen et al. 1997; Rypma et al. 1999, Leung et al. 2002). Our results extend these findings by demonstrating that these load effects are strongest at the start of the delay and then diminish through the delay period. These decaying non-linear load effects suggest these regions are involved in control operations that are not required to scale linearly with increasing memory load. Furthermore, there was no interaction of memory load and rehearsal rate in MFG or SPL regions. This suggests that the operations these regions are performing at high memory loads is independent from the rehearsal processes mentioned above that are manipulated when rehearsal rate is altered.

While the exact function of MFG in WM tasks is unclear, these results are consistent with some of the proposed functions of MFG including the manipulation of information (D'Esposito et al. 1999; Postle et al. 1999), "updating" or continuously modifying the content of WM (Miyake et al. 2000; Shimamura 2000), and the strategic reorganization of information in WM (Rypma et al. 1999; Druzgal and D'Esposito 2003; Bor et al. 2003). While the role of SPL in working memory tasks is also unclear, it has been implicated in both the retrieval of information (Olson & Berryhill 2009) as well as the manipulation of information (Champod & Petrides 2007; Champod & Petrides 2010). In general, any demanding working memory task that activates MFG also seems to activate SPL (D'Esposito et al. 1995; D'Esposito et al. 1999; Rypma et al. 1999; Zarahn et al. 2005). Our results are consistent with this and show that the pattern of effects in both MFG and SPL across both memory load and rehearsal rate are similar (e.g. Figure 3.7). Interestingly, a recent study dissociated MFG and SPL regions, finding that MFG was involved in the monitoring and manipulation of information, while SPL was primarily involved in the manipulation of information in WM (Champod & Petrides 2010).

3.4.2 Storage/Rehearsal Regions

Our results demonstrate that IFG, PM and area Spt are the core storage/rehearsal areas that maintain task-relevant information in verbal WM. Not only were these regions sensitive to manipulations in rehearsal rate, they were also active throughout the long 45 second delay periods. This is consistent with the proposed roles for each of these regions, with IFG thought to be involved in simple motor planning, PM believed to generate the actual motor plans and area Spt thought to be an auditory-motor interface.

Furthermore, our results demonstrate that within area Spt and PM there seems to be a linear increase in activity with increasing rehearsal rate (even across different memory loads). This is consistent with speech studies (that did not contain a memory component as subjects simply had to say "pa" or "ta") that found linear increases in activity with increasing rehearsal rate (Wildgruber et al. 2001; Shergill et al. 2002; Riecker et al. 2005; Riecker 2006). Therefore, there does not seem to be an energy savings when task-relevant information is reactivated at greater rates which would have manifested as some type of non-linear increase in activity. This type of energy savings is suggested by studies on priming and repetition suppression that suggest when a stimulus is repeatedly presented the neural representation becomes sparser as the neurons encoding non-essential features of the stimulus respond less, leading to an overall decrease in activity (Desimone 1996; Wiggs & Martin, 1998). Additionally, our results revealed that rehearsal rate did not interact with load or time through the delay period. This suggests that there is a fixed activation cost for reactivating task-relevant information that is irrespective of the number of items currently held in working memory or time in the delay period.

Our results demonstrate that the memory load effects in PM and area Spt are approximately linear (constant increase in activity across memory loads), in contrast to the load effects in MFG and SPL areas which appear generally non-linear. This has been shown previously and suggests these areas are directly involved in maintaining the task-relevant information as they increase whenever the number of items stored in memory increases.

Our findings revealed that memory load effects dissipated over the long delay periods in this study. This general effect seemed to be present in all ROIs (both control and storage/rehearsal regions) and did not interact with rehearsal rate. Specifically, the activity in the 6-letter condition reached a maximum value early and remained there, while activity levels in 2 and 4-letter slowly increased over time until they were approximately equal to the 6-letter activity by the end of the delay period. It may be that subjects increased attention to the task as it became more difficult as the long delay periods went by (due to fatigue, boredom, etc.) or they anticipated the difficult order/recall probe at the end of the delay period, increasing activity levels in the 2 and 4-letter conditions, but not in the 6-letter condition, where activity levels may have already been at a maximum. Regardless, this seems to demonstrate that in the context of verbal working memory the activity required

to maintain 2-items can be equivalent to the activity required to maintain 6-items, thus memory load may not be an optimal way to operationalize storage. Instead, manipulation of rehearsal may be a more specific measure.

3.4.3 Confound of memory load & rehearsal

One potential confound to memory load manipulations that has not been investigated is rehearsal rate. We found that subjects alter their rehearsal rate based on memory load and rehearse at a faster rate at low memory loads before rehearsing slower at a high memory load (8-letters). This suggests that across lower memory loads subjects rehearse faster in order to maintain the increased numbers of items. However, once a certain memory load is exceeded, subjects devote attentional resources to try and remember the information, which decreases the rate at which they can rehearse. Furthermore, we found that rehearsal rate varied as a function of time during the delay period contingent on the memory load.

While the effect of memory load on rehearsal rate has not been demonstrated previously, our findings are consistent with some earlier studies on rehearsal rate. One previous study found that maximum overt rehearsal for spoken words increased as the list length increased from 2, 3, to 4-items (Cowan et al. 1998). Several other studies have shown that individuals with faster maximum overt speech rates have higher verbal span (Baddeley et al. 1975; Hulme et al. 1984; Cowan et al. 1998). However, it should be noted that while rehearsal rate and verbal span are correlated, it is not clear if rehearsal rate casually influences memory recall.

Therefore, this behavioral data suggests that multiple factors can change rehearsal rate while subjects are maintaining task-relevant information. Combined with the rehearsal rate manipulation fMRI results, this suggests multiple cortical regions can show changes in activity that may be misattributed to certain task manipulations when in fact it really may be secondary to a change in rehearsal rate. This may partly explain why memory load effects have been so inconsistent and discrepant in various cortical regions both among individuals in the same study (Postle et al. 1999) as well as across studies. Specifically, several studies have shown memory load effects in MFG (Rypma et al. 2002; Zarahn et al. 2005), while others have not (Rypma et al. 1999; Postle et al. 1999). Other regions that show inconsistent results include IFG, inferior parietal, temporal, and motor areas (Rypma et al. 1999; Postle et al. 1999; Buchsbaum et al. 2005; Narayanan et al. 2005). Many different sources of variability may help explain these inconsistent findings such as differences in the task (recall versus recognition), number of items (below, at, or above span i.e. <4, =4, >4 items (Cowan 2001)), and analysis (whole-brain versus region of interest; how delay period modeled) (Postle 2006; Buchsbaum & D'Espostio 2008; Curtis & D'Espostio 2003). However, even when many of these external factors are accounted for there still seems to be a large amount of variability in reported findings. For example, even the same lab using similar verbal WM tasks found load effects in MFG and IFG in one study (Rypma et al. 2002), but not in another study (Rypma et al. 1999). Therefore,

this study extends previous findings by revealing that even when the rate of rehearsal is held constant, memory load effects still exist across multiple cortical regions and were not simply due to increases in rehearsal rate.

3.4.4 Individual differences

Our results revealed that in MFG, SPL and IFG regions, memory load effects were negatively correlated with recall and free rehearsal rate, suggesting higher capacity individuals engage these cortical regions less than low capacity individuals. This may suggest that higher capacity individuals are using these cortical areas in a more efficient manner, although it is unclear if this higher efficiency relates to higher neural efficiency (i.e. actual functioning of the neural tissue) or more efficient behavioral strategies (i.e. strategies that engage those cortical areas less across loads). These results are similar to findings of decreased activity in MFG, IFG, and lingual gyri in high capacity subjects (Reichle et al. 2000; Prat et al. 2007; Rypma et al. 2002).

Conversely, PM revealed a significant positive correlation with fMRI recall values (and a non-significant positive correlation with free rehearsal rate), suggesting higher capacity individuals engage PM more than low capacity individuals. One interpretation of this finding is that high capacity individuals are more effortful in their rehearsal across different rehearsal rates, although this is an interpretation based on reverse inference and will require future studies to elucidate.

Together, it seems that high capacity individuals recruit control regions less across memory loads yet recruit storage/rehearsal regions more across rehearsal rates. This seems to suggest high capacity individuals are more efficient with control region(s) yet pay more attention to the rehearsal of the task-relevant information.

4

THE INFLUENCE OF SIGNAL VARIABILITY ON TASK FUNCTIONAL CONNECTIVITY

4.1 Introduction

It is becoming clear that distributed cortical networks are required for complex cognition. Functional connectivity is one way to study these networks and is formally defined as temporal correlations between remote neurophysiological events (Friston 1994). Since fMRI BOLD reflects both action potential and local field potential activity (Logothetis et al. 2001), it is generally believed that if two regions demonstrate correlated fMRI BOLD activity, this reflects synchronous neural activity in communicating regions.

Since functional connectivity is thought to reflect communication between cortical regions, altering task demands is expected to alter the information load and thus modulate functional connectivity. In general, most studies investigating task functional connectivity demonstrate the majority of cortical regions show increases in functional connectivity as task demands increase (Sakai et al. 2002; Fiebach et al. 2006; Chang et al. 2007; Kayser et al. 2010). However, some studies demonstrate not only regions showing increases in functional connectivity as task demands increase, but other areas showing decreases in connectivity as task demands increase (Gruber et al. 2007; Rissman et al. 2007). In particular, during the delay period of a visual working memory study, as the memory load (number of faces) was parametrically increased the IFG demonstrated linearly decreasing functional connectivity with the fusiform face area (FFA), while the hippocampus demonstrated linearly increasing functional connectivity with both the IFG and FFA (Rissman et al. 2007). Therefore, functional connectivity has been reported to increase or decrease depending on the cortical region and particular task demands being studied.

However, task demands may directly alter fMRI BOLD signal properties such as variability, and signal variability may in turn affect functional connectivity measures. One way to measure fMRI BOLD signal variability is the standard deviation across time (Garrett et al. 2010; McIntosh et al. 2010; Garrett et al. 2011; Garrett et al. 2012). It has been demonstrated that task (task versus rest) can modulate the standard deviation of the fMRI BOLD signal over time (Garrett et al. 2012). Since most measures of functional connectivity rely on some form of correlation that quantifies the shared signal variability between two regions, it therefore follows

that the standard deviation may be critical in examining how task demands modulate functional connectivity.

In order to investigate how task demands affect signal variability and functional connectivity, the delay period of a WM task was utilized. A large amount of work has been devoted to studying how task-relevant information is maintained during the delay period of WM tasks (Gazzaley et al. 2004; Fiebach et al. 2006; Rissman et al. 2007) which, in verbal WM, is thought to involve the transfer of information among the various cortical nodes in a network with each subvocal rehearsal. Therefore, in order to investigate 1) how task demands influence fMRI BOLD functional connectivity, and 2) how these results may relate to signal variability, we investigated the mean activity (beta value from multiple linear regression), signal variability (standard deviation across time) and connectivity (linear correlation) of fMRI BOLD during the delay period of a specialized verbal working memory task while memory load and rehearsal rate were orthogonally and parametrically manipulated.

As alluded to above, in verbal WM an articulatory or phonological loop (Baddeley & Hitch 1974) is believed to subserve subvocal rehearsal and therefore allows task-relevant information to be retained over a delay period. A specific set of cortical regions are thought to form the phonological loop network. Univariate activity analyses on the data used in this study (Chapter 3) revealed that these core areas are in fact activated by this particular task. Specifically, a core set of task-active regions demonstrated increased activity to increases in both memory load and subvocal rehearsal rate as task demands increased: IFG, and in particular the IFGpo, PM and area Spt. In addition, cortical areas thought to form a domain general central-executive control network increased activity as memory load task demands increased, but not subvocal rehearsal rate: MFG and SPL.

We predict that as task demands increase (memory load$_{[2,4,6\text{-letters}]}$ or subvocal rehearsal rate$_{[0.8,1.1,1.4,1.7,2.0,2.3,2.6\ Hz]}$), functional connectivity will increase between some or all of the core task-active regions (IFGpo, PM, area Spt) secondary to the increase in information load. In addition, we will examine how changing task demands in subvocal rehearsal rate and memory load affect signal variability and in what manner they influence functional connectivity.

4.2 Methods

Full details on subjects, experimental stimuli, experimental task, fMRI acquisition and pre-processing can be found in the univariate study (Chapter 3). The same data was re-analyzed for this project.

4.2.1 Activity (beta value) Analysis

Data was band-passed filtered to retain frequencies from 0-0.15 Hz (3dBandpass), frequencies in the power-spectrum of the hemodynamic response (Aguirre et al. 1997; Sun et al. 2004). Regression modeling was carried out similar to the univariate study (Chapter 3) and the same stimulus timing and modeling parameters were used. The entire delay period was modeled with a 43-second block regressor, starting two seconds into the delay period. For each scanning run a set of nuisance regressors (constant term plus linear, quadratic, and polynomial terms) and head movement were regressed out of the time series data. For this study, each of the 21 conditions ($LOAD_{[2L,4L,6L]}$ x $RATE_{[0.8,1.1,1.4,1.7,2.0,2.3,2.6\ Hz]}$) were modeled and each of the 42 events (21 conditions x 2 trials each = 42 trials) were individually estimated and given an amplitude value. The median beta value was taken for each of the two extracted blocks in each condition in order to get an estimate for that condition. Data was normalized to group template space and random effects group analyses were performed. Linear contrasts for factors LOAD (-1,0,+1) and RATE (-1,-0.667,-0.333,0,+0.333,+0.667,+1) were computed on beta values using a repeated-measures ANOVA (3dANOVA3).

4.2.2 Connectivity Analysis

To analyze the delay period, 44 second delay period blocks were extracted from the longer runs of data. Data was band-passed filtered to retain frequencies from 0-0.15 Hz, and area Spt, ventricle, and white-matter ROIs were used to extract time series from each extracted block. At the single-subject level, multiple linear regression (3dDeconvolve) was carried out separately for each of the 21 conditions, with each condition containing two extracted delay period blocks (extracted blocks were not concatenated but entered individually into the same regression model). The seed ROI (area Spt) time series, nuisance ROI time series (ventricle, white-matter), head movement, and baseline detrending for each extracted block (constant plus linear term) were all included as covariates in the regression model. r^2 values were converted to correlation coefficient r values before being transformed into a more normal distribution with Fisher's Z transform. Data was normalized to group template space and random effects group analyses were performed. Linear contrasts for factors LOAD (-1,0,+1) and RATE (-1,-0.667,-0.333,0,+0.333,+0.667,+1) were carried out on Fischer Z values using a repeated-measures ANOVA (3dANOVA3).

Nuisance ROIs (ventricle, white-matter) were created based on anatomical constraints using each subject's mean EPI. Ventricle contiguous ten voxel ROIs were created by finding high intensity voxels in the temporal horn of the left hemisphere lateral ventricle. White matter contiguous ten voxel ROIs were created by finding voxels located in the left hemisphere that were superior to the ventricles and medially located, centered in the white-matter and away from gray-matter.

4.2.3 Standard Deviation Analysis

To analyze the encoding period, the first 16 seconds of each 2-letter, 4-letter, and 6-letter trial was extracted as a block. For the delay period, 44 second blocks of data were extracted. To analyze the retrieval period, the first 16 seconds after the delay period (including both the order probe and recall probe) were extracted. A time window of 16 seconds was chosen for encoding and retrieval in order to capture the complete hemodynamic response function (HRF) associated with each respective event.

Extracted blocks were band-passed filtered to retain frequencies 0-0.15 Hz, baseline detrended (constant plus linear term), and head movement and nuisance (ventricle, white-matter) time series were regressed out. The standard deviation across time was calculated (3dTstat) for each voxel over the entire course of the extracted block (16 seconds for encoding and retrieval, 44 seconds for delay; blocks were not concatenated). The median standard deviation was taken for each of the two extracted blocks in each condition in order to get an estimate for that condition (21 conditions x 2 trials each = 42 total trials). Data was normalized to group template space and random effects group analyses were performed. Linear contrasts for factors LOAD (-1,0,+1) and RATE (-1,-0.667,-0.333,0,+0.333,+0.667,+1) were carried out on standard deviation values using a repeated-measures ANOVA (3dANOVA3) and then submitted to permutation testing (randpermute.py, http://kurage.nimh.nih.gov/meglab/Meg/Randpermute).

4.2.4 Finite Impulse Response time courses

Time courses were derived by single-subject regression modeling implementing a cubic spline function (CSPLIN) response model (3dDeconvolve). Each of the 21 conditions ($LOAD_{[2L,4L,6L]}$ x $RATE_{[0.8,1.1,1.4,1.7,2.0,2.3,2.6\ Hz]}$) were modeled to include the entire trial from encoding through retrieval. Specifically, 14 CSPLIN functions were used to model activity over a 70 second time-window from the first presented letter in encoding until after retrieval. An activity estimate (beta value) was generated for each second. For IFGpo, PM and area Spt ROIs, the mean beta value over each ROI for each condition was extracted, and then the mean value over all three ROIs was computed.

4.2.5 Region of Interest Analyses

ROIs of the core task-active regions were created as described in the univariate study (Chapter 3). For each subject, top-10 voxel ROIs for IFGpo, PM and area Spt were derived based on anatomic constraints and maximum *t*-values for the contrast [$TASK_{ALL}$ > $CONTROL_{ALL}$]. Therefore, ROIs were unbiased towards any particular task condition since all task conditions were included in the ROI definition.

ROIs were used to extract activity estimates (beta values) by taking the mean value over the ROIs from volume data after regression modeling. For standard deviation

and connectivity analyses, the mean fMRI BOLD time series for each ROI was extracted and the standard deviation was calculated or time series were entered into a regression model to calculate the correlation coefficient (connectivity). Data for activity estimates (beta value), standard deviation, and connectivity were otherwise processed as described in each relevant section above (filtering, detrending, etc.). Permutation linear contrast analyses were performed with the R package lmPerm. Therefore, connectivity values were not Fisher Z transformed before statistical testing for ROI analysis (Figure 4.5 only).

4.2.6 Correlation: Activity and Standard Deviation

For each subject an activity estimate (beta value) and the standard deviation across time were computed for each of the 42 trials (as described in relevant sections above). A Spearman rank correlation was performed across all 42 trials and a Spearman correlation coefficient value was generated for each subject in native space. Correlation coefficient values were transformed into a more normal distribution with Fisher's Z transform and resulting values were normalized to group template space and submitted to a one-sample *t*-test. The analysis was performed in both ROI and voxelwise fashions separately and the final correlation values from voxelwise analysis were not simply extracted with ROIs. Instead, ROIs were used to extract mean fMRI BOLD time series for standard deviation analysis.

4.2.7 Correlation: Standard Deviation and Connectivity

For each subject, the standard deviation across time and a connectivity value were computed for each of the 42 trials (as described in relevant sections above). The analysis was performed in both ROI and voxelwise fashions. For the two ROIs or voxels used to generate a connectivity value (correlation), the standard deviation across time for each ROI or voxel time series was separately computed and then the median value over the two ROIs or voxels was calculated. For example, for region A and B (or seed region A and voxel B), a connectivity value (correlation) was generated for the time series of A and B, the standard deviation across time was computed for the time series of A, the standard deviation across time was computed for the time series of B, and then the median standard deviation was computed from the two standard deviation values. Subsequently, the connectivity value between the two time series and the median standard deviation of the two time series were entered into a Spearman rank correlation across all 42 trials per subject, and a Spearman correlation coefficient was generated for each subject in native space. Spearman correlation coefficient values were transformed into a more normal distribution with Fisher's Z transform and resulting values were normalized to group template space and submitted to a one-sample *t*-test. ROI and voxelwise analyses were performed separately and the final correlation values from voxelwise analysis were not simply extracted with ROIs. Instead, ROIs were used to extract mean fMRI BOLD time series for standard deviation and connectivity analyses.

4.3 Results

Full details on fMRI behavioral results and fMRI univariate activity results can be found in the univariate activity portion of this study in Chapter 3. Briefly, fMRI behavioral results demonstrated that subjects were subvocally rehearsing throughout the long 45-second delay periods (order probe accuracy grand mean: 71%). Behaviorally for factor LOAD, as task-demands increased there were significant decreases for both order and recall probe accuracies. As task-demands increased for factor RATE, there was a significant decrease in order probe accuracy, but not recall probe accuracy. Univariate activity results revealed a core set of task-active regions that demonstrated increased activity separately to increasing LOAD and increasing RATE. Specifically, IFG, and in particular IFGpo, PM and area Spt were sensitive to manipulations of both LOAD and RATE. In contrast, MFG and SPL increased activity with increasing RATE. No regions demonstrated a significant LOADxRATE interaction.

4.3.1 Connectivity Results

To determine how task demands alter functional connectivity, we performed a correlation analysis on fMRI BOLD time series over the delay period of a verbal working memory task. For each subject, a 10-voxel area Spt ROI time series was used as the "seed" time series and correlated with a time series from every voxel in the brain. Area Spt was used as the seed region because of its central importance in the phonological loop of verbal working memory (Hickok et al. 2003; Buchsbaum et al. 2005; Hickok et al. 2009) and for comparison to previous verbal working memory functional connectivity studies that also used area Spt as a seed region (Buchsbaum et al. 2005). Resulting r values were Fischer Z transformed and entered into linear trend analyses for factors LOAD and RATE. Results demonstrated a decreasing linear trend in connectivity for both LOAD and RATE (Figure 4.1). Specifically, for LOAD at a conventional voxelwise statistical threshold (FDR $q<0.05$), some of the core task-active regions for this task such as IFGpo and PM demonstrated a significant decreasing linear trend, while at a lower statistical threshold ($p<0.05$ uncorrected) there were also significant decreases in MFG and parietal cortex. Therefore, functional connectivity significantly decreased as task demands increased (2, 4, 6-letter) in these regions. RATE also showed a decreasing linear trend in connectivity across conditions, however, in different cortical regions. Specifically, at a conventional voxelwise statistical threshold (FDR $q<0.05$) regions in a non task-active region, superior temporal cortex, demonstrated significant decreases in connectivity, while at a lower threshold ($p<0.05$ uncorrected) this effect also included anterior and posterior superior temporal cortex as well as occipital cortex. Therefore, functional connectivity significantly decreased across 0.8, 1.1, 1.4, 1.7, 2.0, 2.3, 2.6 Hz levels in these regions. For both LOAD and RATE, there were very few regions that showed an increasing linear trend in connectivity, and the regions that did were not task active areas, very small, and were significant only at an extremely low statistical threshold for voxelwise analysis.

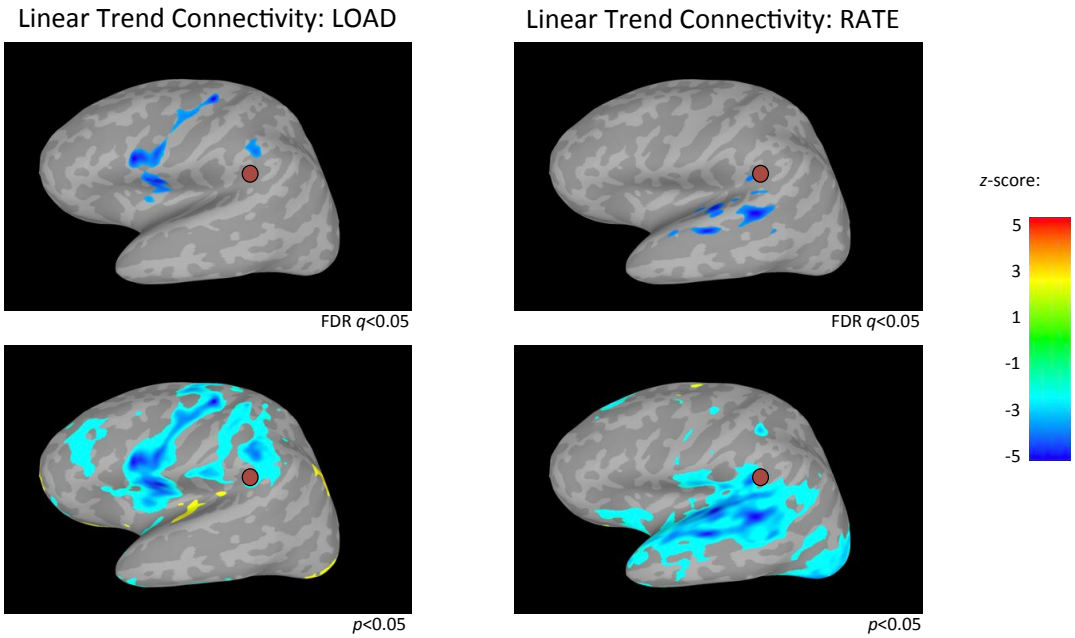

Figure 4.1: Functional connectivity results. At the single-subject level, area Spt ROIs were used to extract fMRI BOLD time courses for each of the 21 conditions ($LOAD_3$ x $RATE_7$) and a voxelwise functional connectivity (linear correlation) analysis was performed using area Spt as the seed region. Correlation coefficient values were Fischer Z transformed and linear trend analyses for factors LOAD and RATE were separately computed. Results show decreasing functional connectivity as task demands increased for both LOAD (left) and RATE (right). For LOAD, decreasing functional connectivity is demonstrated in the core task active areas IFGpo and PM at a conventional voxelwise statistical threshold (FDR q<0.05), as well as MFG and parietal cortex at a lower threshold (p<0.05 uncorrected). Therefore, these regions showed a decrease in functional connectivity as task demands increased: 2, 4, 6-letter. For RATE, decreasing functional connectivity is demonstrated in a generally non task-active region (for this task), superior temporal cortex, at a conventional voxelwise statistical threshold (FDR q<0.05), and in the occipital cortex at a reduced threshold (p<0.05 uncorrected). Therefore, these regions showed a decrease in functional connectivity as task demands increased: 0.8,1.1,1.4,1.7,2.0,2.3,2.6 Hz. Of note are the few regions demonstrating an increasing linear trend in connectivity (yellow on surface maps). For visualization purposes only, maroon circles represents approximate location of area Spt (seed ROI) at the group level. Surface data are z-scores thresholded at FDR corrected q<0.05 and uncorrected p<0.05 from the left hemisphere.

4.3.2 Standard Deviation Results

Since a priori we predicted that some or all of the task active regions would demonstrate an increase in functional connectivity as task demands increased, yet almost all cortical regions (both task-active and non task-active) demonstrated a decrease in connectivity with increasing task demands, we decided to investigate how the standard deviation across time of the fMRI BOLD signal was modulated by task demands. The standard deviation across time was computed for encoding, delay and retrieval periods, and entered into permutation linear trend analyses for factors LOAD and RATE. In general, over the delay period, the same regions that

demonstrated a decreasing linear trend in functional connectivity also demonstrated a decreasing linear trend in standard deviation for both LOAD (Figure 4.2A) and RATE (Figure 4.3A).

Specifically, for LOAD there was a significant decreasing linear trend in standard deviation in MFG, IFG, PM, area Spt and SPL over the delay period (as well as during encoding and retrieval periods), similar to areas that demonstrated a decreasing linear trend in connectivity over the delay period (Figure 4.1). Additionally, frontal polar, anterior temporal lobe, inferior temporal cortex, and some occipital regions also demonstrated a decreasing linear trend over each of the time epochs. Additionally, areas that were not generally task-active also demonstrated decreases in functional connectivity including frontal polar, anterior temporal lobe (during the delay and retrieval), and inferior temporal cortex.

In contrast, only a few regions exhibited an increasing linear trend in standard deviation for LOAD. Superior temporal cortex demonstrated a significant increasing linear trend in standard deviation that was greatest during the encoding period and then greatly diminished through the delay and retrieval periods. Similarly, the occipital pole also showed an increasing linear trend that diminished through time. Finally, the anterior temporal lobe had a small region that also demonstrated an increasing linear trend during encoding. Finite impulse response (FIR) time courses (Figure 4.2B) of the core task-active regions (IFGpo, PM and Spt) are provided as a reference in order to interpret standard deviation results in terms of activity changes (FIR time courses were not used to calculate standard deviation across time). Time courses reveal increases in activity near the start (encoding) and end (retrieval) of trials, while the delay period had relatively constant levels of activity. Furthermore, the 6-letter condition (blue line) appears to demonstrate the greatest level of activity and also demonstrate the least variability over time, particularly during encoding and delay time periods.

In contrast to LOAD, for RATE there were overall fewer regions demonstrating a significant decreasing linear trend in standard deviation and task-active regions were generally not implicated (Figure 4.3A), similar to RATE connectivity results (Figure 4.1). However, in contrast to connectivity results, during the delay period, the most significant decreasing linear trend in standard deviation occurred in precentral and postcentral cortex, as well as parietal cortex. While there were no areas significantly demonstrating a decreasing linear trend in standard deviation in the same areas demonstrating a decreasing trend in connectivity for RATE, at a high statistical threshold (FDR $q<0.05$), at a lower threshold ($p<0.05$ uncorrected) there was a linear decreasing trend in standard deviation in superior temporal cortex during the delay period, similar to connectivity. Encoding and retrieval periods did not demonstrate any regions with significant decreases at a conventional voxelwise statistical threshold (FDR $q<0.05$), but various regions during encoding (postcentral gyrus, parietal, anterior temporal lobe, occipital pole) and retrieval (MFG, middle and inferior cortex, occipital cortex) revealed decreases in standard deviation at a reduced statistical threshold ($p<0.05$ uncorrected). In terms of an increasing

standard deviation, no regions demonstrated a significant increasing linear trend in standard deviation at a conventional voxelwise statistical threshold (FDR q<0.05), but various regions during encoding (MFG, IFG, SPL) and a few regions during the delay (superior frontal cortex, frontal polar) did exhibit increases in standard deviation at a reduced statistical threshold (p<0.05 uncorrected). Critically therefore, for RATE task-active regions (MFG, IFG, PM, area Spt, SPL) did not seem to demonstrate changes in standard deviation with changing task-demands (at a conventional voxelwise statistical threshold).

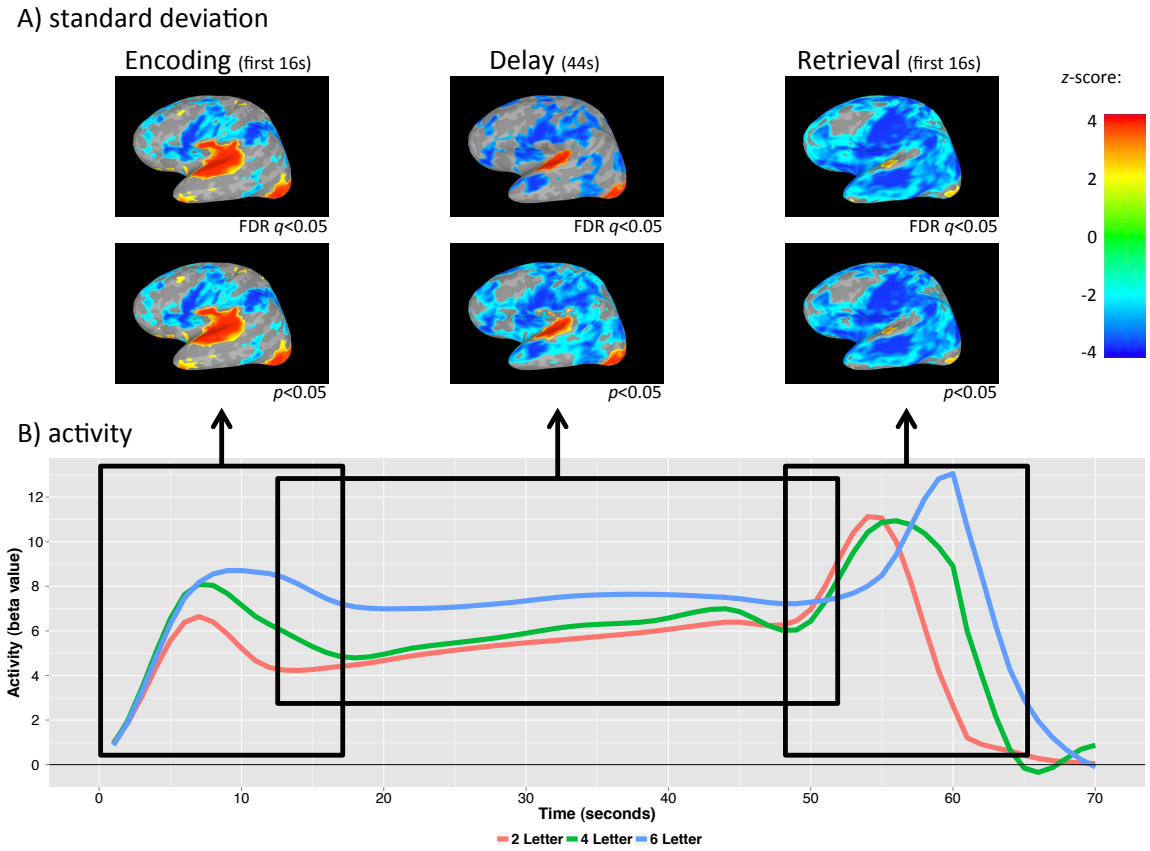

Figure 4.2: Standard deviation across time results for factor LOAD. ***A,*** Standard deviation results for encoding, delay, and retrieval time periods. Results demonstrate that during the delay period some of the same regions that demonstrated decreasing functional connectivity for factor LOAD, demonstrated decreasing standard deviation as task demands increased. Specifically, decreasing standard deviation occurred in MFG, IFG, PM, area Spt and SPL. Additionally, areas without decreasing connectivity also demonstrated decreasing standard deviation including frontal polar, anterior temporal lobe (during delay and retrieval) and inferior temporal cortex. In contrast three regions demonstrated increasing standard deviation with increasing task demands: superior temporal cortex, occipital pole and anterior temporal lobe. In all three of these regions the increase in standard deviation was highest at the start of trials (during encoding) and diminished through time. Regions with significant changes in standard deviation in encoding and retrieval were largely similar to the delay period, with larger areas of increasing standard deviation in encoding and larger areas of decreasing standard deviation in retrieval. ***B,*** FIR time courses for the core task-active ROIs (mean of

IFGpo, PM and Spt) for the entire trial are provided in order to interpret standard deviation results in relation to activity. Results demonstrate that activity increased during encoding, was relatively constant during the delay period, and then increased again during retrieval. Especially during encoding and the delay period, the condition level with the greatest task demands (6-letter, blue line) seemed to demonstrate the largest amount of activity and also exhibit the least amount of variability across time. Black boxes on time courses approximately indicate relevant time epochs. Surface data are z-scores thresholded at FDR corrected $q<0.05$ and uncorrected $p<0.05$ from the left hemisphere. Time courses plotted are group means.

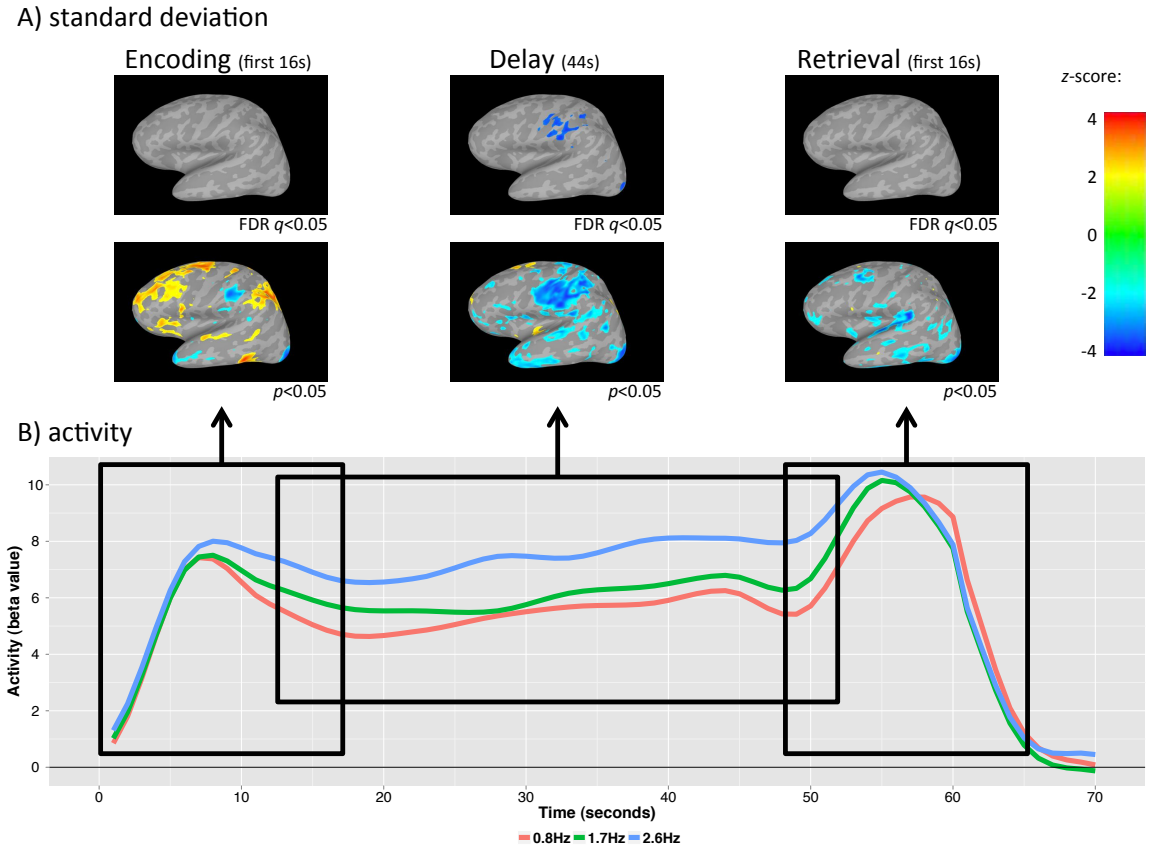

Figure 4.3: Standard deviation across time results for factor RATE. ***A,*** Standard deviation results for encoding, delay, and retrieval time periods. At a conventional voxelwise threshold (FDR $q<0.05$) the only area in any time period to demonstrate a significant change in standard deviation in relation to task demands were in precentral and postcentral cortex and parietal cortex. Over the delay period at a reduced statistical threshold ($p<0.05$ uncorrected), superior temporal cortex demonstrated decreasing standard deviation as task demands increased, the same area that demonstrated a decreasing linear trend in connectivity for RATE (Figure 4.1). In encoding and retrieval only regions at very low voxelwise statistical thresholds ($p<0.05$ uncorrected) demonstrated significant changes. ***B,*** FIR time courses for the core task-active ROIs (mean of IFGpo, PM and Spt) for the entire trial are provided in order to interpret standard deviation results in relation to activity. Only three of the total seven rehearsal rates are plotted in order to make visualization easier. Results demonstrate that activity increased during encoding, was relatively constant during the delay period, and then increased again during retrieval. In contrast to LOAD, for RATE all condition levels seem to

demonstrate approximately the same amount of variability over the delay period. Black boxes on time courses approximately indicate relevant time epochs. Surface data are z-scores thresholded at FDR corrected $q<0.05$ and uncorrected $p<0.05$ from the left hemisphere. Time courses plotted are group means.

4.3.3 Conjunction Results

To formally determine if increasing activity, decreasing standard deviation, and decreasing connectivity effects were all occurring in the same spatial locations during the delay period, a conjunction analysis was performed. Linear trend analyses for activity (beta values), standard deviation, and connectivity (using an area Spt seed) for both LOAD and RATE were independently thresholded at the group level and then combined in various conjunctions (Figure 4.4).

For LOAD, [increasing linear trend in activity] ∩ [decreasing linear trend in standard deviation] was primarily demonstrated in task-active regions including MFG, IFG, PM, area Spt and SPL. Very few other areas demonstrated a significant conjunction for these two measures. As demonstrated by this conjunction analysis, regions with a significant activity effect did not obligatory demonstrate a significant standard deviation effect. Similarly, [decreasing linear trend in standard deviation] ∩ [decreasing linear trend in connectivity] was mainly demonstrated in task-active regions such as IFG, PM and SPL (although the SPL in this conjunction seems to be in a slightly different location than typically activated by this task (Chapter 3). Regions with a significant standard deviation effect did not obligatory demonstrate a significant connectivity effect, however, there were only a few areas that demonstrated a significant connectivity effect without a standard deviation effect (superior PM areas). A triple conjunction [increasing linear trend in activity] ∩ [decreasing linear trend in standard deviation] ∩ [decreasing linear trend in connectivity] was primarily demonstrated in task-active areas including IFG and PM at high statistical thresholds, and MFG, area Spt and SPL at lower statistical thresholds.

In contrast, for RATE many of the task-active regions did not demonstrate significant conjunctions. Specifically, while [increasing linear trend in activity] ∩ [decreasing linear trend in standard deviation] was demonstrated in PM and area Spt (and a very small area in IFG), only area Spt demonstrated [decreasing linear trend in standard deviation] ∩ [decreasing linear trend in connectivity] as well as a significant conjunction involving all three measures. However, since area Spt was used as the seed region in the connectivity analysis it is difficult to interpret what a decrease in connectivity within this same region signifies. Also demonstrating a significant triple conjunction at a lower threshold were some PM and occipital regions. Of note, some of the same superior temporal cortex areas that showed a significant decreasing linear trend in connectivity (Figure 4.1) also demonstrated a significant [decreasing linear trend in standard deviation] ∩ [decreasing linear

trend in connectivity] conjunction, although this area did not demonstrate an activity effect. In summary, for LOAD all three of the effects seemed to be co-occur in the same task-active regions, while for RATE the effects seemed to co-occur in different regions, depending on the conjunction.

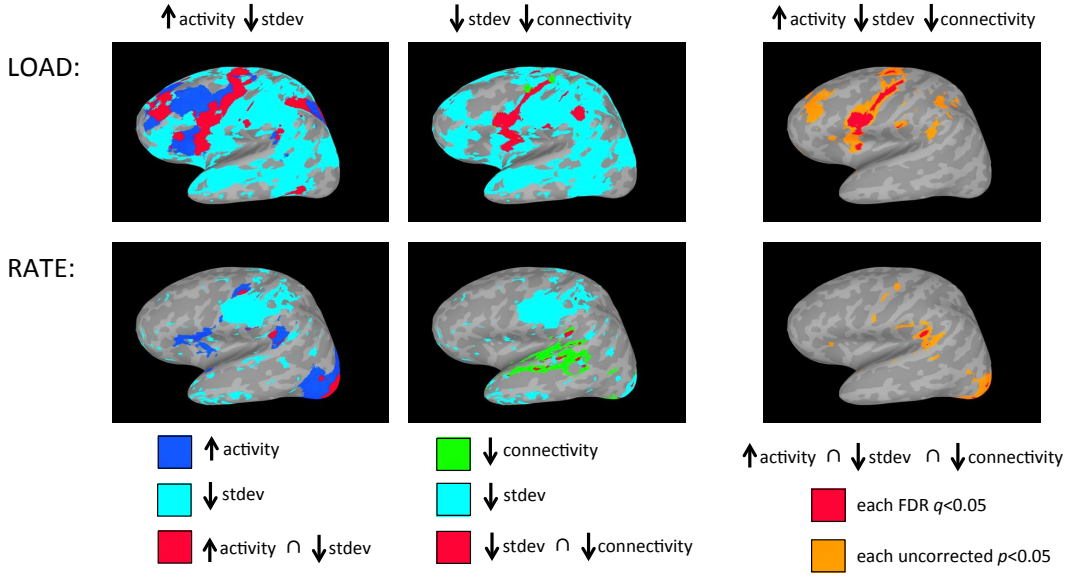

Figure 4.4: Conjunction analysis. Three separate conjunction results for factors LOAD (top) and RATE (bottom). For each conjunction, the left hemisphere individual group linear trend surface maps (activity, standard deviation, connectivity) during the delay period were separately thresholded at single-tail FDR q<0.05 and combined (triple conjunction was additionally presented at separately thresholded at p<0.05 uncorrected). For LOAD, [increasing activity]∩[decreasing standard deviation] occurred in the task-active regions MFG, IFG, PM, area Spt and SPL, while [decreasing standard deviation]∩[decreasing connectivity] occurred in task-active areas IFG, PM and SPL. The triple conjunction, [increasing activity]∩[decreasing standard deviation]∩[decreasing connectivity], was demonstrated at high thresholds in the core task areas IFG and PM, while at lower thresholds, the task-active areas MFG, IFG, PM, area Spt and SPL demonstrated all three effects. For RATE, [increasing activity]∩[decreasing standard deviation] occurred in the task-active regions IFG (very small area), PM and area Spt, while [decreasing standard deviation]∩[decreasing connectivity] occurred only in task-active area Spt as well as superior temporal cortex. The triple conjunction, [increasing activity]∩[decreasing standard deviation]∩[decreasing connectivity], demonstrated that at high thresholds only area Spt demonstrated all three effects (which may be difficult to interpret since it was the seed region), while at lower thresholds, some portions of PM and occipital cortex demonstrated all three effects. In general for both LOAD and RATE, activity/standard deviation/connectivity effects did not obligatorily co-occur together (e.g. there are areas with significant activity changes but no standard deviation changes). The abbreviation stdev (standard deviation across time) is the same as in the rest of the manuscript and was only used in this figure to save space.

4.3.4 Region of Interest Results

To determine the pattern of effects in the core task-active regions for LOAD and RATE, an ROI analysis of activity (beta value), standard deviation, and connectivity was performed (Figure 4.5).

Results for LOAD revealed that the core task-active regions (IFGpo, PM and area Spt) exhibited a negative relationship between activity and standard deviation. Specifically, as task demands increased, activity increased, while standard deviation decreased. Furthermore, both measures seemed to demonstrate the same non-linear effect: a small difference from 2-letter to 4-letter conditions, but then a much larger change from 4-letter to 6-letter conditions. In contrast, core task-active regions seemed to demonstrate a positive relationship between standard deviation and connectivity. Specifically, as task demands increased both the standard deviation and connectivity seemed to decrease. However, the correspondence between these two measures does not seem to be as strong as the correspondence between activity and standard deviation. For example, the connectivity between IFGpo and PM does not appear to strongly resemble the combined standard deviation patterns of IFGpo and PM.

Similarly, results for RATE demonstrated that IFGpo, PM and area Spt exhibited a negative relationship between activity and standard deviation as task demands increased, although the individual patterns for standard deviation are only significant in 1/3 regions (area Spt). Conversely, there does not seem to be a correspondence between standard deviation and connectivity values for RATE in these core task-active regions. While in all three ROIs standard deviation trends or significantly decreases as task demands increase, connectivity seems to increase (IFGpo-PM; $p<0.05$), stay approximately constant (IFGpo-Spt; $p=0.86$), and non-significantly decrease (PM-Spt; $p=0.24$). Permutation linear trend analyses for data in Figure 4.5 is listed in Table 4.1.

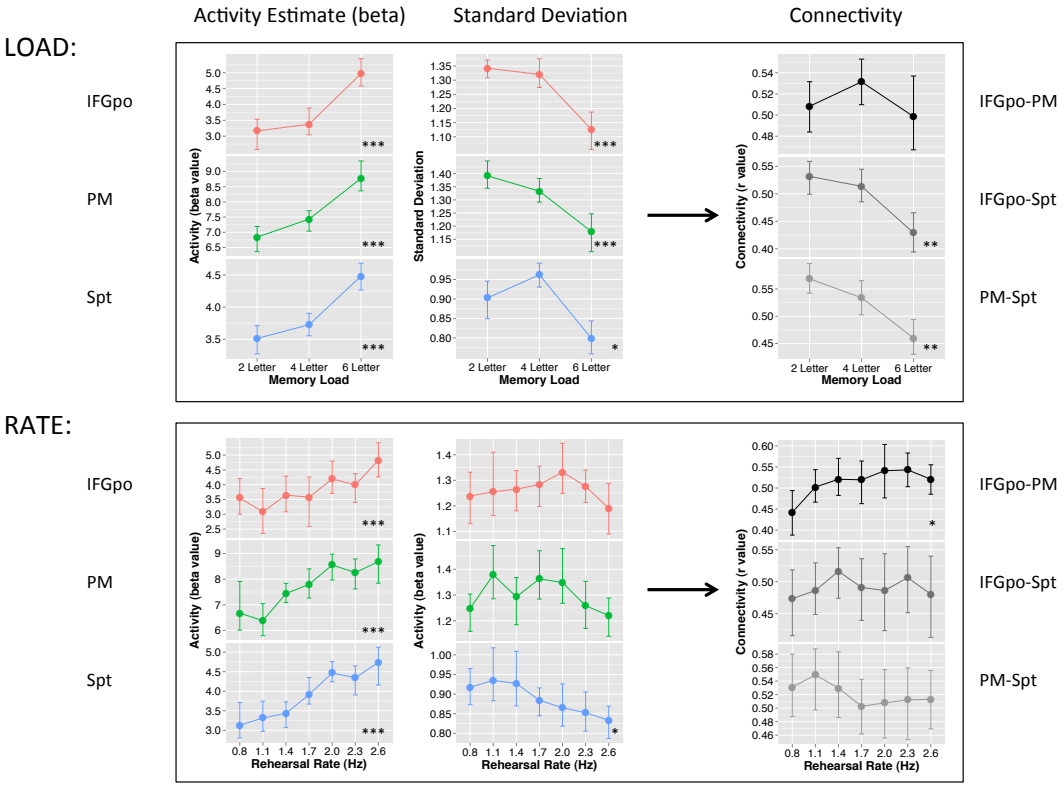

Figure 4.5: Region of interest results. ROI analysis was performed on activity (left), standard deviation across time (middle), and connectivity (right) for the core task-active regions IFGpo, PM and area Spt for factors LOAD (top) and RATE (bottom). For activity and standard deviation the ROI labels are in the left margin; for connectivity the two ROIs used to generate the plotted correlation values are in the right margin. Permutation linear trend statistical results are included as asterisks in the bottom right of each plot. Results for LOAD (top) demonstrate a negative relationship between activity and standard deviation. Specifically, as task demands increased, activity non-linearly increased (small change from 2 to 4-letter, large change from 4 to 6-letter) while standard deviation non-linearly decreased. In contrast, standard deviation and connectivity seem to exhibit a positive relationship with both decreasing as task demands increased. Results for RATE (bottom) demonstrate a negative relationship between activity and standard deviation (although only area Spt demonstrated a significant decreasing trend). However, in contrast to LOAD, for RATE there did not seem to be a systematic relationship between standard deviation and connectivity as the correlation either significantly increased (IFGpo-PM), remained approximately constant (IFGpo-Spt), or non-significantly decreased (PM-Spt). Data plotted are group means. Error bars represent bootstrapped within-subject 95% confidence intervals. ***p<0.0001, **p<0.001, *p<0.05.

Table 4.1: ROI permutation linear trend statistical results.

LOAD:		Activity	Stdev	Connectivity	
IFGpo	linear coefficient	1.28	-0.15	-0.0069	IFGpo-PM
		$p<0.0001$	$p<0.0001$	$p=0.64$	
PM	linear coefficient	1.37	-0.15	-0.073	IFGpo-Spt
		$p<0.0001$	$p<0.0001$	$p<0.001$	
Spt	linear coefficient	0.68	-0.074	-0.077	PM-Spt
		$p<0.0001$	$p<0.01$	$p<0.001$	

RATE:					
IFGpo	linear coefficient	1.17	-0.0067	0.063	IFGpo-PM
		$p<0.0001$	$p=0.98$	$p<0.05$	
PM	linear coefficient	2.056	-0.051	0.0059	IFGpo-Spt
		$p<0.0001$	$p=0.67$	$p=0.86$	
Spt	linear coefficient	1.49	-0.090	-0.028	PM-Spt
		$p<0.0001$	$p<0.05$	$p=0.24$	

4.3.5 Correlation: Activity and Standard Deviation Results

To statistically demonstrate the relationship between activity and standard deviation, a trial-by-trial correlation between activity and standard deviation was performed. For each subject an activity estimate (beta value) and the standard deviation across time was computed for each trial, and a Spearman rank correlation was computed on all 42 trials. Within the core task-active regions IFGpo, PM and area Spt, most subjects demonstrated a negative correlation between activity and standard deviation (Figure 4.6A). Specifically, 18/24 subjects for IFGpo, 16/24 subjects for PM and 19/24 subjects for area Spt all showed a negative correlation. Across all subjects for each ROI, the group median correlation value negative and was significant (Table 4.2).

A Pearson correlation analysis demonstrated similar results (median Pearson correlation coefficient, Fisher Z transform and one-sample *t*-test - IFGpo: -0.17, $p<0.01$; PM: -0.11, $p<0.05$; Spt: -0.15, $p<0.001$). To determine if this negative relationship occurred only in these core task-active regions, the analysis was carried out in a voxelwise fashion (Figure 4.6B, C). Results demonstrated that a negative relationship between activity and standard deviation significantly occurred in primarily task active areas including MFG, IFG, PM, area Spt, SPL and occipital cortex at both high and low thresholds (Figure 4.6B). Notably, only the negative correlation was significant at a conventional group statistical threshold (FDR $q<0.05$). A positive

correlation between activity and standard deviation was significant at a lower threshold (p<0.05 uncorrected) in anterior temporal lobe and lateral parietal cortex. In general, the Spearman correlation coefficient was highest in the same areas that were most significant including MFG, SPL, IFG, PM, area Spt and occipital cortex (Figure 4.6C). However, the areas showing a positive relationship between activity and standard deviation, anterior temporal lobe and parietal cortex, also demonstrated high Spearman correlation coefficients.

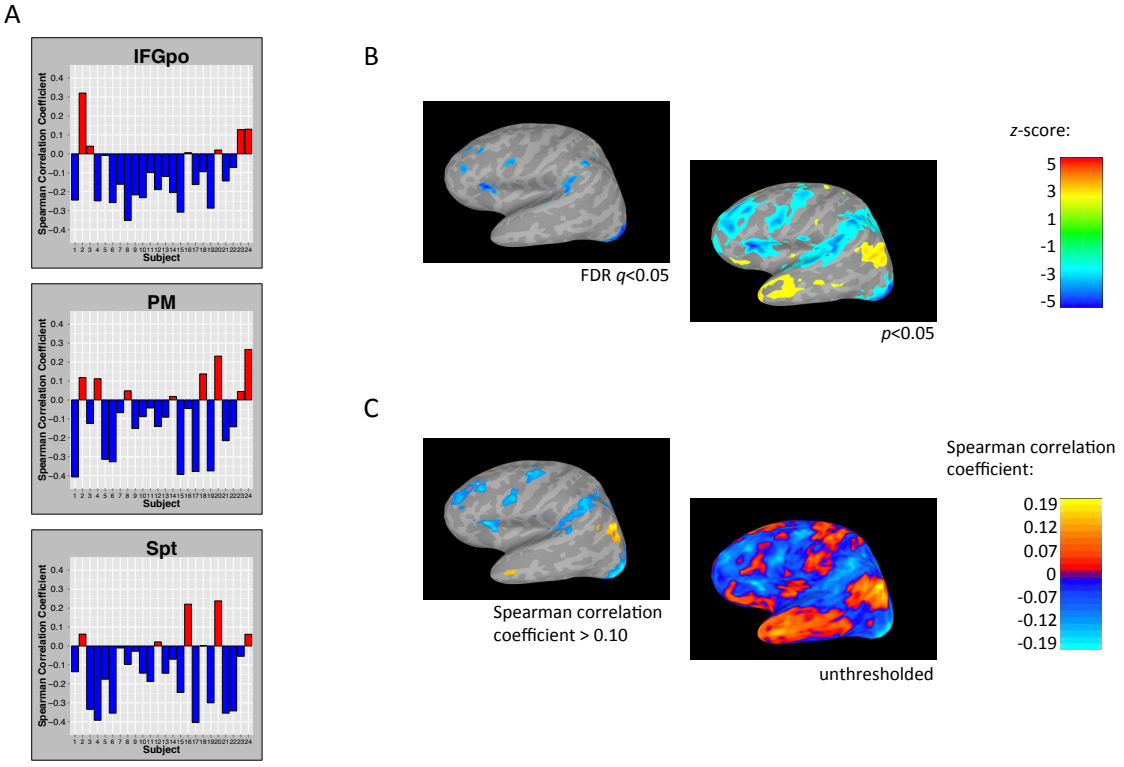

Figure 4.6: Correlation between activity and standard deviation across time. For each subject, activity estimates (beta values) and standard deviation across time for all 42 trials were entered into a Spearman rank correlation. ***A,*** ROI analysis of core task-active regions: IFGpo (top), PM (middle), area Spt (bottom). Bar plots depict Spearman correlation coefficient (y-axis) of each individual subject (x-axis). Red signifies a positive correlation, while blue signifies a negative correlation. Results demonstrate that the majority of subjects have a negative correlation between activity and standard deviation (i.e. most bars are blue). ***B,*** Voxelwise correlation statistical results. Results demonstrate that a negative relationship between activity and standard deviation was statistically significant in primarily task active regions: MFG, IFG, PM, area Spt, SPL and occipital cortex. A positive relationship between activity and standard deviation was only significant at a lower statistical threshold (p<0.05 uncorrected) in anterior temporal lobe and lateral parietal cortex. ***C,*** Whole-brain correlation coefficient results. In general, the Spearman correlation coefficient was highest in the same task-active regions that also demonstrated significant correlations: MFG, IFG, PM, area Spt, SPL and occipital cortex. In addition, the anterior temporal lobe and lateral parietal cortex demonstrated high positive Spearman correlation coefficient values. Surface data are from the left hemisphere and are FDR corrected q<0.05 or uncorrected p<0.05. Group median Spearman correlation coefficient values are displayed on surface maps.

Table 4.2: Group ROI Spearman rank correlation results. Top: median Spearman correlation coefficient value. Bottom: statistical significance after converting correlation values with Fisher Z transform and submitting to one-sample *t*-test.

	IFGpo	PM	Spt
Group Spearman Correlation Coefficient	-0.15	-0.09	-0.14
	$p<0.01$	$p<0.05$	$p<0.01$

4.3.6 Correlation: Standard Deviation and Connectivity

To statistically demonstrate the relationship between standard deviation and connectivity, a trial-by-trial correlation between standard deviation across time and connectivity was performed. For each two time series, a median standard deviation and a connectivity value between the time series were computed for each trial, and a Spearman rank correlation was computed on all 42 trials per subject. Within the core task-active regions IFGpo, PM and area Spt, most subjects demonstrated a positive correlation between standard deviation and connectivity (Figure 4.7A). Specifically, 24/24 subjects for IFGpo-PM, 22/24 subjects for IFGpo-Spt, and 24/24 subjects for PM-Spt all showed a positive correlation. Across all subjects for each ROI, the group median correlation value was positive and was highly significant (Table 4.3).

A Pearson correlation demonstrated similar results (median Pearson correlation coefficient, Fisher Z transform and one-sample *t*-test - IFGpo-PM: 0.35, $p<0.0001$; IFGpo-Spt: 0.34, $p<0.0001$; PM-Spt: 0.39, $p<0.0001$). To determine if this positive relationship occurred only in these main task-active regions, the analysis was carried out in a voxelwise fashion using either IFGpo, PM or area Spt as the seed region (Figure 4.7B, C). Results demonstrated that the positive relationship between standard deviation and connectivity did not only occur in task-active regions, but significantly occurred in many regions across the brain (Figure 4.7B). However, task-active regions such as IFG and PM demonstrated the most significant correlation values. Notably, very few areas showed a statistically significant negative correlation, such as parietal cortex.

In general, depending on the seed region used, the Spearman correlation coefficient was highest in the same areas exhibiting the highest statistical significance. Specifically, the task-active areas MFG, IFG, PM, area Spt, SPL and occipital cortex all demonstrated high Spearman correlation coefficient values (Figure 4.7C). When area Spt was used as a seed region, superior temporal regions also demonstrated high correlation values. Unthresholded maps revealed that only a few regions demonstrated a negative relationship between standard deviation and connectivity. Specifically, portions of the anterior temporal lobe, parietal cortex, frontal pole and superior frontal gyrus revealed negative correlation coefficients.

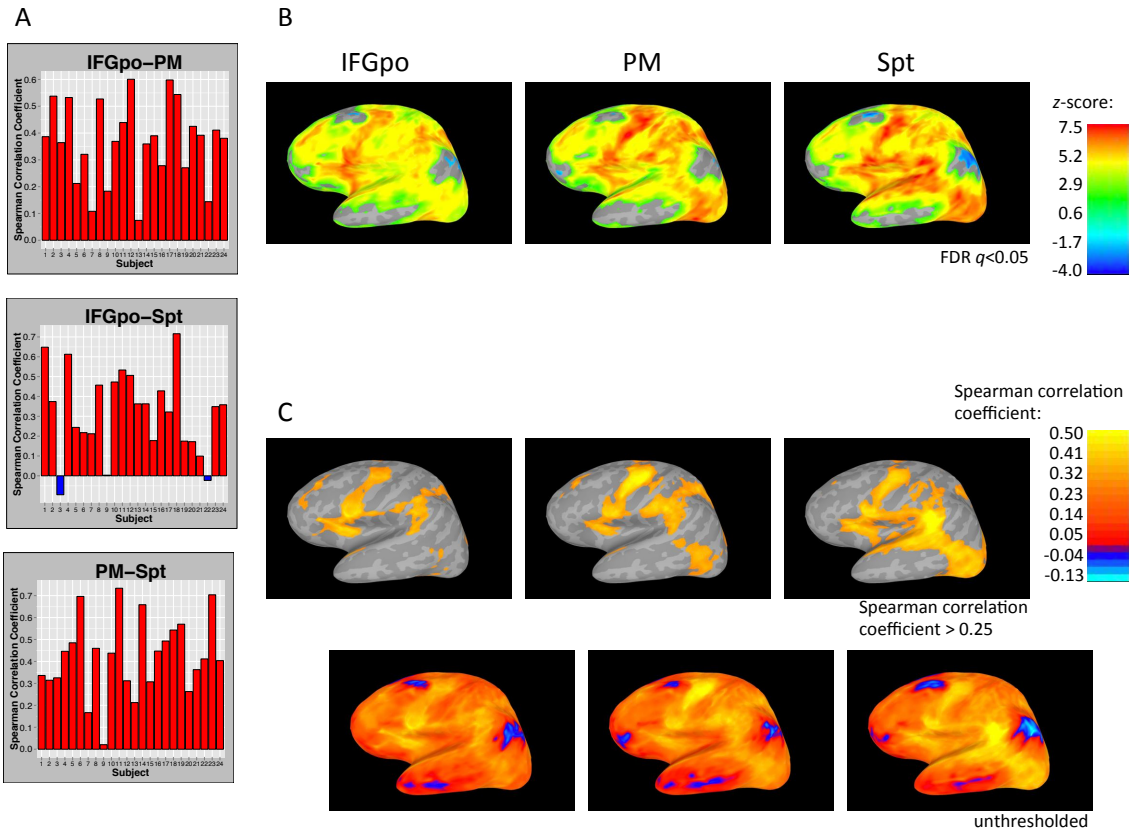

Figure 4.7: Correlation between activity and standard deviation across time. Same analysis depicted in ROI (A) and voxelwise (B, C) forms. The standard deviation across time was calculated separately for the two ROIs (A) or for the seed region and target voxel (B, C) and then the median value for the two was computed. Additionally, the correlation (connectivity) for the fMRI BOLD time series for the two ROIs (A) or for the seed region and target voxel (B, C) was computed. Subsequently, for each subject, the median standard deviation for the two regions and the connectivity value between the two regions for all 42 trials were entered into a Spearman rank correlation. ***A,*** ROI analysis of core task-active regions: IFGpo-PM (top), IFGpo-Spt (middle), PM-Spt (bottom). Bar plots depict Spearman correlation coefficient (*y*-axis) of each individual subject (x-axis). Red signifies a positive correlation, while blue signifies a negative correlation. Results demonstrate that the majority of subjects have a positive correlation between standard deviation and connectivity (i.e. most bars are red). ***B,*** Voxelwise correlation statistical results using three different seed regions: IFGpo (left), PM (middle), area Spt (right). Results demonstrate that the correlation between standard deviation and connectivity was statistically significant in many areas, including both task-active areas and areas not generally active in this task. Very few areas, such as parietal cortex, demonstrated a statistically significant negative correlation between standard deviation and connectivity. ***C,*** Voxelwise correlation coefficient results using three different seed regions: IFGpo (left), PM (middle), area Spt (right). In general, the Spearman correlation coefficient was highest in the core task-active areas: IFG, PM and area Spt. Additionally, the task-active areas MFG, SPL and occipital cortex also demonstrated high correlation coefficient values. Unthresholded maps (bottom) demonstrated that very few regions exhibited a negative correlation between standard deviation and connectivity: anterior temporal lobe, parietal cortex, frontal pole and superior frontal gyrus. Surface data are from the left hemisphere and are FDR corrected $q<0.05$ or uncorrected $p<0.05$. Median Spearman correlation coefficient values are displayed on surface maps.

Table 4.3: Group ROI Spearman rank correlation results. Top: median Spearman correlation coefficient value. Bottom: statistical significance after converting correlation values with Fisher Z transform and submitting to one-sample *t*-test.

	IFGpo-PM	IFGpo-Spt	PM-Spt
Group Spearman Correlation Coefficient	0.38	0.35	0.42
	$p<0.0001$	$p<0.0001$	$p<0.0001$

4.4 Discussion

The activity (beta value), standard deviation across time, and functional connectivity (linear correlation) of the fMRI BOLD signal was investigated in the core task-active regions (IFGpo, PM, area Spt) during the delay period of a verbal working task while the factors load and rate were manipulated. Decreasing functional connectivity was found in both task-active areas (for load) and non task-active areas (for rate) as task demands increased for both factors. When the standard deviation across time of the fMRI BOLD signal was investigated, the same decreasing linear trend was demonstrated in many of the same regions that the functional connectivity analysis revealed decreases in. A conjunction analysis formally demonstrated that increasing activity, decreasing standard deviation and decreasing connectivity were occurring in task-active regions for load, while for rate there were regions demonstrating two out of the three conjunctions, but very few areas demonstrating all three conjunctions (both in task-active or non task-active regions). AN ROI analysis on the core task-active regions for load revealed that as activity increased, standard deviation decreased and connectivity decreased as task demands increased, while for rate there seemed to be a weak relationship between activity and standard deviation and no relationship between standard deviation and connectivity. The relationship between activity and standard deviation was formally investigated by a trial-by-trial correlation analysis of the two measures and in general revealed the two parameters were negatively correlated, especially in task-active areas. A similar correlation analysis performed on standard deviation and connectivity, revealed that standard deviation and connectivity were in general positively correlated, especially in task-active regions.

4.4.1 Decrease in Functional Connectivity

In contrast to our predictions, we found linear decreasing functional connectivity as task demands increased in both load and rate conditions (Figure 4.1). These decreases occurred both in task-active regions (load) as well as non task-active regions (rate). A priori we had predicted that at least some (if not all) of the core task-active regions (IFGpo, PM, area Spt) would demonstrate increased functional connectivity with increased task demands in response to an increase in information, which seems to be the general finding in the majority of cortical areas in task-related functional connectivity studies (Sakai et al. 2002; Woodward et al. 2006;

Fiebach et al. 2006; Kayser et al. 2010). However, in regards specifically to verbal WM, it may be hard to form predictions since only a few studies have reported functional connectivity findings. In a beta-series functional connectivity analysis during the delay period, it was demonstrated that an inferotemporal cortex seed was more correlated with MFG, anterior insula, middle occipital gyrus and cerebellum for 5-words greater than 2-words. In the voxelwise analysis, no areas demonstrated a decrease in functional connectivity (Fiebach et al. 2006). In a psychophysiological interactions effective connectivity analysis during the delay period, it was demonstrated that a left anterior caudate seed increased connectivity with left posterior parietal cortex, ventrolateral prefrontal cortex and pre-supplementary motor area for a high-load relative to low-load condition (remember 5 different numbers versus remember 5 of the same number). While their connectivity analysis only examined regions that demonstrated significant univariate load effects, they report 16 left and right cortical areas that demonstrated increased connectivity with a caudate seed as memory load increased and no areas that decreased connectivity (Chang et al. 2007). It should be noted that these connectivity techniques are different than the analyses used in the current study and it's unclear how they relate. It should also be noted that not all verbal WM studies only found increases in connectivity as some have found decreases (see below for details), and one study found although memory load task-demands altered univariate activity they did not alter connectivity (Narayanan et al. 2005). Furthermore, although our prediction assumes that task demands will increase connectivity, an increase in information may not necessitate an increase in functional connectivity, as increases or decreases in functional connectivity may be more related to the context of the operation being performed by each cortical region in a network (Fuster 1995; McIntosh 2000; Fuster 2003). It is currently unknown exactly what modulates functional connectivity and what increases or decreases in connectivity functionally signifies.

We cannot definitely rule out that the decrease in functional connectivity represents a neural process such as a decrease in neural communication between cortical regions as task demands increase. There have been a few reports in the literature of decreased connectivity due to task demands in healthy subjects, although none demonstrating uniform decreases across all cortical areas. During a visuospatial working memory task an electroencephalography (EEG) study found decreases in alpha-band functional connectivity, however, this was only short-range connectivity (among frontal electrodes) as long-range connectivity (frontal to parietal electrodes) showed theta-band increases in functional connectivity (Sauseng et al. 2005). In an fMRI verbal WM task it was demonstrated that during a subvocal rehearse condition relative to an articulatory suppression condition, left ventral PM cortex showed negative psychophysiological interaction connectivity with left intraparietal sulcus, bilateral inferior parietal lobule, anterior intermediate frontal sulcus (BA 46), left inferior frontal sulcus and pre-supplementary motor area (Gruber et al. 2007). Additionally, Broca's area demonstrated negative connectivity with bilateral inferior frontal sulcus, but only at non-significant thresholds. In other words, this study seems to demonstrate increases in activity in the phonological

loop are correlated with decreases in activity in domain general central-executive areas (e.g. frontal and parietal cortex) relative to task demands. However, the authors do not comment on nor provide the data on how connectivity within the phonological loop is altered by task demands. In a delayed face recognition task, an fMRI study found as memory load was parametrically increased the right IFG showed linearly decreasing functional connectivity with the FFA while, in contrast, the hippocampus showed linearly increasing functional connectivity with the IFG and FFA over the delay period (Rissman et al. 2007). The authors believed that at low memory loads the IFG-FFA network was all that was required to maintain the task-relevant information, but at higher memory loads its capacity was exceeded, requiring the involvement of the hippocampus in the network. It should be noted that this study used beta-series correlation as their measure for functional connectivity, which may or may not be similar to this study's correlations on the actual fMRI BOLD time series. What seemed counterintuitive about our finding was not just decreased connectivity, but that almost all areas showing significant changes in connectivity were exhibiting decreases in connectivity. If some regions had demonstrated a decrease in connectivity while others had demonstrated an increase in connectivity, then we may have not fully investigated why the connectivity was decreasing with increasing task demands.

It is known that the fMRI BOLD signal correlates with different LFP frequencies in different conditions (Goldman et al. 2002; Laufs et al. 2003; Moosmann et al. 2003; Kayser et al. 2004; Mukamel et al. 2005; Goense & Logothetis 2008; Maier et al. 2008; Scheeringa et al. 2008). It has also been shown in some EEG and magnetoencephalography (MEG) studies that certain frequency bands demonstrate decreases in connectivity while other frequency bands show concomitant increases in connectivity (Sauseng et al. 2005; Bartolomei et al. 2006). Therefore, one possible explanation for our finding of decreased functional connectivity is that both increases and decreases in connectivity are in fact occurring, but fMRI BOLD is more sensitive to decreases in connectivity.

In direct contrast to our predictions, another possibility is that although task-active regions demonstrate increases in activity, they may uniformly demonstrate decreases in functional connectivity. This may occur as limited cortical resources are devoted to local processing at the expense of network processing. Although we were unable to locate any evidence for this in the literature, it remains a possibility.

4.4.2 Standard Deviation and Task

In order to investigate the counterintuitive decreasing functional connectivity findings, the standard deviation across time was investigated. While it is common in fMRI analysis to compute a mean activity estimate in some fashion (here, estimated by a beta value from multiple linear regression), it is becoming evident that there are measures other than the mean activity level that have useful information in fMRI BOLD. One measure that has become important recently is signal variability. While signal variability can be measured in a multitude of ways such as mean squared

successive difference (Samanez-Larkin et al. 2010), maybe the most intuitive and commonly used measure is standard deviation. The standard deviation of the fMRI BOLD signal has been shown to exhibit a spatially coherent pattern that relates to age (Garrett et al. 2010), decreases with normal aging (McIntosh et al. 2010), increases in young subjects in task relative to fixation (Garrett et al. 2012) and who were faster and more consistent on various tasks (Garrett et al. 2011) when compared to older, poorer performing subjects.

In general, we found that standard deviation decreased as task-demands increased for both load and rate (Figures 4.2, 4.3). Specifically, for load, the standard deviation decreased as task-demands increased during encoding, delay, and retrieval (Figure 4.2) in most task-active areas. As suggested by the FIR time courses, this effect may be due to higher levels of activity having a restricted range of variability. In contrast, two areas demonstrated an increase in standard deviation as task-demands increased: superior temporal cortex and occipital cortex. While these areas are not generally active during the delay period when task conditions are compared, they are activated during the encoding period (data not shown). Specifically, superior temporal cortex contains auditory responsive regions while occipital cortex contains visually responsive regions. Therefore, these regions are most likely responding to the letters being presented in a visual and auditory manner during encoding. We therefore believe their FIR time courses would appear different than those presented for encoding and would instead reveal a typical HRF that begins and returns to baseline after the stimulus event, thus leading to an increase in standard deviation as task demands increase.

While there have a few studies investigating the standard deviation of fMRI BOLD signals, we were unable to find any study investigating signal variability comparing task-to-task or parametric manipulations within the same task, as our study demonstrates. One study that did investigate the standard deviation of the fMRI BOLD signal that did have multiple tasks, matched behavioral performance across tasks and did not report or comment on any task-versus-task standard deviation changes (Garrett et al. 2012). However, several studies have investigated signal variability in task relative to rest. One study assessed the standard deviation of the fMRI BOLD signal in rest (view fixation cross) versus three different task conditions: perceptual matching, attentional cueing and delayed match to sample tasks. They demonstrated that all three tasks increased the standard deviation of the signal relative to rest in a variety of different brain regions (Garrett et al. 2012). However, other studies have revealed a decrease in signal variability with activation. Specifically, it has been shown that signal variance (McAvoy et al. 2008) and standard deviation (Bianciardi et al. 2009) decrease in the visual cortex in an eyes-open versus eyes-closed condition, and a detrended fluctuation analysis revealed a reduction in variance in many cortical areas during a button-press task relative to resting-state fixation in a variety of cortical areas (He 2011). Additionally, signal variability has been shown to decrease in the default-mode network in a 2-back working memory task relative to rest (Fransson 2006). It is unclear why these various studies found discrepant results. Some of the differences may be

attributable to the measure of signal variability used and the time window analyzed. Regardless, our results seem to agree with the later findings that signal variability decreases in task relative to rest. Our results extend these findings by suggesting that as task-demands increase signal variability continues to decrease.

4.4.3 Activity (beta value) and Standard Deviation

We found that activity (beta values) and standard deviation of the fMRI BOLD signal were related, occurring spatially in the same regions (Figure 4.4) and exhibiting a negative relationship with one another (Figure 4.5, 4.6). Specifically, in conjunction analyses for load and rate, both effects occurred primarily in task-active regions and did not obligatorily occur together, suggesting this relationship is not solely a general property of fMRI BOLD but is modulated to some degree by task. Furthermore, we found a negative relationship between activity (beta values) and standard deviation, such that higher activity values correspond with lower standard deviation values. As mentioned above, this may be due to higher levels of activity having a restricted range of variability (as suggested by FIR time courses). In contrast, two areas demonstrated a positive relationship between activity and standard deviation, anterior temporal pole and lateral parietal cortex (Figure 4.6). Notably, these areas demonstrated significant decreases in activity as task-demands increased in the univariate study (Figure 3.4 & 3.5, Chapter 3). Considering these areas are commonly implicated in the default mode network, they may be activated at rest and then deactivate during task.

Other studies have compared the mean signal with standard deviation, but generally as they relate to changes with age. Specifically, a few studies calculated the mean as a percentage change within a block, calculated the standard deviation, and then analyzed each separately with age in a partial least squares (PLS) analysis. The resulting brain patterns can be displayed on surface maps and conjunction maps can be constructed. These analyses have revealed that age-based standard deviation and mean-based patterns are nearly spatially orthogonal (McIntosh et al. 2010; Garrett et al. 2010; Garrett et al. 2011; Garrett et al. 2012). In contrast, one study investigated these parameters not in the context of age but across varying task conditions. The standard deviation and various task conditions were entered into a PLS analysis and results were displayed as spatial maps. However, the results are hard to interpret in relation to the mean activity since they did not provide the corresponding mean activity maps. Some of the cortical areas on these standard deviation map are typical task-positive regions such as inferior and dorsolateral prefrontal regions. However, other general task-active regions such as sensorimotor cortex regions did not display standard deviation changes (Garrett et al 2012). While these results superficially seem at odds with our findings, it may be hard to compare results as the latent variables in PLS may or may not be comparable to the metrics used in this study.

4.4.4 Standard Deviation and Functional Connectivity

Functional connectivity is a multivariate measure defined as temporal correlations between remote neurophysiological events (Friston, 1994). Therefore, most measures of functional connectivity rely on some form of correlation between time series across regions. For example, beta-series correlation (Rissman et al. 2004) and coherence (Sun et al. 2004) are both essentially correlations. The definition of correlation between X and Y is the covariance of X and Y divided by the product of the standard deviations of X and Y:

$$corr(X,Y) = \frac{cov(X,Y)}{\sigma_X \sigma_Y}$$

While the covariance indicates the degree of linear relationship between two variables, the product of the standard deviation is required to make the resulting correlation coefficient scale-free (so the correlation coefficient does not depend on the scale of measurement of the variables, e.g. inches or feet). The product of the standard deviations also represents the maximum possible value of the covariance – when perfectly linear, the covariance equals the product of the standard deviation. Critically, signal variability can affect both the covariance and the standard deviation (as the two parameters are somewhat dependent on one another), thus influencing the correlation coefficient.

We found that signal variability (standard deviation) and connectivity (correlation) of the fMRI BOLD signal were related, occurring spatially in the same regions (Figure 4.4) and exhibiting a positive relationship with one another (Figure 4.5, 4.7). Specifically, in conjunction analyses for load (but not rate), both effects occurred primarily in task-active regions and did not obligatorily occur together, suggesting this relationship is not solely a general property of fMRI BOLD but is modulated to some degree by task. Furthermore, we found a positive relationship between standard deviation and connectivity, such that lower standard deviation values corresponded with lower connectivity values, and higher standard deviation values were associated with higher connectivity values. While these results are only correlational in nature, we believe that signal variability is influencing the correlation coefficient. Specifically, our data demonstrate that the correlation coefficient decreased and the standard deviation decreased, therefore the covariance must have decreased as well. Furthermore, the covariance must have decreased more than the product of the standard deviation (if the covariance and product of standard deviation decreased proportionally then the correlation value would have remained the same). In other words, when there is a decrease in standard deviation of the signal there seems to be disproportionally less covariance between the two time series than the product of standard deviations of the two time series, leading to a smaller correlation coefficient. In contrast (and similar to the opposite correlation between activity and standard deviation, above), two areas demonstrated a negative relationship between standard deviation and connectivity:

portions of the anterior temporal pole and lateral parietal cortex (Figure 4.7). Notably, these areas demonstrated significant decreases in activity as task-demands increased in the univariate study (Figure 3.4 & 3.5, Chapter 3). Considering these areas are commonly implicated in the default mode network, they may be activated at rest and then deactivate during task.

Therefore, our results seem to suggest that signal variability may influence the correlation coefficient. Despite this possibility, the relationship between these two parameters has not been directly investigated in fMRI BOLD. While a few studies have examined the variability in functional connectivity across time in resting-state (Chang & Glover 2010; de Pasquale et al. 2010), they did not report on why or what was causing these fluctuations in connectivity. However, one resting-state fMRI study found that caffeine significantly increased the variability of functional connectivity between left and right motor cortices over time, and this effect was primarily due to phase differences between BOLD signals (Rack-Gomer & Liu 2012). It is unclear how these phase differences relate to signal variability or the findings of this study. Another resting-state fMRI study had the necessary data (independently calculated fMRI BOLD variance and fMRI BOLD correlations) to investigate the relationship between the two parameters, but did not report on the relationship or provide the relevant data for readers to form any conclusions (McAvoy et al. 2008). A resting-state EEG study demonstrated that functional connectivity (measured by phase lag index) and variability (measured by information content) were related as nodes from a graph theory analysis with greater degree, betweeness, and efficiency were more likely to have a higher amount of variability (Misic et al. 2011). Similarly, a second EEG study demonstrated that as variability increased with age (measured by local entropy), functional connectivity increased as well (measured by distributed entropy and phase locking) (Vakorin et al. 2011). Therefore, while both of these EEG studies used more complicated measures of signal variability and functional connectivity than this study, both found a positive correlation between signal variability and functional connectivity in agreement with the findings reported here.

4.4.5 Load versus Rate

While this study investigated how the task demands of two different factors (load and rate) influenced activity, standard deviation, and connectivity during the delay period, the two factors are critically different in that load is explicitly manipulated before the delay period (during encoding) while rate is explicitly manipulated during the delay period. Since it is well known that the HRF acts as a low-pass filter, it may be predicted that if one of the two factors would have a larger impact on the standard deviation of the fMRI BOLD signal during the delay period, it would be rate. Specifically, the faster the rehearsal rate over the delay period, the less variable (flatter) the elevated fMRI BOLD block activity would be after passing through the low-pass filter of the HRF, resulting in a decrease in standard deviation. However, while some task-active areas demonstrated a decrease in standard deviation for rate (PM and area Spt in conjunction analysis, Figure 4.4; area Spt in ROI analysis, Table

4.1), the decreased standard deviation effect was much more consistent in the task-active areas for load. Furthermore, it appeared that for load all three effects (increasing activity, decreasing standard deviation, and decreasing connectivity) occurred in all task-active regions, but for rate the effects were not as spatially consistent. Specifically, for rate, while increasing activity and decreasing standard deviation generally occurred in the main task-active regions, decreasing standard deviation and decreasing connectivity generally occurred in superior temporal cortex (which mentioned above, contains auditory responsive regions and may be responding to auditory stimuli).

It is unclear exactly why all three effects are occurring primarily for load but not rate. However, these results seem to reflect univariate activity results to some degree, as load activity effects were found to be much stronger than rate activity effects in the univariate study (e.g. Figure 3.4, Chapter 3). Therefore, if these three effects are a causal chain of events that are initiated by activity, there may be an activity threshold required to set the events in motion. However, it also appears that load and rate modulate activity over the delay period differently. If the FIR time courses for load (Figure 4.2) and for rate (Figure 4.3) are examined, there seems to be a load x slope interaction, but not a rate x slope interaction. Specifically, for load, the factor level with greatest task-demands (6-letter, blue line) seems flat relative to the other two conditions which have a positive slope (green, red lines), versus rate where all three plotted conditions seems to have the same positive slope (blue, green, red lines). This difference may lead to a more pronounced effect of task demands on standard deviation in load versus rate (as seems to be the case when comparing Figure 4.2 with Figure 4.3), which may then transfer into a greater functional connectivity effect.

4.4.6 Generalizability to other working memory studies

While many fMRI studies have investigated functional connectivity during WM tasks, it is unclear exactly how they relate to the current study. Typical WM paradigms do not explicitly control behavior during the delay period and generally assume that subjects are rehearsing the task-relevant information in some fashion for approximately 10-15 seconds before subjects are asked to recall or recognize the information at retrieval. In contrast, this study rigorously enforced very fast and regular subvocal rehearsals at constant frequencies for extremely long delay periods (45 seconds), and ensured this activity continued throughout the entire delay period. Therefore, it would be expected that the resulting fMRI BOLD time series from this study would be much more constant and less variable than the fMRI BOLD time series from other WM studies in the literature. Additionally, most WM studies do not run functional connectivity analyses directly on the fMRI BOLD time series as this study did, but instead perform a beta-series correlation functional connectivity analysis (Rissman et al. 2004) in order to eliminate issues concerning contamination of one task phase into another (e.g. encoding activity into delay period), an issue this study addressed by employing extremely long delay periods.

5

TEMPORAL DYNAMICS AND FUNCTIONAL CONNECTIVITY OF CORTICAL NETWORKS SUBSERVING VERBAL WORKING MEMORY

5.1 Introduction

Verbal WM tasks generally involve three phases: an encoding period during which the incoming task-relevant information is perceived and converted into a construct that can be stored, a delay period during which the task-relevant information is actively maintained and manipulated by subvocal rehearsal processes within the phonological loop, and a retrieval period during which the task-relevant information is accessed and recovered from memory. In verbal WM during both encoding and delay periods a separate but consistent set of cortical areas are known to be active. During auditory encoding both primary auditory cortex (Heschl's gyrus, HG) in STG as well as area Spt are known to be active (Buchsbaum et al. 2005), while during the maintenance and manipulation of verbal information over the delay period the phonological loop is known to be active: IFG, and in particular IFGpo, PM and area Spt (Buchsbaum et al. 2005; Chein & Fiez 2001). While many studies have consistently identified these cortical areas as being involved in verbal WM tasks, there is little evidence demonstrating how the different areas relate to each other in a network or even if they form a network.

One way to examine how cortical areas relate to one another is to investigate the timing of activation across cortical regions. The time-to-onset (e.g. the time it takes to achieve 20% of the maximum or peak activity) as well as the time-to-peak (Neumann et al. 2003) are two ways that the timing of regions has been studied in fMRI. In the few studies that have looked at the language system and timing, it has generally been found that language comprehension activates posterior areas such as area Spt (Wernicke's area) first, followed by frontal areas like IFG (Broca's area), while language production studies have often found the reverse order (Thierry et al. 1999; Heim & Friederici 2003). However, timing analyses are not standard in fMRI and have certain design requirements such as allowing enough time for the HRF to be estimated and knowing precisely when the events behaviorally occur, which make these analyses difficult to apply to the delay period of WM tasks.

While a timing analysis can lead to important information regarding the relation of one cortical region to another, functional connectivity analyses are required to directly show that different cortical regions are functioning as a network. However, many fMRI WM tasks use short delay periods which allows preceding encoding

period activity to contaminate delay period activity. Therefore, much of what is known about functional connectivity during the delay period is from a special technique known as beta-series correlation (Rissman et al. 2004) which may or may not relate to functional connectivity as determined by correlations directly on the fMRI BOLD signal. Additionally, no connectivity study has been designed based on the previous results (Chapter 4) which revealed that increased standard deviation of the fMRI BOLD signal is related to increased functional connectivity.

Therefore, in order to investigate the timing across regions and the functional network formed during 1) encoding and 2) the delay period of a verbal WM task, substitute tasks were used which are free from the constraints of traditional verbal WM paradigms. Specifically, a listen task was substituted for the encoding period of a verbal WM task, while a subvocal rehearsal task was substituted for the delay period of a verbal WM task. Each task was designed specifically for timing and connectivity analyses including long time blocks of continuous activity, adequate time between events to maximize signal variability, and precise behavioral control with the aid of visual pacing circles. While not exactly analogous to a verbal WM task, these tasks allow the activated cortical regions to be examined in novel ways.

We predict that during the listen condition, both primary auditory cortex (including HG), and area Spt will be active and that primary auditory cortex will activate before area Spt. We further predict that the two regions will demonstrate functional connectivity. In contrast, during subvocal rehearsal we predict that area Spt will primarily form a functional network with IFG and PM regions.

5.2 Methods

5.2.1 Subjects

Thirty-seven subjects gave informed written consent according to procedures approved by the University of California and participated in the study. All were right-handed, native English speakers, had normal or corrected-to-normal vision and normal hearing. All subjects were healthy with no neurological or psychiatric disease. One subject had unusable data due to a technical error (no transistor-transistor logic pulses being emitted from fMRI scanner) and five subjects were removed due to poor behavioral performance. This left a total of thirty-one subjects (19 females; age: 18-23, mean: 19.9).

5.2.2 Experimental Stimuli

Five low-frequency words were pseudorandomly chosen from the MRC Psycholinguistic Database (www.psy.uwa.edu.au/mrcdatabase/uwa_mrc.htm), with the only constraints that the words had to be two syllables as well as have a Kucera-Francis written frequency range of 1-5 (out of a possible 1-20). Words were chosen and converted to a female voice with text-to-speech software (built in Mac software,

voice: Victoria). Words were randomly chosen that had durations of 600msec. The final five words were: ballast, seaweed, pinkie, gourmet, and rubbish. For listen scrambled word condition (control sounds), each word was separated into six 100ms segments, randomly shuffled, and concatenated back together.

5.2.3 fMRI Task

Each trial began with a five second instruction period where an instruction was visually presented which included the condition as well as the target word to be used (if the condition involved a word). Each condition was pseudorandomly paired with a target word with the only constraint that each of the five target words was used twice with each condition overall and no target word could be used twice in the same run. This was followed by a ten second rest period where only a cross-hair was presented, followed by the start of the 60 second task block.

For each condition, during the 60 second task block a visual pacing cue (gray circle) was visually presented for a duration of 600ms ten separate times (Figure 5.1). Intervals between each pacing cue were chosen to give the HRF time to reach peak and then appreciably decrease while still keeping subjects behaviorally engaged, as well as sample the HRF at multiple time-points. Specifically, intervals of: 4000, 4200, 4500, 4800, 5100, 5400, 5700, 6100, 6600, and 7400ms were chosen based on pilot data. For each run, the intervals were randomly shuffled and then used for the interval times for all five conditions in that run (i.e. the timing of the gray pacing circles were identical in all five conditions). What subjects did when they observed a gray flashing circle differed depending on condition.

In REST condition blocks, subjects were instructed to observe the gray flashing circles as they appeared on the screen. In LISTEN SCRAMBLED WORD blocks, subjects were instructed to listen to the scrambled word, auditorily presented with each gray pacing circle. In LISTEN WORD blocks, subjects were instructed to listen to the target word, which was auditorily presented with each gray pacing circle. In SUBVOCAL REHEARSAL blocks, subjects were instructed to subvocally rehearse the target word one time, when they saw they gray pacing circle. In LISTEN THEN SUBVOCAL REHEARSAL blocks, the target word was auditorily presented with the gray flashing circle and subjects were instructed to wait until they saw a green pacing circle before subvocally rehearsing. The time interval between the listen gray circle and the subvocal rehearse green circle was pseudorandomly jittered by shuffling a distribution of interval times (500, 700, 1000, 1300, 1500, 1600, 1800, 2000ms) with the only constraint that each interval time be used once. Instead of a green circle cue, 20% of the time a red circle was presented with the instruction to do nothing (so don't subvocally rehearse the word you just heard). These catch trials were randomly mixed with the regular trials and the interval time between the gray pacing circle and the red circle were pseudorandomly chosen from the same distribution as the green pacing circles, with the only constraint that all interval times had to be used before they could be repeated.

After each 60 second task block there was a two second rest period followed by a multiple choice question (five seconds long), with the same question for all five conditions: “Word just using?” along with four possible answers visually listed. Three of the answers were randomly chosen from the list of five task words while one answer was always “none”. For subvocal rehearsal, listen word, and listen then subvocal rehearsal, the correct answer was whichever word was being used. However, if the correct word was not included on the list or the condition was rest or listen scrambled word, then the correct answer was “none”. Correct answers were balanced for answer position and the correct answer was “none” for subvocal rehearsal, listen word, and listen then subvocal rehearsal on 20% of trials. Responses were recorded with a button box and subsequently scored. A set of inter-trial interval times (3000, 3000, 4000, 5000ms) were randomly shuffled for the rest period between trials.

Each fMRI session contained ten runs that lasted approximately 7.5 minutes. Each run contained each condition (rest, subvocal rehearsal, listen word, listen scrambled word, listen then subvocal rehearsal) presented once in random order. Therefore, in total, each fMRI session contained ten 60 second blocks of each condition (two blocks for each target word).

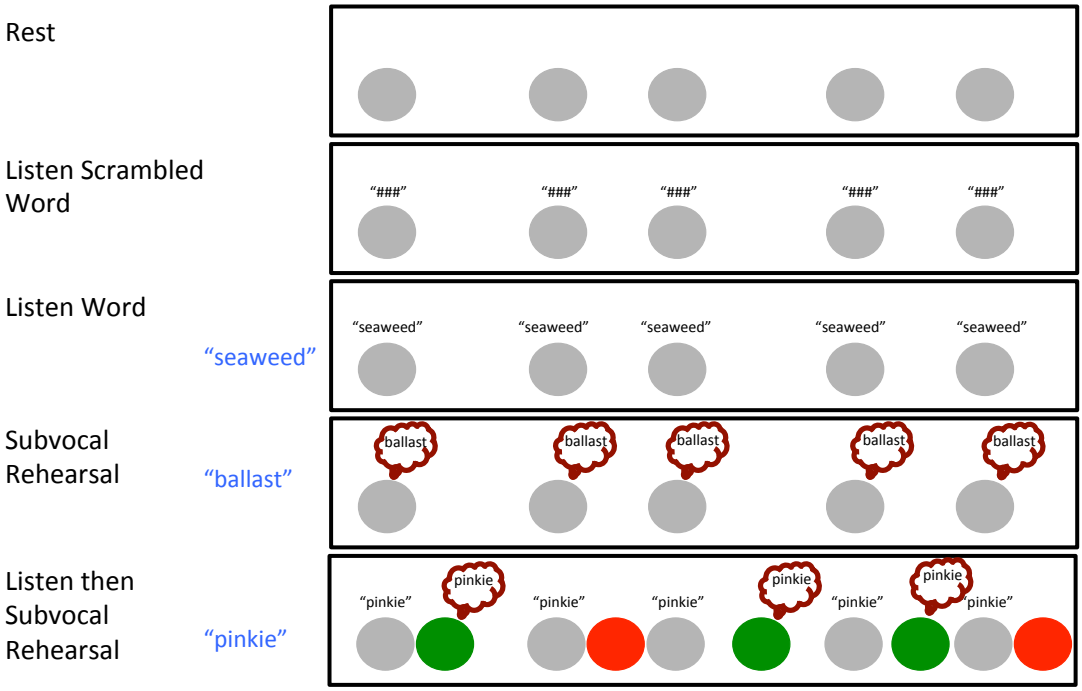

Figure 5.1: fMRI task design. Subjects (n=31) were presented with one of five conditions (listed left) which consisted of 10 events over a 60 second block. In REST blocks subjects were instructed to simply observe gray flashing circles. In LISTEN SCRAMBLED WORD blocks subjects heard the scrambled word each time a gray circle flashed. In LISTEN WORD blocks subjects heard the target word each time a gray circle flashed. In SUBVOCAL REHEARSAL blocks subjects were instructed to subvocally rehearse the target word for that trial each time they visualized a gray flashing circle. In LISTEN THEN SUBVOCAL REHEARSAL blocks subjects were instructed to listen to the word when a gray circle flashed and then wait until either a green circle flashed, at which time they were instructed to rehearse the target word, or a red circle flashed, at which time they were instructed to do nothing. If a given condition block required a word, one of five words was pseudorandomly chosen and presented along with the block instructions: ballast, seaweed, gourmet, rubbish, or pinkie. At the end of each block a multiple choice test was given. Note that in all conditions just a gray flashing circle was presented and words shown above circles in figure are to make explanation easier.

5.2.4 Functional Magnetic Resonance Imaging

5.2.4.1 Acquisition

MR data were acquired with a Siemens TIM/Trio 3 Tesla scanner (Berlin/Munich, Germany). Functional data were obtained using a 32-channel radiofrequency head coil and a 2-shot T_2^*-weighted EPI sequence sensitive to BOLD contrast (TR = 1600msec, TE = 25msec, 224mm field of view with a 72x72 matrix size, in-plane resolution 3.1mm x 3.1mm). Each functional volume contained 27 contiguous 3.3mm-thick axial slices separated by a 0.5mm interslice gap acquired in a

descending fashion. High-resolution whole-brain MP Flash T_1-weighted scans were acquired for anatomical localization.

Presentation software (Neurobehavioral Systems, Albany, CA) was used for auditory and visual stimulus delivery. Auditory stimuli were delivered via MRI-compatible form-fitting foam insert earphones (Sensimetrics, MA). Visual stimuli were presented via a liquid crystal display projector (Avotec, FL) which displayed images on a screen located in the center of the scanner bore. Subjects viewed the screen by looking at a mirror mounted on the radiofrequency coil. Button responses in the fMRI scanner were recorded with a 4-button inline fiber optic response pad (Current Designs, PA).

5.2.4.2 Pre-Processing

MRI data were converted to NifTI format. Functional data were slice-time corrected and realigned to the first acquired volume using the AFNI (Cox 1996) program 3dVolreg and spatially smoothed with a 5-mm full-width at half-maximum Gaussian kernel. No runs were removed for excessive head motion (>3mm within a single run). One run for one subject was removed due to a technical error (no transistor-transistor logic pulses being emitted from fMRI scanner). All subsequent statistical analyses were performed on these realigned and smoothed images.

In order to view the functional results on the group anatomy of the same subjects who generated them, a study specific group template was created with the program ANTS. In an iterative fashion, each subject's high-resolution anatomical scan was nonlinearly warped (SyN algorithm) into registration with one another, and a group mean image was generated. The study specific group template was then normalized to MNI space with a 12-parameter affine transformation. Each subject's high-resolution anatomical scan was nonlinearly normalized to this study specific group template in MNI space utilizing the SyN algorithm (ANTS). These warping parameters were then applied to the native space EPI data/statistical maps as needed to transform them into normalized template space. The study specific group template and group functional data were converted to surface maps for visualization purposes (SUMA).

5.2.4.3 Statistical Analyses

Regression modeling within each subject was performed with the AFNI program 3dDeconvolve. Most events were modeled with a one parameter SPM gamma variate basis function (included in AFNI: SPMG1). For listen then subvocal rehearsal condition, an amplitude modulated response model was utilized. Linear repetition suppression effects were regressed out with an amplitude modulated regressor using mean-centered trial number within block as a modulator. All instruction and answer periods were also modeled with a SPMG1 function. For each scanning run a set of nuisance regressors (constant term plus linear, quadratic, and polynomial terms up to and including eight) were included to remove low frequency noise.

Head movement was also regressed out of the time series data. Statistical contrasts at the single-subject level were carried out in native space and were computed as weighted sums of the estimated beta coefficients divided by an estimate of the standard error, resulting in a *t*-statistic. Each subject's *t*-statistic map was normalized to group template space. Random effects group analyses were computed on *t*-values instead of beta coefficients because *t*-values are more normally distributed at the group level (Thirion et al. 2007). Left-hemisphere group results were corrected for multiple comparisons by thresholding to $q<0.05$ using the FDR method.

5.2.4.4 Region of Interest Definition

ROI were created to be used in timing and connectivity analyses. ROIs were created for the main areas of interest: IFGpo, PM, HG and area Spt. In general, cortical ROIs were first anatomically constrained and then searched within for the most active voxels in native space on a subject-by-subject basis. In the end, each subject had a native-space ROI defined for every area of interest.

For IFGpo and PM the anatomical regions were derived from the Harvard-Oxford Cortical and Subcortical Structural Atlas (included in FSL: http://www.fmrib.ox.ac.uk/). Anatomical regions were taken in normalized space at 100% thresholded probability and a group level [SUBVOCAL REHEARSAL$_{(p<0.001)}$] ∩ [LISTEN WORD$_{(p<0.001)}$] conjunction mask was applied. Within these regions the voxel with the highest *t*-value for the contrast [SUBVOCAL REHEARSAL] + [LISTEN WORD] was identified and encircled with a 10mm sphere. These spheres were then re-intersected back with the original atlas mask. Because area Spt is functionally (as opposed to anatomically) defined, at the group level the voxel with the highest *t*-value located near the Sylvian fissure at the parietal-temporal boundary was located (so no Harvard-Oxford atlas mask was used) and encircled with a 10mm sphere. Because the Harvard-Oxford atlas mask for HG was so small to begin with, the top-voxel and 10mm sphere at the group level was not used and instead the entire anatomical mask was used in the second step of ROI definition (below).

These group masks were then non-linearly reverse normalized into native space for each subject. Because these ROIs were to be used in a timing analysis, all voxels in ROIs had to contain active voxels for the two main conditions of interest, subvocal rehearsal and listen word. This was achieved by creating a conjunction mask of [SUBVOCAL REHEARSAL$_{(p<0.05)}$] ∩ [LISTEN WORD$_{(p<0.05)}$] and multiplying the reverse normalized group mask for each subject. Subsequently, within this mask the voxel with the highest *t*-value for the contrast [SUBVOCAL REHEARSAL] + [LISTEN WORD] was identified and the top-9 highest *t*-value contiguous voxels were found, resulting in a top-10 voxel ROI. However, in some instances the requirement to only include active voxels (i.e. the conjunction mask) was so restrictive that some subjects did not have certain ROIs defined or the number of contiguous voxels surrounding the top-voxel resulted in ROIs that were less than 10 voxels. Specifically, two subjects did not have an IFGpo ROI, one subject did not have a PM

ROI, six subjects did not have a HG ROI, and three subjects did not have an area Spt ROI. For defined ROIs, the group mean number of voxels for each ROI was at or near ten: IFGpo: 9.8 voxels, PM: 10 voxels, HG 9.6 voxels, area Spt: 8.9 voxels.

Subsequently, each subject's Spt ROI was manually assessed. In five subjects the Spt ROIs were incorrectly located. In these five subjects the top voxel was manually located that was clearly in the planum temporale and this top voxel was used to create the ROI.

Ventricle and white matter nuisance ROIs were also created. Pure anatomical ROIs were manually created using each subject's mean EPI. Ventricle 10 voxel contiguous voxel ROIs were created by finding high intensity voxels in the temporal horn of the left hemisphere lateral ventricle. White matter 10 voxel contiguous voxel ROIs were created by finding voxels located in the left hemisphere that were superior to the ventricles and medially located. Voxels away from gray matter were chosen.

5.2.4.5 Timing Analysis

Trial averaged time courses were derived by single-subject regression modeling implementing a CSPLIN response model (3dDeconvolve). Each event was modeled with 8 basis functions over a 16 second time-window. An activity estimate (beta value) was generated by interpolation for every 100ms. Linear repetition suppression effects and motion were regressed out of the signal. For each scanning run a set of nuisance regressors (constant term plus linear, quadratic, and polynomial terms up to and including eight) were included to remove low frequency noise.

For voxelwise timing analysis to ensure only active voxels were included, an activity mask was generated for each condition. Activity maps (*t*-values) for each condition were thresholded at $p<0.05$ and surviving voxels were used to mask the FIR time courses (e.g. subvocal rehearsal at $p<0.05$ was used to mask subvocal rehearsal FIR time courses). Both time-to-onset (time to 20% of peak) and time-to-peak were calculated before being warped to normalized space. Resulting maps were used to calculate group median times and were used in non-parametric group *t*-tests and masked with [SUBVOCAL REHEARSAL$_{(\text{FDR } q<0.05)}$] + [LISTEN WORD$_{(FDR\ q<0.05)}$] to aid in viewing. For ROI timing analysis, activity masks were not used since only voxels that passed the [SUBVOCAL REHEARSAL$_{(p<0.05)}$] ∩ [LISTEN WORD$_{(p<0.05)}$] conjunction were used to generate the ROIs. For each ROI the mean FIR time course was extracted and time-to-onset (time to 20% of peak) and time-to-peak were calculated.

5.2.4.6 Functional Connectivity Analysis

Each 60 second task block was extracted from the longer run. Within each subject's native space an area Spt ROI was used to extract fMRI BOLD time-series. A correlation analysis on the BOLD time series was then carried out with an area Spt

seed utilizing multiple linear regression (3dDeconvolve) with regressors of no interest (motion, white-matter, ventricle) and nuisance regressors (constant and linear terms). The correlation coefficient was calculated and then Fisher Z transformed to make the distribution more normal. Each subject's Fisher Z map was then normalized to template space and group testing was carried out with paired t-tests (3dttest++). For ROI analysis, IFGpo, PM, HG and area Spt ROIs were used to extract fMRI BOLD time series. Motion, white-matter, ventricle and nuisance terms (constant plus linear) were regressed out of each time series before the ten time series in each condition were concatenated. Correlations (1dCorrelate) were then carried out on each condition specific concatenated time series.

5.2.4.7 Analysis of fMRI Behavioral Data

fMRI behavioral data was scored as either "correct", "incorrect", or "no response" (both "incorrect" and "no response" were counted as errors). Subjects that did not have an average score => 90% correct were removed to ensure all subjects were not falling asleep or inattentive while in the scanner (n=5 removed, mean accuracy=74%). One subject scored 92% overall but had one run where they scored 40% correct. Therefore, this one run was removed from all behavioral and fMRI analyses.

5.3 Results

5.3.1 Behavioral Data

Analysis of the behavioral data revealed performance on the multiple choice questions was near ceiling (Figure 5.2) as expected. Group-averaged behavioral accuracy was very similar across conditions with REST: 97%, LISTEN SCRAMBLED WORD: 96%, LISTEN WORD: 97%, SUBVOCAL REHEARSAL: 97% and LISTEN THEN SUBVOCAL REHEARSE: 98%. Of the total errors, 56% were due to "no response" and 44% were due to "incorrect". None of the conditions were statistically different from one another (p>0.05 by permutation statistical testing).

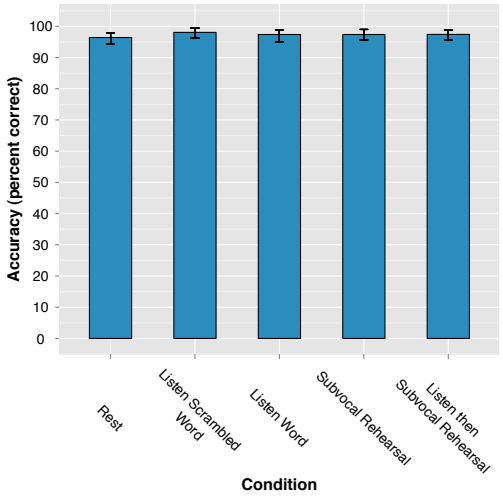

Figure 5.2: fMRI behavioral data. Accuracy data from multiple choice test given at the end of each condition block was graded as either correct or error (including both incorrect answers and no response). Results demonstrated that performance in all conditions was near ceiling and approximately equal across conditions. None of the conditions were statistically different from one another (p>0.05 by permutation statistical testing).

5.3.2 Functional Magnetic Resonance Imaging Results

To determine how the two conditions of interest modulate activity levels, activity estimates (t-values) were entered into a paired t-test at the group level (Figure 5.3). SUBVOCAL REHEARSAL versus LISTEN WORD revealed that IFG, PM, STS, area Spt and SPL were significantly more active. LISTEN WORD versus REST revealed that STS was significantly more active at a conventional voxelwise statistical threshold (FDR q<0.05), while superior frontal cortex, area Spt, and SPL were significant at a reduced threshold (p<0.05 uncorrected). SUBVOCAL REHEARSAL versus LISTEN WORD revealed that IFG, PM, anterior temporal lobe and parietal areas were significantly more active in SUBVOCAL REHEARSAL, while STG was significantly more active in LISTEN WORD.

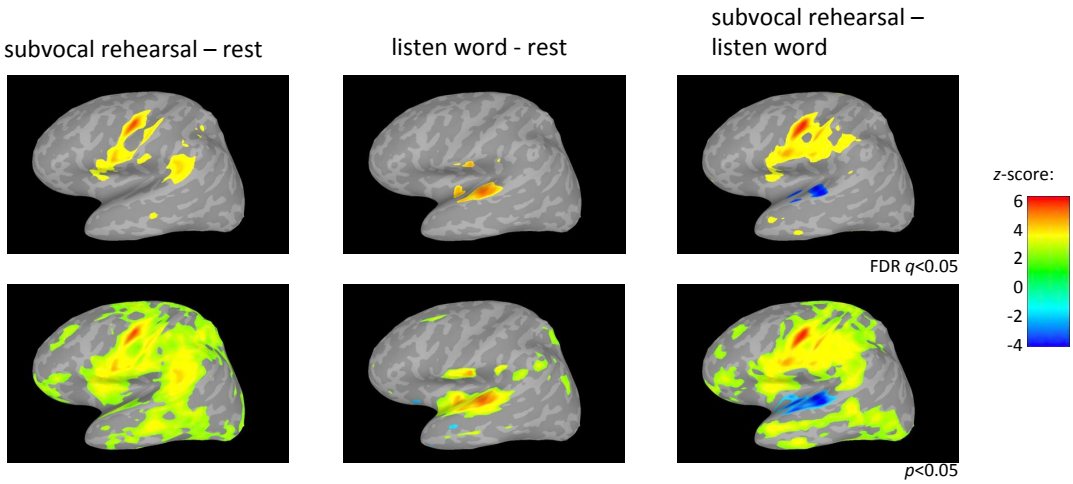

Figure 5.3: Group fMRI activity results. Activity estimates (*t*-values) for each condition were entered into a paired *t*-test. When SUBVOCAL REHEASAL was contrasted against REST (left), IFG, PM, STS, area Spt and small portions of SPL were significantly more active at a conventional voxelwise statistical threshold (FDR $q<0.05$). When LISTEN WORD was contrasted against REST (middle), STG was significantly more active at a high threshold (FDR $q<0.05$), while at a reduced threshold superior frontal cortex, area Spt, and SPL were significantly active ($p<0.05$). When SUBVOCAL REHEARSAL was contrasted against LISTEN WORD (right), IFG, PM, anterior temporal lobe and parietal areas were more active in SUBVOCAL REHEARSAL, while STG was significantly more active in LISTEN WORD (FDR $q<0.05$). Data from left hemisphere; data shown are *z*-scores thresholded at FDR $q<0.05$ and uncorrected $p<0.05$.

5.3.3 Timing Results

Time courses were modeled with FIR basis functions and two commonly used timing measures were calculated: time-to-onset (time to 20% of peak) and time-to-peak (Figure 5.4). For LISTEN WORD, both time-to-onset and time-to-peak revealed that activity began first in STG/STS before approximately occurring in area Spt and middle temporal gyrus followed approximately by IFG and PM regions. Conversely, for SUBVOCAL REHEARSAL, both time-to-onset and time-to-peak revealed that activity occurred approximately at the same time in IFG, PM and area Spt and much later in STG/STS. The timing across conditions was statistically assessed with a non-parametric *t*-test. Results demonstrated that for time-to-onset STG/STS was significantly different as were small regions of IFG, PM and Spt. Comparing conditions in time-to-peak similarly revealed significant differences in STG/STS and very small regions of IFG, PM and Spt.

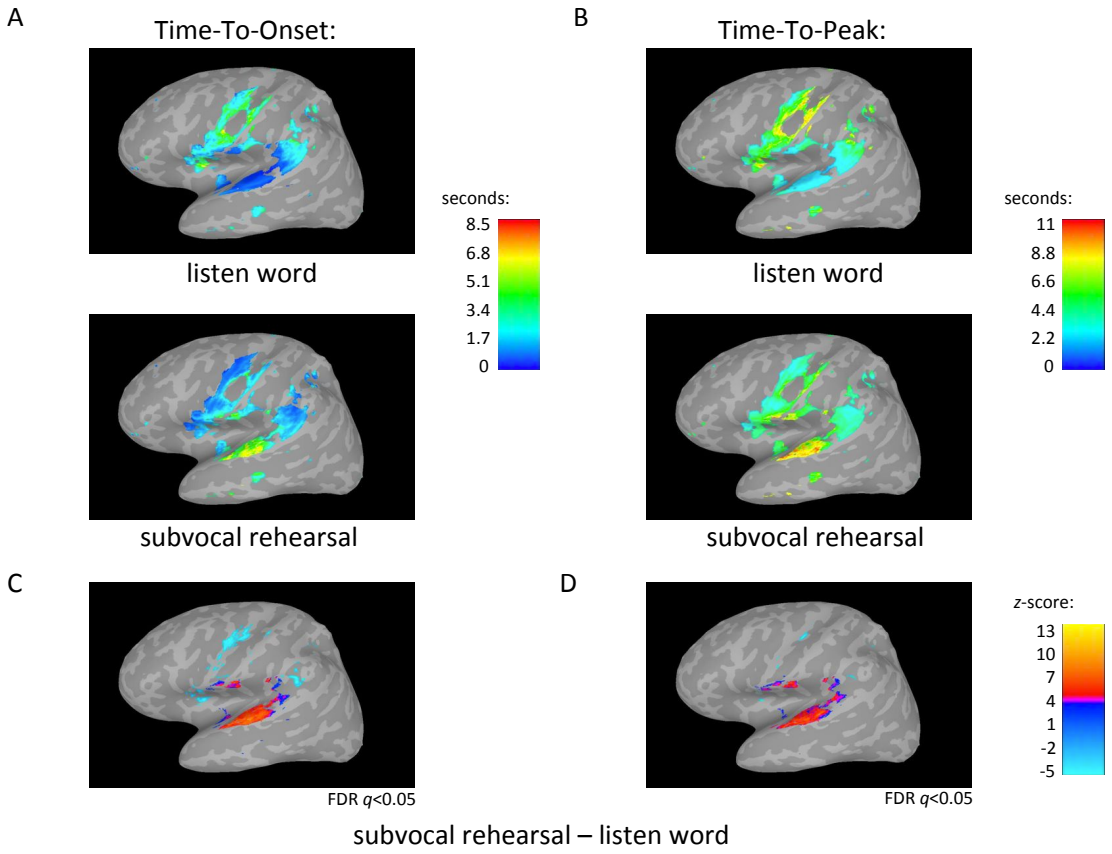

Figure 5.4: Voxelwise timing results. Trial averaged FIR time courses were generated for each condition and then multiplied by a corresponding activity mask (p<0.05) to ensure only active regions were included in the analysis. Therefore, for the LISTEN WORD condition for each subject in native space the LISTEN WORD activity map (t-values) were thresholded at p<0.05 and only surviving voxels were used in the FIR timing analysis. Both time-to-onset (time to 20% of peak) and time-to-peak were calculated and then spatially normalized and the median value across the group was calculated. For visualization, group values were masked with [SUBVOCAL REHEARSAL $_{(\text{FDR } q<0.05)}$] + [LISTEN WORD $_{(\text{FDR } q<0.05)}$] from Figure 5.3 (for visualization to focus on group active regions). ***A,B,*** time-to-onset and time-to-peak results for LISTEN WORD (top) and SUBVOCAL REHEARSAL (bottom). Results demonstrate that in LISTEN WORD activity starts first in STG/STS before approximately occurring in area Spt and middle temporal gyrus, followed approximately by IFG and PM regions. Conversely, in SUBVOCAL REHEARSAL activity seems to approximately occur at the same time in IFG, PM, and area Spt followed much later by activity in STG/STS. ***C,D,*** non-parametric t-test results for [SUBVOCAL REHEARSAL] – [LISTEN WORD] for time-to-onset (left) and time-to-peak (right) masked by active regions (as described above) and thresholded at FDR q<0.05 within those surviving regions. Results demonstrate that both timing measures were significantly different in STG/STS across the two conditions, and that small areas of IFG, PM and Spt were significantly different across conditions, more so in time-to-onset than time-to-peak. Data from left hemisphere only.

To examine the timing across IFG, PM and area Spt in more detail, an ROI timing analysis was performed. For each subject FIR time courses were extracted with functionally defined ROIs in native space and subsequently analyzed. For LISTEN WORD, both timing measures revealed that activity began first in PM (median time-to-onset: 0.75 seconds; median time-to-peak: 3.00 seconds), then area Spt (median time-to-onset: 1.10 seconds; median time-to-peak: 3.10 seconds) followed by IFGpo (median time-to-onset: 1.50 seconds; median time-to-peak: 4.50 seconds). Similarly, for SUBVOCAL REHEARSAL, activity began first in PM (median time-to-onset: 0.95 seconds; median time-to-peak: 4.15 seconds), followed by area Spt (median time-to-onset: 1.00 seconds; median time-to-peak: 4.50 seconds), and then IFGpo (median time-to-onset: 1.40 seconds; median time-to-peak: 5.00 seconds). Both timing measures were entered into a 2-way permutation repeated-measures ANOVA with CONDITION and ROI modeled as within-subject factors and SUBJECT modeled as a random effect, however, neither the main effect of CONDITION, the main effect of ROI, nor the interaction of CONDITIONxROI was significant (all $p>0.05$) for both timing measures. However, while inspecting individual FIR time courses it was noted that many did not resemble typical HRFs (double and triple peaks, etc.) which led to peaks outside of the generally reported 4-6 seconds. Therefore, it is unclear how much the voxelwise and group timing results can be trusted and the issue needs to be further investigated.

5.3.4 Connectivity Results

To obtain evidence that the active regions form a distributed functional network, an area Spt seed functional connectivity analysis was preformed. For LISTEN WORD and SUBVOCAL REHEARSAL an area Spt fMRI BOLD time series was extracted and correlated with the fMRI BOLD time-series of every voxel. The functional connectivity in the two conditions was directly compared with a paired *t*-test (Figure 5.5). In LISTEN WORD relative to SUBVOCAL REHEARSAL, area Spt had significant correlations with STG/STS at a conventional statistical threshold (FDR $q<0.05$), and with MFG and frontal polar at a lower threshold ($p<0.05$). In SUBVOCAL REHEARSAL relative to LISTEN WORD, area Spt had significant correlations with PM, postcentral gyrus, and parietal regions at a conventional voxelwise statistical threshold (FDR $q<0.05$), and IFG and inferior temporal regions at lower threshold ($p<0.05$). Therefore, area Spt had significant correlations with different cortical regions in SUBVOCAL REHEARSAL versus LISTEN WORD.

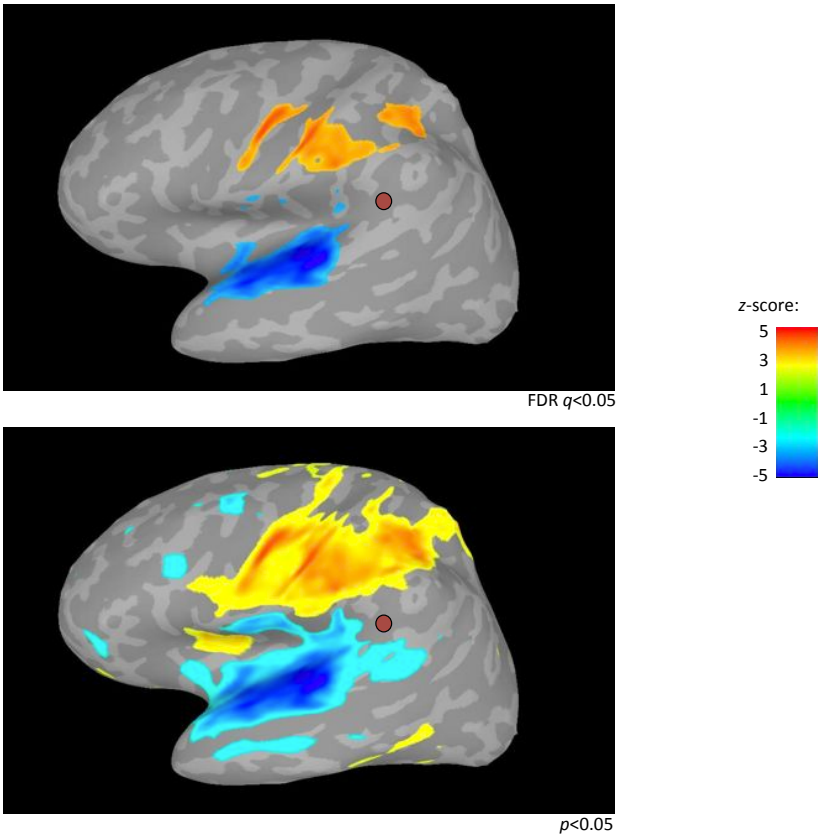

Figure 5.5: Functional connectivity results. An area Spt seed was used in an fMRI BOLD correlation analysis for LISTEN WORD and SUBVOCAL REHEARSAL. Correlation values were Fisher Z transformed and submitted to a paired *t*-test to determine connectivity differences between the two conditions. Results demonstrate that area Spt is significantly more correlated in LISTEN WORD with STG/STS areas, while in SUBVOCAL REHEARSAL area Spt is more correlated with PM, postcentral gyrus, and parietal regions at a conventional voxelwise threshold (FDR $q<0.05$) and with IFG and inferior temporal regions at a lower threshold ($p<0.05$). For visualization purposes only, maroon circles represents approximate location of area Spt (seed ROI) at the group level. Data from left hemisphere; data shown are *z*-scores thresholded at FDR $q<0.05$ and uncorrected $p<0.05$.

To further examine connectivity in key regions, ROI connectivity analyses were performed. All pairwise combinations of ROIs were entered into a correlation analysis. One ROI pair was significantly more correlated in LISTEN WORD relative to REST: HG-Spt (median *r* value for listen: 0.63; $p<0.01$, df=23, permutation *t*-test). Conversely, three ROI pairs were more significantly correlated in SUBVOCAL REHEARSAL relative to REST: IFGpo-PM (median *r* value for rehearse: 0.51; $p<0.01$, df=28, permutation *t*-test) IFGpo-Spt (median *r* value for rehearse: 0.59; $p<0.01$, df=26, permutation *t*-test) and PM-Spt (median *r* value for rehearse: 0.60; $p<0.01$, df=27, permutation *t*-test). When correlation values for LISTEN WORD and SUBVOCAL REHEARSAL were directly compared, only two ROI pairs were significantly different. PM-Spt was more correlated in SUBVOCAL REHEARSAL than

LISTEN WORD (p<0.05, df=27, permutation t-test), while HG-Spt was more correlated in LISTEN WORD than SUBVOCAL REHEARSAL (p<0.001, df=23, permutation t-test).

5.4 Discussion

In this fMRI study we investigated both the timing and functional connectivity during two important phases of verbal WM: encoding (with a listen word task), and the delay period (with a subvocal rehearsal task). We demonstrated that during the listen word task primary auditory cortex activated before area Spt and that the two regions functionally formed a network. Furthermore, we demonstrated that during the subvocal rehearsal task activity occurred first in PM, then area Spt, followed by IFGpo. We then also demonstrated that these three regions formed a functional network.

5.4.1 Timing

Our results demonstrate that during listening, activity occurred first in STG/STS before occurring in area Spt. While the task used in this study is a listening task and not a language comprehension task per se, the two tasks do share some resemblances and in general, our results agree with other language comprehension timing studies. Specifically, an fMRI study using target auditory stimuli found that it took 3 seconds after stimulus to reach peak in primary auditory cortex and 4 seconds to reach peak in superior temporal gyrus anteriorly and posteriorly from primary auditory cortex, although the differences were not significant (Belin et al. 1999). Similarly, in an fMRI auditory sentence comprehension task, it was demonstrated that activity first occurred in Heschl's gyrus with longer latencies in anterior and posterior directions (Brauer et al. 2008).

Our results also demonstrate during listening that activity occurred first in PM, then in area Spt, followed by activity in IFGpo. While most language and verbal WM timing studies do not comment on PM, the relationship between area Spt and IFGpo seems to agree with findings from other studies. Specifically, both fMRI and MEG studies have demonstrated earlier temporal (Wernicke's) activation than IFG (Broca's) activation in language comprehension tasks (Thierry et al. 1999; Kober et al. 2001; Heim & Friederici 2003; Brauer et al. 2008; Pulvermuller & Shtyrov 2009) with a difference between time-to-peak across regions of approximately 3 seconds being reported with fMRI: Wernicke's 2.85 seconds, Broca's 5.61 seconds (Thierry et al. 1999).

In contrast to language comprehension studies, language production timing studies have generally found the reverse. For example, an fMRI study found earlier time-to-peak in Broca's area than Wernicke's area with a difference across regions of approximately 3 seconds: Wernicke's 7.00 seconds, Broca's 4.39 seconds (Heim & Friederici 2003). This seems to be at odds with our results, as we found that during

subvocal rehearsal activity first occurred in PM, then area Spt, followed by IFGpo. However, there are some studies with findings that may agree with our results. An electrocorticography (ECoG) study reported that speech production begins in the peri-rolandic cortices (pre- and post-central gyri) before occurring in other areas, including posterior middle temporal gyrus and then spreading to posterior superior temporal sulcus (Edwards et al. 2010). In an ECoG meta-analysis review paper, it was found that in auditory language production tasks activity began in middle and posterior superior temporal gyrus and sulcus (200-500ms post-stimulus) as well as in inferior frontal peri-rolandic areas before occurring in STG and STS as well as supramarginal gyrus, IFG, and peri-rolandic areas (Llorens et al. 2011).

As explained above, in general it is believed that comprehension and production engage the same language cortical regions but with variable dynamics. One set of theoretical models used to explain these findings essentially states that conceptually speech production is the reverse of speech perception: from the conceptual, to the word form, to phonological representation levels (Dell et al. 1997; Levelt et al. 1998; Jacquemot & Scott 2006). Also as explained above, our results do not support models that state language production and language comprehension are the reverse of each other and instead suggest the two processes may engage the same cortical regions with the same cortical dynamics. However, as mentioned above, this may be due to our task not being exactly a comprehension task but more of a listening task. Although subjects were instructed and trained not to rehearse during listening, we cannot rule out that after hearing a target word they then subvocally rehearsed the word, leading to similar results between the subvocal rehearsal and listen word conditions. Another theoretical concern in language are serial versus parallel models. Some recent studies have found evidence in support of parallel instead of serial models (Rodriguez-Fornells et al. 2002; Edwards et al. 2010). While in this study it is difficult to delineate what exactly are overlapping and non-overlapping activations, it seems as though PM and area Spt activations are occurring very close in time while IFGpo occurs much later. Therefore, it may be the case that these results suggest parallel processing with PM and area Spt followed by serial processing with IFGpo.

5.4.2 Caveats with timing

fMRI timing studies have to be interpreted with caution since fMRI BOLD activity and not the electrophysiological signal is being measured. For example, it has been revealed that larger blood vessel diameter leads to longer temporal delays (Lee et al. 1995). It is also well known that different cortical areas exhibit different fMRI BOLD time courses (Thierry et al. 1999; Duann et al. 2002; Anemuller et al. 2006). Therefore, it is not clear how the underlying electrical activity maps onto the neurovascular cascade measured by fMRI BOLD, but one technique is to study the timing across the same set of regions with different tasks to determine if the timing changes. Essentially, the neurovascular coupling to the underlying electrophysiological activity is kept constant, therefore any changes in timing can be attributed to timing changes in the underlying electrical activity as a function of task.

While it has been shown that area Spt responds to speech perception (Buchsbaum et al. 2005), there is also mounting evidence that regions such as IFG and PM traditionally associated with speech production are also involved in speech perception (Wilson et al. 2004; Edwards et al. 2010). Therefore, this study was designed to activate the same set of regions (IFG, PM, Spt) with two different tasks (listen word, subvocal rehearsal) with the hope of finding a ROIxCONDITION interaction in timing. However, none of the ROI timing results were significant including the ROIxCONDITION interaction. However, as noted with the surface maps it appears that the listen word condition used in this task did not activate IFG and PM even at a very low voxelwise statistical threshold (p<0.05 uncorrected). It is unclear why the results of this study seem to be at odds with other studies, but it may be due to the listen word condition used in this task. Specifically, hearing a single word repeated ten times over a 60 second time period may not activate areas such as IFG and PM.

5.4.3 Connectivity

Due to many of the technical constraints required for functional and effective connectivity analyses, there have been only a few verbal working memory studies that have reported functional connectivity findings that relate to our findings. In a verbal WM fMRI task using beta-series correlation during the delay period, it was demonstrated that an area Spt seed showed greater connectivity with dorsolateral prefrontal cortex and PM, while a middle STS seed had greater connectivity with IFG (Buchsbaum et al. 2005). While it is unclear exactly how beta-series correlations compare with correlations directly on the fMRI BOLD signal, and the tasks compared are not exactly equivalent, we found no evidence that the ROI used in our study in STG/STS (Heschl's gyrus) exhibited any connectivity with any other regions except area Spt. However, it is not even clear the same region of STG/STS was used in both studies. In a second fMRI study using a Sternberg task involving letters, ROI correlations on the fMRI BOLD signal during the delay period revealed a functional network involving MFG (BA 9), IFG (BA 44), primary motor cortex (BA 4), and parietal cortex (BA 40) (Narayanan et al. 2005). With the exception of the dorsolateral prefrontal cortex, these results are very similar to ours showing functional connectivity between IFG, PM and area Spt during subvocal rehearsal.

In addition to verbal WM studies, there have been a few language studies that have looked at functional or effective connectivity. In general, their results agree with our findings and in some cases their causality findings add to our results. An fMRI language study found that Broca's and Wernicke's areas were correlated at rest, and that during a listening task this correlation increased and Broca's area became additionally correlated with left premotor cortex (Hampson et al. 2002). In an ECoG word production study it was demonstrated that perisylvian language sites had causal interactions with mouth and tongue areas of motor cortex with spoken language, but causal interactions with hand and arm areas of motor cortex with sign language (Korzeniewska et al. 2011).

6

CONCLUSIONS AND FUTURE DIRECTIONS

6.1 Summary of novel experimental results

In the series of studies presented we examined the cortical mechanisms underlying verbal WM. While the initial study (Chapter 2) was designed specifically to study connectivity in verbal WM, the connectivity analyses ultimately returned a null result which was counterintuitive considering the task was specifically designed for this purpose. However, the long delay periods used in this study demonstrated that control regions MFG and SPL could be temporally dissociated from storage/rehearsal regions IFG, PM and area Spt.

During the first study, the novel use of visual pacing cues to prompt subvocal rehearsal made us realize that in addition to memory load, subvocal rehearsal rate could be manipulated. Therefore, the second study (Chapter 3) investigated memory load and rehearsal rate effects in verbal WM. This demonstrated that control regions MFG and SPL were not sensitive to manipulations in rehearsal rate but were non-linearly sensitive to manipulations in memory load. In contrast, storage/rehearsal regions IFG, PM and area Spt were sensitive to manipulations in both rehearsal rate and memory load. It was also revealed that all task-active regions (not just MFG and SPL) demonstrated decreasing memory load effects through time, while in the regions sensitive to rehearsal rate, the effects persisted through time. It was also revealed that memory load and rehearsal rate were confounded behaviorally and that individual differences in verbal span may be partly explained by high capacity individuals having less activity in MFG, SPL and IFG, but more activity in PM. After these univariate effects were examined in detail, this same data-set was examined with a connectivity analysis (Chapter 4). It was discovered that increasing task demands decreased the standard deviation of the fMRI BOLD signal over the delay period, which seemed to then decrease functional connectivity (correlation) measures. These effects seemed especially prominent in task-active areas across memory load conditions. These results help clarify the counterintuitive functional connectivity finding of the first study (Chapter 2) as functional connectivity seems to be strongly related to signal variability.

Realizing there was an association between the standard deviation of the fMRI BOLD signal and the correlation between signals across regions, the third study (Chapter 5) was designed to maximize signal variability while still keeping subjects behaviorally engaged. This led to the development of substitute tasks for the

encoding period (listen to word condition) and the delay period (subvocal rehearsal condition) of typical verbal WM tasks. This study demonstrated that during the listen word condition primary auditory cortex and area Spt were functionally connected and that activity occurred in primary auditory cortex before area Spt. Furthermore, during the subvocal rehearsal condition IFG, PM and area Spt were functionally connected as a network and activity occurred first in PM, then area Spt, followed by IFGpo.

Broadly, these results demonstrate that numerous cortical regions that engage in different types of information processing underlie verbal WM. These regions were divided into control and storage regions based on dissociations using different behavioral manipulations: time, memory load and rehearsal rate. How they function together, as a network, was also studied and revealed that different nodes of the networks were active at different times within a condition but that different functional networks formed during different conditions. While these results add to the already large body of work pertaining to verbal WM, much more remains to be discovered in the future.

6.2 Future Directions

A key cortical area in verbal working memory tasks is area Spt, thought to be involved in sensory-motor integration of speech (Buchsbaum et al. 2005). While anatomically a sub-portion of the temporoparietal junction (Galaburda & Sanides 1980), area Spt is functionally defined within this anatomically constrained region. Specifically, area Spt is defined as being a region of cortex within the posterior Sylvian fissure (Sylvian-parietal-temporal junction) that has both auditory and motor properties (Hickok et al. 2003). However, due to the high anatomical variability of the Sylvian fissure it can be difficult to identify area Spt manually, and it is even more difficult to develop a efficient automated procedure to locate the area (Figure 6.1).

One way the individual anatomical variability of area Spt can be investigated is with diffusion tensor imaging (DTI). Because the most efficacious anatomical tracers require antemortem injections, most human anatomy has been inferred from primate studies (Greicius et al. 2008). However, with the advent of DTI, human anatomy can be studied non-invasively in vivo. DTI data measures the diffusion of water molecules in the brain and uses the direction of diffusivity to infer the existence and orientation of white matter tracts in the brain. Therefore, using functional fMRI BOLD data collected during a verbal WM task in conjunction with DTI data collected during the same session from the same subjects, it can be determined if some of the anatomical variability of area Spt can be explained by location of white-matter tracts, such as the arcuate fasciculus and superior longitudinal fasciculus (Saur et al. 2008).

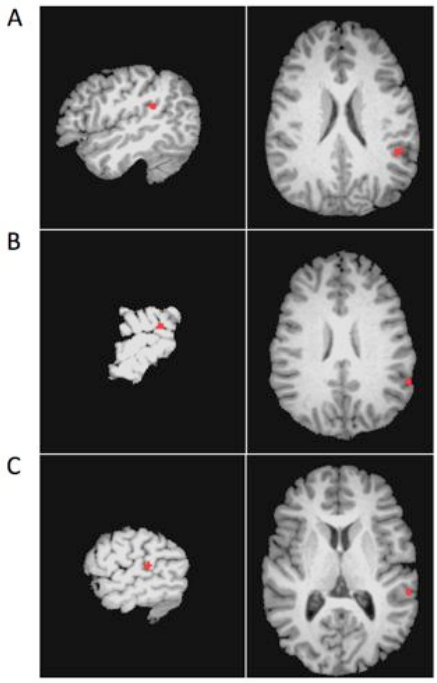

Figure 6.1: Variability of functionally defined area Spt. fMRI data showing the location of the top-10 most significant voxels on sagittal (left) and axial (right) slices derived from a functional contrast for three individual subjects. ***A,*** Subject with a medially located area Spt. ***B,*** Subject with a laterally located area Spt. ***C,*** Subject with a Sylvian fissure that splits into ascending and descending branches. In this particular subject, area Spt happens to be located on the descending branch.

REFERENCES

Aguirre, G. K., Zarahn, E., & D'Esposito, M. (1997). Empirical analyses of BOLD fMRI statistics. II. Spatially smoothed data collected under null-hypothesis and experimental conditions. *Neuroimage*, 5(3), 199–212.

Aldridge, J. W., Garcia, H. R., & Mena, G. (1987). Habituation as a necessary condition for maintenance rehearsal. *Journal of Memory and Language*, 26(6), 632–637.

Anemüller, J., Duann, J.-R., Sejnowski, T. J., & Makeig, S. (2006). Spatio-temporal dynamics in fMRI recordings revealed with complex independent component analysis. *Neurocomputing*, 69(13-15), 1502–1512.

Anderson, J. R. (1983). *The architecture of cognition*. Cambridge, MA: Harvard University Press.

Awh, E., Jonides, J., Smith, E. E., Schumacher, E. H., Koeppe, R. A., & Katz, S. (1996). Dissociation of storage and rehearsal in verbal working memory: Evidence from positron emission tomography. *Psychological Science*, 7, 25–31.

Baddeley, A. D. (1986). *Working memory*. Oxford, UK: Oxford University Press.

Baddeley, A. D., Hitch, G. J. (1974). *Recent advances in learning and motivation.* New York, NY: Academic Press, 47-89.

Baddeley, A. D., Thomson, N., Buchanan, M. (1975). Word length and the structure of short-term memory. *Journal of verbal learning and verbal behavior*, 14, 575-589.

Badre, D., & Wagner, A. D. (2007). Left ventrolateral prefrontal cortex and the cognitive control of memory. *Neuropsychologia*, 45(13), 2883–901.

Bartolomei, F., Bosma, I., Klein, M., Baayen, J. C., Reijneveld, J. C., Postma, T. J., Heimans, J. J., et al. (2006). Disturbed functional connectivity in brain tumour patients: evaluation by graph analysis of synchronization matrices. *Clin Neurophysiol*, 117(9), 2039–49.

Becker, J. T., MacAndrew, D. K., & Fiez, J. A. (1999). A comment on the functional localization of the phonological storage subsystem of working memory. *Brain and cognition*, 41(1), 27–38.

Belin, P., Zatorre, R. J., Hoge, R., Evans, A. C., & Pike, B. (1999). Event-related fMRI of the auditory cortex. *Neuroimage*, 10(4), 417–29.

Bianciardi, M., Fukunaga, M., Gelderen, P. van, Horovitz, S. G., Zwart, J. A. de, & Duyn, J. H. (2009). Modulation of spontaneous fMRI activity in human visual cortex by behavioral state. *Neuroimage*, 45(1), 160–168.

Bor, D., Duncan, J., Wiseman, R. J., & Owen, A. M. (2003). Encoding strategies dissociate prefrontal activity from working memory demand. *Neuron*, 37(2), 361–7.

Brauer, J., Neumann, J., & Friederici, A. D. (2008). Temporal dynamics of perisylvian activation during language processing in children and adults. *Neuroimage*, 41(4), 1484–92.

Brovelli, A., Ding, M., Ledberg, A., Chen, Y., Nakamura, R., & Bressler, S. L. (2004). Beta oscillations in a large-scale sensorimotor cortical network: directional influences revealed by Granger causality. *Proc Natl Acad Sci USA*, 101(26), 9849–54.

Buchsbaum, B., & D'Esposito. M. (2008). The search for the phonological store: from loop to convolution. *Journal of cognitive neuroscience*, 20(5), 762-78.

Buchsbaum, B., Olsen, R., Koch, P., & Berman, K. (2005). Human dorsal and ventral auditory streams subserve rehearsal-based and echoic processes during verbal working memory. *Neuron*, 48(4), 687–697.

Camos, V., Lagner, P., & Barrouillet, P. (2009). Two maintenance mechanisms of verbal information in working memory. *Journal of Memory and Language*, 61(3), 457–469.

Champod, A. S, & Petrides, M. (2010). Dissociation within the frontoparietal network in verbal working memory: a parametric functional magnetic resonance imaging study. *Journal of Neuroscience*, 30(10), 3849–3856.

Champod, Anne Sophie, & Petrides, M. (2007). Dissociable roles of the posterior parietal and the prefrontal cortex in manipulation and monitoring processes. *Proc Natl Acad Sci USA*, 104(37), 14837–42.

Chang, C., Crottazherbette, S., & Menon, V. (2007). Temporal dynamics of basal ganglia response and connectivity during verbal working memory. *Neuroimage*, 34(3), 1253–1269.

Chang, C., & Glover, G. H. (2010). Time–frequency dynamics of resting-state brain connectivity measured with fMRI. *Neuroimage*, 50(1), 81–98.

Chao, L. L., & Knight, R. T. (1998). Contribution of human prefrontal cortex to delay performance. *Journal of cognitive neuroscience*, 10(2), 167–77.

Chein, J., & Fiez, J. (2001). Dissociation of verbal working memory system components using a delayed serial recall task. *Cerebral Cortex*, 11(11), 1003-14.

Chen, S., & Desmond, J. (2005). Cerebrocerebellar networks during articulatory rehearsal and verbal working memory tasks. *Neuroimage*, 24(2), 332–338.

Cohen, J. D., Perlstein, W. M., Braver, T. S., Nystrom, L. E., Noll, D. C., Jonides, J., & Smith, E. E. (1997). Temporal dynamics of brain activation during a working memory task. *Nature*, 386(6625), 604–8.

Constantinidis, C., Franowicz, M. N., & Goldman-Rakic, P. S. (2001). The sensory nature of mnemonic representation in the primate prefrontal cortex. *Nat Neurosci*, 4(3), 311–6.

Cowan, N. (1995). *Attention and memory: an integrated framework*. New York, NY: Oxford University Press.

Cowan, N. (2001). The magical number 4 in short-term memory: a reconsideration of mental storage capacity. *Behav Brain Sci*, 24(1), 87-114.

Cowan, N., Wood, N. L., Wood, P. K., Keller, T. A., Nugent, L. D., & Keller, C. V. (1998). Two separate verbal processing rates contributing to short-term memory span. *Journal of experimental psychology*, 127(2), 141–60.

Cox, R. W. (1996). AFNI: software for analysis and visualization of functional magnetic resonance neuroimages. *Computers and Biomedical Research*, 29(3), 162–173.

Curtis, C. E., & D'Esposito, M. (2003). Persistent activity in the prefrontal cortex during working memory. *Trends in Cognitive Sciences*, 7(9), 415–423.

D'Esposito, M. (2007). From cognitive to neural models of working memory. *Philosophical Transactions of the Royal Society B: Biological Sciences*, 362(1481), 761.

D'Esposito, M., & Postle, B. R. (1999). The dependence of span and delayed-response performance on prefrontal cortex. *Neuropsychologia*, 37(11), 1303–1315.

D'Esposito, M., Detre, J. A., Alsop, D. C., Shin, R. K., Atlas, S., & Grossman, M. (1995). The neural basis of the central executive system of working memory. *Nature*, 378(6554), 279–81.

D'Esposito, M., Postle, B. R., & Rypma, B. (2000). Prefrontal cortical contributions to working memory: evidence from event-related fMRI studies. *Experimental brain research*, 133(1), 3–11.

Dasí, C., Soler, M., Cervera, T., & Ruiz, J. (2008). Influence of articulation rate on two memory tasks in young and older adults. *Percept Mot Skills*, 106(2), 579-89.

Dell, G. S., Schwartz, M. F., Martin, N., Saffran, E. M., & Gagnon, D. A. (1997). Lexical access in aphasic and nonaphasic speakers. *Psychol Rev*, 104(4), 801–38.

Desimone, R. (1996). Neural mechanisms for visual memory and their role in attention. *Proc Natl Acad Sci USA*, 93(24), 13494–9.

Desmond, J. E., Gabrieli, J. D., Wagner, A. D., Ginier, B. L., & Glover, G. H. (1997). Lobular patterns of cerebellar activation in verbal working-memory and finger-tapping tasks as revealed by functional MRI. *J Neurosci*, 17(24), 9675–85.

Douglas, R. J., & Martin, K. A. . (2004). Neural circuits of the neocortex. *Annual Review of Neuroscience*, 27(1), 419–451.

Druzgal, T. J., & D'Esposito, M. (2003). Dissecting contributions of prefrontal cortex and fusiform face area to face working memory. *Journal of cognitive neuroscience*, 15(6), 771–84.

Duann, J.R., Jung, T.P., Kuo, W.J., Yeh, T.C., Makeig, S., Hsieh, J.C., & Sejnowski, T. J. (2002). Single-trial variability in event-related BOLD signals. *Neuroimage*, 15(4), 823–835.

Edwards, E., Nagarajan, S. S., Dalal, S. S., Canolty, R. T., Kirsch, H. E., Barbaro, N. M., & Knight, R. T. (2010). Spatiotemporal imaging of cortical activation during verb generation and picture naming. *Neuroimage*, 50(1), 291–301.

Fiebach, C., Rissman, J., & D'Esposito, M. (2006). Modulation of inferotemporal cortex activation during verbal working memory maintenance. *Neuron*, 51(2), 251–261.

Fransson, P. (2006). How default is the default mode of brain function? Further evidence from intrinsic BOLD signal fluctuations. *Neuropsychologia*, 44(14), 2836–45.

Frey, S., Campbell, J. S. W., Pike, G. B., & Petrides, M. (2008). Dissociating the human language pathways with high angular resolution diffusion fiber tractography. *Journal of Neuroscience*, 28(45), 11435–11444.

Fries, P. (2005). A mechanism for cognitive dynamics: neuronal communication through neuronal coherence. *Trends in Cognitive Sciences*, 9(10), 474–480.

Friston, K. J. (1994). Functional and effective connectivity in neuroimaging: A synthesis. *Human brain mapping*, 2(1-2), 56–78.

Funahashi, S., Chafee, M. V., & Goldman-Rakic, P. S. (1993). Prefrontal neuronal activity in rhesus monkeys performing a delayed anti-saccade task. *Nature*, 365(6448), 753–6.

Fuster, J. M. (1995). *Memory in the cerebral cortex.* Cambridge, UK: The MIT Press.

Fuster, J. M. (2003). *Cortex and mind.* New York, NY: Oxford University Press.

Fuster, J. M., & Alexander, G. E. (1971). Neuron activity related to short-term memory. *Science*, 173(3997), 652-654.

Galaburda, A., & Sanides, F. (1980). Cytoarchitectonic organization of the human auditory cortex. *J. Comp. Neurol.*, 190(3), 597–610.

Garrett, D. D., Kovacevic, N., Mcintosh, A. R., & Grady, C. L. (2010). Blood oxygen level-dependent signal variability is more than just noise. *Journal of Neuroscience*, 30(14), 4914–4921.

Garrett, D. D., Kovacevic, N., Mcintosh, A. R., & Grady, C. L. (2011). The importance of being variable. *Journal of Neuroscience*, 31(12), 4496–4503.

Garrett, D. D., Kovacevic, N., Mcintosh, A. R., & Grady, C. L. (2012). The modulation of BOLD variability between cognitive states varies by age and processing speed. *Cerebral Cortex*, 1–10.

Gazzaley, A., Rissman, J., & D'Esposito, M. (2004). Functional connectivity during working memory maintenance. *Cogn Affect Behav Neurosci*, 4(4), 580–99.

Glenberg, A. M., & Fernandez, A. (1988). Evidence for auditory temporal distinctiveness: modality effects in order and frequency judgments. *Journal of experimental psychology: Learning, memory, and cognition*, 14(4), 728–39.

Goense, J., & Logothetis, N. (2008). Neurophysiology of the BOLD fMRI signal in awake monkeys. *Current Biology*, 18(9), 631–640.

Goldman, R. I., Stern, J. M., Engel, J., & Cohen, M. S. (2002). Simultaneous EEG and fMRI of the alpha rhythm. *Neuroreport*, 13(18), 2487–92.

Greene, R. L. (1987). Effects of maintenance rehearsal on human memory. *Psychological Bulletin*, 102(3), 403–413.

Greicius, M. D., Supekar, K., Menon, V., & Dougherty, R. F. (2008). Resting-state functional connectivity reflects structural connectivity in the default mode network. *Cerebral Cortex*, 19(1), 72–78.

Gruber, O., Müller, T., & Falkai, P. (2007). Dynamic interactions between neural systems underlying different components of verbal working memory. *J Neural Transm*, 114(8), 1047–1050.

Hampson, M., Peterson, B. S., Skudlarski, P., Gatenby, J. C., & Gore, J. C. (2002). Detection of functional connectivity using temporal correlations in MR images. *Human brain mapping*, 15(4), 247–262.

He, B. J. (2011). Scale-free properties of the functional magnetic resonance imaging signal during rest and task. *Journal of Neuroscience*, 31(39), 13786–95.

Heim, S., & Friederici, A. D. (2003). Phonological processing in language production: time course of brain activity. *Neuroreport*, 14(16), 2031–3.

Henson, R. N. A. (2006). Efficient experimental design for fMRI. *Statistical parametric mapping: the analysis of functional brain images*. London: Elsevier, 193–210.

Hickok, G., Okada, K., & Serences, J. (2009). Area Spt in the human planum temporale supports sensory-motor integration for speech processing. *J Neurophysiol*, 101(5), 2725-32.

Hickok, G., Buchsbaum, B., Humphries, C., & Muftuler, T. (2003). Auditory-motor interaction revealed by fMRI: speech, music, and working memory in area Spt. *Journal of cognitive neuroscience*, 15(5), 673–82.

Hulme, C., Thomson, N., Muir, C., & Lawrence, A. (1984). Speech rate and the development of short-term memory span. *Journal of Experimental Child Psychology*, 38(2), 241–253.

Jacquemot, C., & Scott, S. (2006). What is the relationship between phonological short-term memory and speech processing? *Trends in Cognitive Sciences*, 10(11), 480–486.

Johnson, J. A., & Zatorre, R. J. (2005). Attention to simultaneous unrelated auditory and visual events: behavioral and neural correlates. *Cerebral Cortex*, 15(10), 1609–20.

Kayser, A. S., Buchsbaum, B. R., Erickson, D. T., & D'Esposito, M. (2010). The functional anatomy of a perceptual decision in the human brain. *J Neurophysiol*, 103(3), 1179–94.

Kayser, C., Kim, M., Ugurbil, K., Kim, D.-S., & König, P. (2004). A comparison of hemodynamic and neural responses in cat visual cortex using complex stimuli. *Cerebral Cortex*, 14(8), 881–91.

Knecht, S., Deppe, M., Dräger, B., Bobe, L., Lohmann, H., Ringelstein, E., & Henningsen, H. (2000). Language lateralization in healthy right-handers. *Brain*, 123 (1), 74–81.

Kober, H., Möller, M., Nimsky, C., Vieth, J., Fahlbusch, R., & Ganslandt, O. (2001). New approach to localize speech relevant brain areas and hemispheric dominance using spatially filtered magnetoencephalography. *Hum. Brain Mapp.*, 14(4), 236–50.

Koechlin, E., & Jubault, T. (2006). Broca's area and the hierarchical organization of human behavior. *Neuron*, 50(6), 963–974.

Korzeniewska, A., Franaszczuk, P. J., Crainiceanu, C. M., Kuś, R., & Crone, N. E. (2011). Dynamics of large-scale cortical interactions at high gamma frequencies during word production: event related causality analysis of human electrocorticography. *Neuroimage*, 56(4), 2218–2237.

Kubota, K., & Niki, H. (1971). Prefrontal cortical unit activity and delayed alternation performance in monkeys. *J Neurophysiol*, 34(3), 337–347.

Lachaux, J., George, N., Tallonbaudry, C., Martinerie, J., Hugueville, L., Minotti, L., Kahane, P., et al. (2005). The many faces of the gamma band response to complex visual stimuli. *Neuroimage*, 25(2), 491–501.

Laufs, H., Kleinschmidt, A., Beyerle, A., Eger, E., Salek-Haddadi, A., Preibisch, C., & Krakow, K. (2003). EEG-correlated fMRI of human alpha activity. *Neuroimage*, 19(4), 1463–76.

Lee, A. T., Glover, G. H., & Meyer, C. H. (1995). Discrimination of large venous vessels in time-course spiral blood-oxygen-level-dependent magnetic-resonance functional neuroimaging. *Magn Reson Med*, 33(6), 745–54.

Leung, H.-C., Gore, J. C., & Goldman-Rakic, P. S. (2002). Sustained mnemonic response in the human middle frontal gyrus during on-line storage of spatial memoranda. *Journal of cognitive neuroscience*, 14(4), 659–71.

Levelt, W. J., Praamstra, P., Meyer, A. S., Helenius, P., & Salmelin, R. (1998). An MEG study of picture naming. *Journal of cognitive neuroscience*, 10(5), 553–67.

Llorens, A., Trébuchon, A., Liégeois-Chauvel, C., & Alario, F.-X. (2011). Intra-cranial recordings of brain activity during language production. *Front. Psychology*, 2, 1–12.

Logothetis, N. K., Pauls, J., Augath, M., Trinath, T., & Oeltermann, A. (2001). Neurophysiological investigation of the basis of the fMRI signal. *Nature*, 412(6843), 150–7.

Maier, A., Wilke, M., Aura, C., Zhu, C., Ye, F. Q., & Leopold, D. A. (2008). Divergence of fMRI and neural signals in V1 during perceptual suppression in the awake monkey. *Nat Neurosci*, 11(10), 1193–1200.

Mcavoy, M., Larson-Prior, L., Nolan, T. S., Vaishnavi, S. N., Raichle, M. E., & D'avossa, G. (2008). Resting states affect spontaneous BOLD oscillations in sensory and paralimbic cortex. *Journal of Neurophysiology*, 100(2), 922–931.

McIntosh, A. R. (2000). Towards a network theory of cognition. *Neural Netw*, 13(8-9), 861–70.

McIntosh, A. R., Kovacevic, N., Lippe, S., Garrett, D., Grady, C., & Jirsa, V. (2010). The development of a noisy brain. *Arch Ital Biol*, 148(3), 323–37.

Miller, E., & Cohen, J. (2001). An integrative theory of prefrontal cortex function. *Annual Review of Neuroscience*, 24, 167-202.

Misic, B. M., Vakorin, V. A., Paus, T. s, & Mcintosh, A. R. (2011). Functional embedding predicts the variability of neural activity. *Front. Syst. Neurosci*, 5, 90.

Miyake, A., Friedman, N. P., Emerson, M. J., Witzki, A. H., Howerter, A., & Wager, T. D. (2000). The unity and diversity of executive functions and their contributions to complex "frontal lobe" tasks: a latent variable analysis. *Cognitive Psychology*, 41(1), 49–100.

Moosmann, M., Ritter, P., Krastel, I., Brink, A., Thees, S., Blankenburg, F., Taskin, B., et al. (2003). Correlates of alpha rhythm in functional magnetic resonance imaging and near infrared spectroscopy. *Neuroimage*, 20(1), 145–58.

Mukamel, R., Gelbard, H., Arieli, A., Hasson, U., Fried, I., & Malach, R. (2005). Coupling between neuronal firing, field potentials, and FMRI in human auditory cortex. *Science*, 309(5736), 951–4.

Narayanan, N. S., Prabhakaran, V., Bunge, S. A., Christoff, K., Fine, E. M., & Gabrieli, J. D. E. (2005). The role of the prefrontal cortex in the maintenance of verbal working memory: an event-related fMRI analysis. *Neuropsychology*, 19(2), 223–232.

Naveh-Benjamin, M., & Jonides, J. (1984). Maintenance rehearsal: a two-component analysis. *Journal of experimental psychology: learning, memory, and cognition*, 10(3), 369–385.

Neumann, J., Lohmann, G., Zysset, S., & Cramon, D. Y. (2003). Within-subject variability of BOLD response dynamics. *Neuroimage*, 19(3), 784–96.

Oberauer, K. (2002). Access to information in working memory: exploring the focus of attention. *Journal of experimental psychology: learning, memory, and cognition*, 28(3), 411–421.

O'Connor, N., Hermelin, B. (1972). Seeing and hearing in space and time. *Percept Psychophys*, *11*, 46-48.

O'Connor, N., Hermelin, B. (1973). The spatial or temporal organization of short-term memory. *Q J Exp Psychol*, *25*, 335-343.

Olson, I. R., & Berryhill, M. (2009). Some surprising findings on the involvement of the parietal lobe in human memory. *Neurobiology of Learning and Memory*, 91(2), 155–65.

Page, M. P., & Norris, D. (1998). The primacy model: a new model of immediate serial recall. *Psychological Review*, 105(4), 761–81.

Pasquale, F. D., Penna, S. D., Snyder, A. Z., Lewis, C., Mantini, D., Marzetti, L., Belardinelli, P., et al. (2010). Temporal dynamics of spontaneous MEG activity in brain networks. *Proc Natl Acad Sci USA*, 107(13), 6040–6045.

Paulesu, E., Frith, C. D., & Frackowiak, R. S. (1993). The neural correlates of the verbal component of working memory. *Nature*, 362(6418), 342–5.

Phaf, R. H., & Wolters, G. (1993). Attentional shifts in maintenance rehearsal. *The American Journal of Psychology*, 353–382.

Postle, B. R. (2006). Working memory as an emergent property of the mind and brain. *Neuroscience*, 139(1), 23–38.

Postle, B. R., Berger, J. S., & D'Esposito, M. (1999). Functional neuroanatomical double dissociation of mnemonic and executive control processes contributing to working memory performance. *Proc Natl Acad Sci USA*, 96(22), 12959–64.

Prat, C. S., Keller, T. A., & Just, M. A. (2007). Individual differences in sentence comprehension: a functional magnetic resonance imaging investigation of syntactic and lexical processing demands. *Journal of cognitive neuroscience*, 19(12), 1950–63.

Pulvermüller, F., & Shtyrov, Y. (2009). Spatiotemporal signatures of large-scale synfire chains for speech processing as revealed by MEG. *Cerebral Cortex*, 19(1), 79–88.

Rack-Gomer, A. L., & Liu, T. T. (2012). Caffeine increases the temporal variability of resting-state BOLD connectivity in the motor cortex. *Neuroimage*, 59(3), 2994–3002.

Raye, C., Johnson, M., Mitchell, K., & Reeder, J. (2002). Neuroimaging a single thought: dorsolateral PFC activity associated with refreshing just-activated information. *Neuroimage*, 15(2), 447-53.

Reichle, E. D., Carpenter, P. A., & Just, M. A. (2000). The neural bases of strategy and skill in sentence-picture verification. *Cognitive Psychology*, 40(4), 261–95.

Riecker, A., Mathiak, K., Wildgruber, D., Erb, M., Hertrich, I., Grodd, W., & Ackermann, H. (2005). fMRI reveals two distinct cerebral networks subserving speech motor control. *Neurology*, 64(4), 700–6.

Riecker, A., Kassubek, J., Gröschel, K., Grodd, W., & Ackermann, H. (2006). The cerebral control of speech tempo: opposite relationship between speaking rate and BOLD signal changes at striatal and cerebellar structures. *Neuroimage*, 29(1), 46–53.

Rissman, J., Gazzaley, A., & D'Esposito, M. (2004). Measuring functional connectivity during distinct stages of a cognitive task. *Neuroimage*, 23(2), 752–763.

Rissman, J., Gazzaley, A., & D'Esposito, M. (2007). Dynamic adjustments in prefrontal, hippocampal, and inferior temporal interactions with increasing visual working memory load. *Cerebral Cortex*, 18(7), 1618–1629.

Rodriguez-Fornells, A., Schmitt, B. M., Kutas, M., & Münte, T. F. (2002). Electrophysiological estimates of the time course of semantic and phonological encoding during listening and naming. *Neuropsychologia*, 40(7), 778–87.

Roebroeck, A., Formisano, E., & Goebel, R. (2005). Mapping directed influence over the brain using Granger causality and fMRI. *Neuroimage*, 25(1), 230–42.

Romanski, L. M. (2004). Domain specificity in the primate prefrontal cortex. *Cogn Affect Behav Neurosci*, 4(4), 421–429.

Romanski, L. M., Tian, B., Fritz, J., Mishkin, M., Goldman-Rakic, P. S., & Rauschecker, J. P. (1999). Dual streams of auditory afferents target multiple domains in the primate prefrontal cortex. *Nat Neurosci*, 2(12), 1131–6.

Ruchkin, D. S., Grafman, J., Cameron, K., & Berndt, R. S. (2003). Working memory retention systems: a state of activated long-term memory. *Behav Brain Sci*, 26(6), 709-28; discussion 728–77.

Rypma, B., & D'Esposito, M. (1999). The roles of prefrontal brain regions in components of working memory: effects of memory load and individual differences. *Proc Natl Acad Sci USA*, 96(11), 6558–63.

Rypma, B., Berger, J. S., Prabhakaran, V., Bly, B. M., Kimberg, D. Y., Biswal, B. B., & D'Esposito, M. (2006). Neural correlates of cognitive efficiency. *Neuroimage*, 33(3), 969–979.

Rypma, B., Prabhakaran, V., Desmond, J. E., Glover, G. H., & Gabrieli, J. D. (1999). Load-dependent roles of frontal brain regions in the maintenance of working memory. *Neuroimage*, 9(2), 216–26.

Rypma, B., Berger, J. S., & D'Esposito, M. (2002). The influence of working-memory demand and subject performance on prefrontal cortical activity. *Journal of cognitive neuroscience*, 14(5), 721–31.

Sakai, K., Rowe, J. B., & Passingham, R. E. (2002). Active maintenance in prefrontal area 46 creates distractor-resistant memory. *Nat Neurosci*, 5(5), 479-84.

Samanez-Larkin, G. R., Kuhnen, C. M., Yoo, D. J., & Knutson, B. (2010). Variability in nucleus accumbens activity mediates age-related suboptimal financial risk taking. *Journal of Neuroscience*, 30(4), 1426–1434.

Saur, D., Kreher, B. W., Schnell, S., Kümmerer, D., Kellmeyer, P., Vry, M.S., Umarova, R., et al. (2008). Ventral and dorsal pathways for language. *Proc Natl Acad Sci USA*, 105(46), 18035–40.

Sauseng, P., Klimesch, W., Schabus, M., & Doppelmayr, M. (2005). Fronto-parietal EEG coherence in theta and upper alpha reflect central executive functions of working memory. *Int J Psychophysiol*, 57(2), 97–103.

Scheeringa, R., Bastiaansen, M. C., Petersson, K. M., Oostenveld, R., Norris, D. G., & Hagoort, P. (2008). Frontal theta EEG activity correlates negatively with the default mode network in resting state. *Int J Psychophysiol*, 67(3), 242–51.

Scott, S. K., & Johnsrude, I. S. (2003). The neuroanatomical and functional organization of speech perception. *Trends in Neurosciences*, 26(2), 100–107.

Shergill, S. S., Brammer, M. J., Fukuda, R., Bullmore, E., Amaro, E., Murray, R. M., & McGuire, P. K. (2002). Modulation of activity in temporal cortex during generation of inner speech. *Hum Brain Mapp*, 16(4), 219–27.

Shimamura, A. (2000). The role of the prefrontal cortex in dynamic filtering. *Psychobiology*, 28 (2), 207-218.

Smith, E. E., Jonides, J., & Koeppe, R. A. (1996). Dissociating verbal and spatial working memory using PET. *Cerebral Cortex*, 6(1), 11–20.

Smith, E. E., Jonides, J., Koeppe, R. A., Awh, E., Schumacher, E. H., & Minoshima, S. (1995). Spatial versus object working memory: PET investigations. *Journal of cognitive neuroscience*, 7(3), 337–356.

Sun, F. T., Miller, L. M., & D'Esposito, M. (2004). Measuring interregional functional connectivity using coherence and partial coherence analyses of fMRI data. *Neuroimage*, 21(2), 647–58.

Tallon-Baudry, C., Bertrand, O., & Fischer, C. (2001). Oscillatory synchrony between human extrastriate areas during visual short-term memory maintenance. *J Neurosci*, 21(20), RC177.

Tallon-Baudry, C., Mandon, S., Freiwald, W. A., & Kreiter, A. K. (2004). Oscillatory synchrony in the monkey temporal lobe correlates with performance in a visual short-term memory task. *Cerebral Cortex*, 14(7), 713–720.

Thierry, G., Boulanouar, K., Kherif, F., Ranjeva, J. P., & Démonet, J. F. (1999). Temporal sorting of neural components underlying phonological processing. *Neuroreport*, 10(12), 2599–603.

Thirion, B., Pinel, P., Mériaux, S., Roche, A., Dehaene, S., & Poline, J. B. (2007). Analysis of a large fMRI cohort: statistical and methodological issues for group analyses. *Neuroimage*, 35(1), 105–20.

Tomita, H., Ohbayashi, M., Nakahara, K., Hasegawa, I., & Miyashita, Y. (1999). Top-down signal from prefrontal cortex in executive control of memory retrieval. *Nature*, 401(6754), 699–703.

Vakorin, V. A, Lippe, S., & Mcintosh, A. R. (2011). Variability of brain signals processed locally transforms into higher connectivity with brain development. *Journal of Neuroscience*, 31(17), 6405–6413.

Varela, F., Lachaux, J. P., Rodriguez, E., & Martinerie, J. (2001). The brainweb: phase synchronization and large-scale integration. *Nat Rev Neurosci*, 2(4), 229–39.

Wagner, A. D., Maril, A., Bjork, R. A., & Schacter, D. L. (2001). Prefrontal contributions to executive control: fMRI evidence for functional distinctions within lateral prefrontal cortex. *Neuroimage*, 14(6), 1337–1347.

Wiggs, C. L., & Martin, A. (1998). Properties and mechanisms of perceptual priming. *Current Opinion in Neurobiology*, 8(2), 227–33.

Wildgruber, D., Ackermann, H., & Grodd, W. (2001). Differential contributions of motor cortex, basal ganglia, and cerebellum to speech motor control: effects of syllable repetition rate evaluated by fMRI. *Neuroimage*, 13(1), 101–9.

Wilson, S. M., Saygin, A. P., Sereno, M. I., & Iacoboni, M. (2004). Listening to speech activates motor areas involved in speech production. *Nat Neurosci*, 7(7), 701–702.

Woodward, T., Cairo, T., Ruff, C., Takane, Y., Hunter, M., & Ngan, E. (2006). Functional connectivity reveals load dependent neural systems underlying encoding and maintenance in verbal working memory. *Neuroscience*, 139(1), 317–325.

Zarahn, E., Rakitin, B., Abela, D., Flynn, J., & Stern, Y. (2005). Positive evidence against human hippocampal involvement in working memory maintenance of familiar stimuli. *Cerebral Cortex*, 15(3), 303–16.